Dissertation

submitted to the

Combined Faculties for the Natural Sciences and for Mathematics

of the Ruperto-Carola University of Heidelberg, Germany

for the degree of

Doctor of Natural Sciences

Presented by

Diplom: Lina Vasiliauskaite

Born in: Vilkaviskis, Lithuania

Oral examination: 24th November, 2016

EMBRYONIC FUNCTIONS OF REPROGRAMMING MUTANTS MIWI2, MILI AND DNMT3L INFLUENCE ADULT MALE GERMLINE MAINTENANCE

Referees: Prof. Dr. Ramesh Pillai

Prof. Dr. Ingrid Lohmann

TABLE OF CONTENTS

EMBRYONIC FUNCTIONS OF REPROGRAMMING MUTANTS MIWI2, MILI AND DNMT3L INFLUENCE ADULT MALE GERMLINE MAINTENANCE

Summary

Miwi2 and Mili are involved in piRNA production and transposon silencing in fetal gonads. It is known that the loss of Miwi2 leads to a complete exhaustion of germline in male mice. Whether the absence of Mili results in the same phenotype, has not been established yet. In this study we show that Mili is also required for germ cell maintenance, but presents a much weaker phenotype than Miwi2 with only a partial loss of the germ line observed in aged mice. The difference between the two mutant phenotypes could be explained by the fact that in Mili deficient fetal testes a small amount of piRNAs is produced that can mount a residual defense against transposable elements as determined by bisulfite sequencing data. We have determined that piRNAs made in the absence of Mili make up a small pool of piRNAs that are also present in the wild type mice. Mili mutant piRNAs are mainly primary in nature and are most likely bound by Miwi2 since Miwi2 partially retains its nuclear localization in the absence of Mili in mouse fetal gonadocytes. In summary, a primary piRNA biogenesis pathways exist in mouse in the absence of Mili that contribute to both germ line reprogramming and maintenance.

Miwi2 and Dnmt3L are involved in de novo DNA methylation in fetal gonads. Miwi2 and Dnmt3L mutant mice exhibit a depletion of germline with age. Dnmt3L mutant mice completely lose germ cells within a two-month period, while Miwi2 mutant mice exhibit Sertoli-only phenotype at nine-month of age. Nonetheless, the phenotype of both reprogramming mutants indicates Miwi2 and Dnmt3L's possible role in germline maintenance. In this study we have shown that the main role of Miwi2 and Dnmt3L in establishing and maintaining the population of undifferentiated spermatogonia precursor cell population in the adult is executed through their role in reprogramming fetal gonadocytes. We have observed that even though Miwi2- and Dnmt3L-deficient spermatogonial precursor cells exhibit transposon de-repression, no apparent loss these cells can be associated with DNA damage. We hypothesize that actively transcribed TE containing locus generates hybrid transcripts triggering abnormal gene expression program in spermatogonia stem cells, which leads to a great reduction in the numbers of actual GFRa1pos stem cells observed n Miwi2 and Dnmt3L mutant testis. Overall, this study shows the importance of germ cell reprograming in establishing a healthy, functional stem cell population in the adult tissue.

EMBRYONALE FUNKTIONEN DER REPROGRAMMIERUNGS-MUTANTEN MIWI2, MILI UND DNMT3L BEEINFLUSSEN DEN ERHALT DER ADULTEN MÄNNLICHE KEIMBAHN

Zusammenfassung

Miwi2 und Mili sind in der piRNA Produktion und der Stilllegung von Transposons in fötalen Hoden involviert. Es ist bereits bekannt, dass der Verlust von Miwi2 zu einem Totalverlust der Keimbahnzell en in männlichen Mäusen führt. Ob jedoch der Verlust von Mili zu einem ähnlichen Phänotyp führt, wurde bisher noch nicht erforscht. In dieser Studie zeigen wir, dass Mili ebenfalls für die Keimzell-Erhaltung benötigt wird, jedoch einen schwächeren Phänotypals Miwi2 zeigt, der sich in teilweisem Verlust von Keimzellen in gealterten Mäusen manifestiert. Der Unterschied zwischen den Phänotypen der zwei Mutanten konnte durch die Produktion von kleinen Mengen piRNAs in Mili-defizienten fötalen Hoden erklärt werden. Diese ermöglichen eine Restantwort auf transponierbare Elemente, welche durch Bisulfit-Sequenzierungs Daten demonstriert wird. Wir beschreiben, dass piRNAs, die in Abwesenheit von Mili produziert werden, eine kleine Gruppe piRNAs darstellen, die auch in Wildtyp-Mäusen präsent ist. Diese piRNAs sind hauptsächlich primärer Natur und sehr wahrscheinlich an Miwi2 gebunden, da Miwi2 trotz Abwesenheit von Mili auch weiterhin teilweise eine nukleare Lokalisation in fötalen Hoden aufweist. Zusammenfassend legtdiese Studie nahe, dass ein tertiärer piRNA Biogeneseweg in Maushoden existiert, der zu Keimzell-Reprogrammierung und -Erhaltung beiträgt.

Miwi2 und Dnmt3L sind in der de novo DNA Methylierung DNA in fötalen Hoden involviert. Männliche Miwi2 und Dnmt3L knockout Mäuse zeigen einen Verlust der männlichen Keimbahn im Alter. Die Dnmt3L knockout Mäuse verlieren die Keimzellen dabei innerhalb von zwei Monaten, während die Miwi2 Mutanten mit neun Monaten ein Sertoli-only Syndrom aufweisen. Beide Phänotypen weisen daher auf eine Funktion von Miwi2 und Dnmt3L in der Erhaltung der Keimbahn hin. In dieser Studie haben wir gezeigt, dass die primäre Rolle von Miwi2 und Dnmt3L in der Etablierung und Erhaltung der adulten Population undifferenzierter spermatogonialer Stammzellen in ihrer Funktion während der fötalen Reprogrammierung von Gonadozy ten begründet liegt. Wir konnten demonstrieren, dass trotz deutlicher Transposon-Aktivierung in Miwi2- und Dnmt3L-defizienten Spermatogonien Vorläuferzellen der Verlust dieser Zellen nicht mit DNA Schäden korreliert werden kann. Wir stellen daher die Hypothese auf, dass ein aktiv transkribierter Transposonlocus zur Expression von hybriden Transkripten führt, die ein verändertes Genexpressions-Programm in spermatogonialen Stammzellen induzieren. Dieses wiederum würde zu einer deutlichen Reduktion an undifferenzierten GFRa1^{pos} Stammzellen im Hoden führen, wie wir sie in Miwi2 und Dnmt3L knockout Hoden beobachten. Zusammengenommen zeigt diese Studie die Bedeutung der fötalen Keimzellen-Reprogrammierung für die Etablierung einer funktionellen Stammzellpopulation in adulten Gewebe.

INTRODUCTION

MALE MOUSE GERMLINE

Male mouse germline development and spermatogenesis

In an early mouse embryo at around the embryonic day 6.5 (E6.5) a group of cells are specified as primordial germ cells (PGCs) by suppression of somatic gene expression program and induction of germline specific genes (Ohinata *et al.*, 2005). Specified PGCs migrate in the embryo to genital ridges where gonads will develop (Buehr *et al.*, 1993). PGCs reach genital ridges at E11.5 where they are enclosed by precursors of somatic support Sertoli cells and form seminiferous cords (Merchant-Larios *et al.*, 1993). In a newly formed gonad sex-specific differentiation begins: in males PGCs become prospermatogonia (also called fetal gonadocytes), while in female – oogonia. Shortly after gonad colonization prospermatogonia enter mitotic arrest and rest in G1/G0 until after birth (McLaren and Southee, 1997). After the birth during postnatal days 3-6 prospermatogonia migrate to the basal compartment of the seminiferous epithelium, enter cell cycle and establish a population of spermatogonial stem cells (SSCs) (de Rooij and Grootegoed, 1998). At the same time a seminiferous cord develops a lumen and becomes a seminiferous tubule (de Rooij and Grootegoed, 1998)(de Rooij and Grootegoed, 1998)(de Rooij and Grootegoed, 1998)(de Rooij and Grootegoed, 1998)(de Rooij and Grootegoed, 1998). SSCs are responsible for continuous production of mature spermatozoa in a process called spermatogenesis.

There are three phases of spermatogenesis: mitotic, meiotic and spermiogenesis. During mitotic phase spermatogonial stem cells divide several times and give rise to more differentiated spermatogonia which in turn differentiate into primary spermatocytes, which undergo two rounds of meiotic divisions (meiosis I and meiosis II) to produce haploid cells. Haploid cells first develop as round spermatids and give rise to elongating spermatids and subsequently to mature spermatozoa in a process called spermiogenesis (de Rooij and Grootegoed, 1998). Spermatogenesis is a precisely timed process, which is most evident during the first wave of spermatogenesis in prepubertal mouse testes. Spermatogonial stem cell population is defined by day 6 after the birth (P6) (Bellve *et al.*, 1977). During the next two days spermatogonia divide and differentiate and the first meiotic cells – primary spermatocytes in leptonene phase are present at day 10. At day 12 zygotene spermatocytes appear, while early stages of pachytene are reached at day 14. Pachytene spermatocytes develop further until day 18-20. First round spermatids occur at day 20 (Bellve *et al.*, 1977; Nebel *et al.*, 1961) and the whole spermatogenesis process takes 35 days to complete (Oakberg, 1956).

Spermatogonial stem cells

Classification of spermatogonial stem cells

It is agreed that the most primitive spermatogonia found in the mouse testes is a type A spermatogonial stem cell. Type A spermatogonia divide mitotically and differentiate into intermediate (In) and then B type spermatogonia. B-type spermatogonia develop into primary spermatocytes (Bellve *et al.*, 1977). Initially, the types of spermatogonia were defined based on their nuclear morphology: type A cell's nucleus is mainly euchromatic, type B cell's nucleus has a lot of heterochromatin, while In spermatogonia have intermediate levels of heterochromatin (Phillips *et al.*, 2010). When a spermatogonial stem cell, which is called A-single spermatogonia or A_s, divides, it produces either two daughter A_s cells (a self-renewal division) or gives rise to two cells that stay interconnected *via* cytoplasmic bridge and are called A-paired spermatogonia or A_{pr}. A_{pr} in turn divides again and forms a chain of four cells – A-aligned4, A_{al4}. Subsequent mitotic divisions result in longer chains of cells – A_{al8}, A_{al16}, A_{al32} (De Rooij, 1988) (Figure 1). A_{al} further on develop into A_1, A_2, A_3 and A_4 spermatogonia (Oakberg, 1971). The population A_s, A_{pr} and A_{al} spermatogonia in mouse testes is also called spermatogonial precursor cells (SPCs) due to a fact that they differentiate and produce meiotic cells as described. The initial ^{3}H-thymidine labeling experiments of dividing germ cells lead to a conclusion that most likely A_s is the stem cell of the testis, since observed A_s spermatogonia retained ^{3}H-thymidine label the longest, in agreement that tissue stem cells do not divide as often as their progeny (Oakberg, 1971). Currently, it is believed that the cells with a stem cell potential reside in a population of A_s, A_{pr} and A_{al4}, whereas spermatogonia in longer chains are more committed to differentiation. A molecular basis of such a classification will be discussed later. Therefore, a population of the actual stem cells is a subset of SPCs.

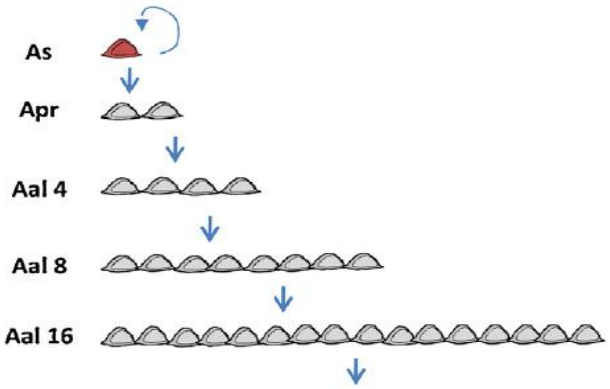

Figure 1. A-type spermatogonia divide to produce long chains of interconnected cells. Modified from Boitani *et al.* (2016).

Regulation of a germ stem cell fate by cytokine signaling and their niche

The niche for spermatogonial stem cells is created by the main somatic cell of the tubule – the Sertoli cell. Sertoli cells provide microenvironment and make contacts with spermatogonia (de Rooij, 2009; Oatley *et al.*, 2011b). Undifferentiated spermatogonia are located at the basal part of seminiferous tubules. More primitive spermatogonia have a tendency to reside in the areas of the tubule that face interstitial tissue and vasculature (Chiarini-Garcia *et al.*, 2001; Yoshida *et al.*, 2007).The fate of SSCs is determined mainly by the cues received in the niche *via* paracrine signaling. Sertoli cells excrete GDNF (glial cell-line derived neurotrophic factor), which is the primary cytokine controlling SSCs self-renewal and differentiation. Spermatogonia in turn express Gfra1/Ret co-receptor complex which responds to GDNF (Hofmann *et al.*, 2005; Naughton *et al.*, 2006). A precise dosage of GDNF is important to maintain a spermatogonial population. Mice harboring only one GDNF-mutant allele showed depletion of germ cells and reduced proliferation rate of spermatogonia, while overexpression of GDNF resulted in large mostly A_s cell clumps that were unable to differentiate (Meng *et al.*, 2000). Increased replication of undifferentiated spermatogonia was also observed in a seminiferous tubule culture system treated with an access of GDNF (Parker *et al.*, 2014). In addition, loss of any of the genes – *Gdnf, Gfra1* or *Ret*, results in a complete loss of germ cells by P28 (Naughton *et al.*, 2006), while a short-term inhibition of Ret reduces proliferation of A_s, A_{pr} and A_{al} spermatogonia and forces them to differentiate (Parker *et al.*, 2014). Overall, these data indicate that in the absence of GDNF spermatogonial stem cells tend to differentiate while at high levels of GDNF self-renewal divisions are favored.

It was found that intracellular signaling by GDNF is exerted *via* Akt/PI3K, Src kinases and MEK/ERK pathways to promote spermatogonial stem cell survival and self-renewal proliferation (Braydich-Stolle *et al.*, 2007; Hasegawa *et al.*, 2013; He *et al.*, 2008; Lee *et al.*, 2007; Oatley *et al.*, 2007; Takashima *et al.*, 2015). Such an effect of GDNF signaling is mediated *via* inducing expression of such transcriptions factors like Bcl6b, Etv5, c-Fos, N-Myc, Foxo1 (Braydich-Stolle *et al.*, 2007; Goertz *et al.*, 2011; He *et al.*, 2008; Oatley *et al.*, 2007) , as well as regulating cell cycle molecules like cyclin A, cyclin E2 or CDK1 (He *et al.*, 2008; Lee *et al.*, 2007). At the same time GDNF is involved in downregulating genes that prime spermatogonia for differentiation, eg. Neurogenin3 (Ngn3), Nanos3, even c-Kit (Grasso *et al.*, 2012; Hasegawa *et al.*, 2013; Lee *et al.*, 2007; Takashima *et al.*, 2015).

Fibroblast growth factor 2 (FGF2), secreted by Sertoli cells, was also found to be important in driving spermatogonial stem cell proliferation (Ebata *et al.*, 2011; Ishii *et al.*, 2012). Most likely the signaling by FGF2 is exerted *via* FGFR1 present on spermatogonia (Takashima *et al.*, 2015). Interestingly, FGF2 was shown to function *via* MEK/ERK and

Akt/PI3K signaling pathway (Ishii *et al.*, 2012; Takashima *et al.*, 2015) to upregulate expression of Blc6b and Etv5, the same pathway induced by GDNF (Ishii *et al.*, 2012). Moreover, FGF2 was implicated in enhancing the effect of GDNF, since cultured SSCs can survive without FGF2, but not GDNF (Ebata *et al.*, 2011; Ishii *et al.*, 2012). Nonetheless, Takashima and colleagues reported that a small population of spermatogonia is able to survive GDNF deficit *in vivo* and interestingly FGF2 deficit increases the levels of GDNF (Takashima *et al.*, 2015), indicating a delicate interplay of regulating spermatogonial stem cell proliferation and survival *via* GDNF and FGF2. In addition, colony stimulating factor 1 (CSF1) expression was identified in interstitial Leyding and peritubular myoid cells in the testes, while undifferentiated spermatogonia were found to express CSF1R – a receptor for CSF1. CSF1 was shown to enhance self-renewal division of SSCs in culture (Oatley *et al.*, 2009). Furthermore, Wnt/β-catenin pathway was found to be functional in undifferentiated spermatogonia in mice and control proliferation of these cells (Takase and Nusse, 2016). All in all, employment of multiple cytokines and signaling pathways indicate complicated and at the same time redundant regulatory system to assure proper spermatogonial stem cell self-renewal and differentiation. It is worth mentioning that, even though mouse models were analyzed extensively, most of the advances in understanding the spermatogonial stem cell fate control by cytokines have been reached in studying cultured SSCs – a culture system first reported and developed in Shinohara's lab (Kanatsu-Shinohara *et al.*, 2003). Cultured SSCs were shown to express spermatogonia characteristic markers and possess a stem cell activity by transplantation (Ebata *et al.*, 2011; He *et al.*, 2008; Ishii *et al.*, 2012; Kanatsu-Shinohara *et al.*, 2003; Lee *et al.*, 2007; Oatley *et al.*, 2007). To note, cultured SSCs can be engineered in a similar manner as mouse embryonic stem cells. Transplanted to a sterile recipient modified SSCs contribute to progeny harboring introduced transgene (Kanatsu-Shinohara *et al.*, 2005). Thus, spermatogonial stem cell research has not only scientific, but also a potential clinical value.

Extended self-renewal capacity of spermatogonia

It has been established that aging mice exhibit reduced fertility: 50% of 1-year-old and 75% of 2-year-old mice have atrophied testes (Zhang *et al.*, 2006). It has been debated whether this effect is manifested due to a SSC self-renewal failure or whether aged somatic support cells cannot provide proper niche and maintenance for the stem cells or both. Experimental evidence points that at the age of two years mice show an impairment in both – SSCs and more so in their niche (Zhang *et al.*, 2006). It is possible that SSCs function can be irreversibly influence by their environment, because SSCs can maintain self-renewal capacity

for more than two years when serially transplanted (Ogawa *et al.*, 2003; Ryu *et al.*, 2006). Even 1-year-old or 2-year-old spermatogonial stem cells show comparable colonization activity to "young" spermatogonia when transplanted into young recipients (Zhang *et al.*, 2006). These experiments suggest that spermatogonial stem cells have an extended self-renewal capacity, which, as discussed before, is tightly regulated. In order to make use of this knowledge, there is a great need to understand SSCs biology in more detail. During last decade most of the effort was diverted into the research to identify molecular markers which would allow to define and distinguish undifferentiated spermatogonial stem cells with an actual stem cell activity.

In a search of SSC markers: SSC population heterogeneity and hierarchy

The discovery that GDNF is the key ruler of spermatogonial stem cell fate and that spermatogonial stem cells express Gfra1/Ret receptor complex for GDNF led to a proposal that Gfra1/Ret expressing cells define an actual stem cell population in the testes. Gfra1 was suggested as a spermatogonial stem cell marker (Hofmann *et al.*, 2005; Meng *et al.*, 2000). Indeed, Gfra1 was found to be expressed mainly in A_s, A_{pr} and A_{al4} spermatogonia (Grisanti *et al.*, 2009; Hara *et al.*, 2014; Hofmann *et al.*, 2005; Nakagawa *et al.*, 2010). Even though it was discovered that 10% of A_s and 20% of A_{pr} did not express Gfra1 (Grisanti *et al.*, 2009), indicating that Gfra1 positive cells are either a subset of the actual stem cells or Gfra1 negative cells present rather a transit amplifying stem cell population than actual stem cells. One of the most reliable functional assays to test whether a population possesses a stem cell activity is a reconstitution of sterile recipient's testes by transplantation, a technique developed by Brinster and colleagues a couple of decades ago (Brinster and Zimmermann, 1994). Transplantation was used to determine whether Grfa1 expressing cells are indeed real stem cells of the testes. When SSCs from a 10 days old mouse were transplanted into a recipient, Gfra1-enriched population gave higher reconstitution rate than Gfra1-depleted population, consistent with the assumption that Gfra1 expressing cells have a stem cell potential (Buageaw *et al.*, 2005). Yet, interestingly, the same approach using donor cells from adult mice revealed that Gfra1-depleted spermatogonial cells had higher colonization activity than Gfra1-enriched cells (Grisanti *et al.*, 2009). The possible explanation for this outcome is that postnatal spermatogonia are different than adult spermatogonia (Ebata *et al.*, 2007). More importantly, Hara and colleagues have shown that Grfa1 expressing spermatogonial stem cells mostly contribute to a steady-state or homeostatic spermatogenesis (Hara *et al.*, 2014), whereas a transplantation creates a great challenge for the stem cell to replenish empty testicular tissue. By lineage tracing experiment it was shown that Grfa1 expressing cells

differentiated continually and gave rise to mature spermatozoa, at the same time maintaining a constant stem cell pool over a prolonged period of time (Hara *et al.*, 2014). On the other hand, a contribution of Grfa1 expressing cells to regeneration of chemically depleted testes was minimal (Hara *et al.*, 2014). Overall, it is accepted that the actual stem cell activity within steady-state, undisturbed mouse testes resides in a population of A_s, A_{pr} and A_{al4} Gfra1 expressing cells.

Over the years molecular identity of spermatogonial stem cells has been extensively researched. It was discovered that mice deficient of an RNA-binding protein Nanos2 very rapidly loose germ cells, when deletion of Nanos2 is induced in an adult animal (Sada *et al.*, 2009). Moreover, overexpression of Nanos2 causes accumulation of undifferentiated cells that cannot differentiate (Sada *et al.*, 2009). To sum, Nanos2 deficient or overexpressing mice very closely resemble the phenotype of GDNF deficiency (Meng *et al.*, 2000). This finding lead to a hypothesis that Nanos2, as well as Gfra1, define a stem cell population in mouse testes. Several lines of experiment are in agreement with this hypothesis. Firstly, in a linage tracing experiment Nanos2 was found to contribute to an entire spermatogenic process, as well as maintain constant number of Nanos2 expressing cells over the time (Sada *et al.*, 2009). Secondly, Nanos2 was described to be expressed in A_s, A_{pr} and A_{al4} spermatogonia (Sada *et al.*, 2009; Suzuki *et al.*, 2009). Finally, all Gfra1 expressing cells were lost upon Nanos2 deletion (Sada *et al.*, 2009). All in all, Nanos2 expressing spermatogonia contribute to a pool of actual stem cells in the testes. Whether Nanos2 is involved in testicular regeneration, was not tested. However, Nanos2 was shown to have more "extended" expression pattern than Gfra1 since 66% of Nanos2 expressing cells were Gfra1 positive, but all Gfra1 positive cells were also Nanos2 positive (Suzuki *et al.*, 2009). Interestingly, GDNF signaling was implicated in maintaining the expression of Nanos2 in undifferentiated spermatogonia (Sada *et al.*, 2012).

Another gene, coding a transcription factor Neurogenin3 (Ngn3), was found to be involved in a germ stem cell biology. Ngn3 is expressed in a population of A_s, A_{pr} and A_{al} spermatogonia. Very few Ngn3 positive A_s and A_{pr} spermatogonia are found, while many A_{al} spermatogonia, even long chains of A_{al16} or A_{al32}, are marked by Ngn3 expression (Yoshida *et al.*, 2004; Nakagawa *et al.*, 2007). In a steady-state spermatogenesis Ngn3 is believed to contribute very little if any to a pool of actual stem cells. Linage tracing studies have indicated that most of the cells "marked" as descendants of Ngn3 disappear from testes within two months or some of the labeled clusters of cells do not contain spermatogonia stem cells at all (Nakagawa *et al.*, 2007). This experiment led to a conclusion that Ngn3 expressing population functions as transit amplifying cells that in turn are derived from Gfra1 positive

cells (Ikami *et al.*, 2015; Nakagawa *et al.*, 2007). Double positive – Gfra1 and Ngn3 expressing – cells are occasionally detected (Nakagawa *et al.*, 2010). Interestingly, very few Ngn3 expressing cells were observed to support a steady-state spermatogenesis in a long-term manner, however, the number of cells that contributed to spermatogenesis in regenerating testicular tissue or gave colonies after transplantation was much greater (Nakagawa *et al.*, 2007). Moreover, under such conditions Ngn3 expressing cells were observed to convert to Gfra1 expressing cells at a very low frequency (Nakagawa *et al.*, 2010), contributing to the expansion of Gfra1 cells in regenerating testes (Hara *et al.*, 2014; Nakagawa *et al.*, 2010). It was shown that Ngn3 positive A_{pr} and A_{al} spermatogonia can fragment by severing intercellular bridges and replenish Gfra1 population (Nakagawa *et al.*, 2007). Even though fragmentation events are more common in regenerating testes, it also naturally happens during stead-state spermatogenesis. Gfra1 expressing cells population was also found to fragment under homeostasis (Hara *et al.*, 2014) (Figure 2). In summary, Gfra1 expressing cells give rise to a transit amplifying Ngn3 positive spermatogonia population which will differentiate further in undisturbed testes. Cells that express both Gfra1 and Ngn3 are not very common (Nakagawa *et al.*, 2010). Considering that Nanos2 shows "broader" expression profile, it is possible that transition from Gfra1 to Ngn3 happens *via* Nanos2 and Ngn3 intermediate population. Indeed, it was discovered that 38% of Ngn3 expressing cells are also Nanos2 positive (Suzuki *et al.*, 2009). Nonetheless, this hypothesis needs further experimental validation. However, in regenerating tissue Ngn3 expressing cells act as potential stem cells by regaining capability of self-renewal and re-initiating spermatogenesis. Eventually potential stem cells defined by Ngn3 expression revert into actual Gfra1 expressing stem cells and restore their population. This model could also explain why Gfra1 expressing cells do not exhibit a robust transplantation activity (Grisanti *et al.*, 2009), yet a fully functional spermatogonial population is restored.

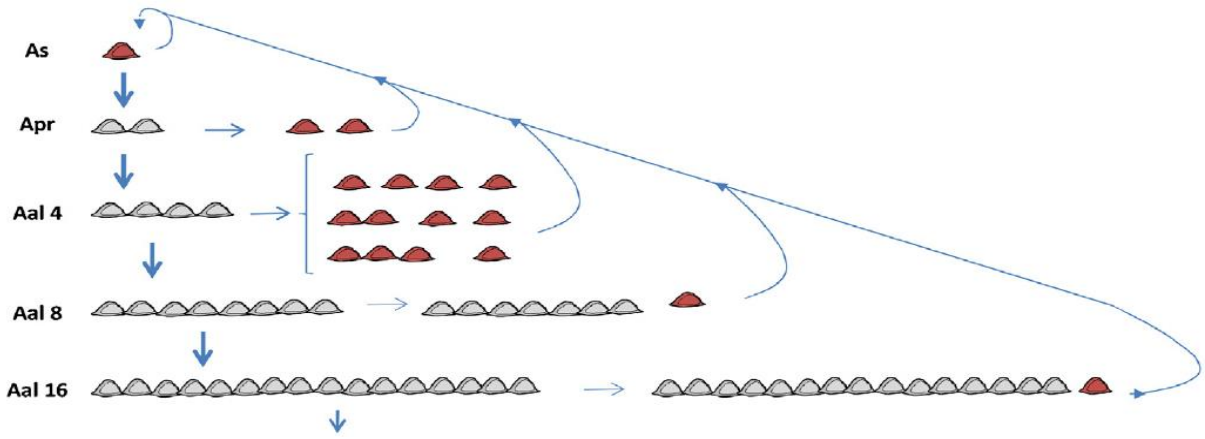

Figure 2. Fragmentation of A_{pr} and A_{al} spermatogonia can replenish an actual stem cell pool. Modified from Boitani *et al.* (2016).

Several other genes were investigated to understand their role in undifferentiated spermatogonia in adult mouse testes. Nanos3 was shown to be expressed in A_s, A_{pr} and A_{al} spermatogonia by 90% overlap with Gfra1 and 99% with Ngn3 (Suzuki *et al.*, 2009). Both Nanos2 and Nanos3 mutant mice are born without a germline (Tsuda *et al.*, 2003). A conditional allele for Nanos3 is not available to evaluate its function in adult spermatogonia, however, it is possible that Nanos3 has a similar role in undifferentiated spermatogonia as does Nanos2. A transcription factor PLZF was identified to be important in germ stem cell maintenance, since absence of PLZF causes gradual loss of germline due to a spermatogonial stem cell depletion (Buaas *et al.*, 2004; Costoya *et al.*, 2004). It was discovered that PLZF is important for keeping spermatogonia in undifferentiated state by opposing function of transcription factor Sall4, which is important for differentiation program induction, and suppressing function of translation promoting complex mTORC1 (Hobbs *et al.*, 2012; Hobbs *et al.*, 2010). Many A_s, A_{pr} and A_{al} spermatogonia were found to be PLZF positive (Buaas *et al.*, 2004). In addition, PLZF expression pattern was found to overlap with Nanos2, Grfa1 and Ngn3 (Nakagawa *et al.*, 2010; Sada *et al.*, 2009). Overall, it can be summarized that PLZF (and probably Nanos3) is a marker of spermatogonial precursor cells (SPCs), whereas Gfra1 and Nanos2 mark an actual stem cell population (SSCs) and Ngn3 – transit amplifying and potential stem cell population in adult mouse testes.

The initial germline stem cell theory explained that only A_s spermatogonia is the actual stem cell. However, as presented here, current experimental evidence points to a model where stem cell activity resides in A_s, A_{pr} and short-chained A_{al} spermatogonia – a population mainly defined by Gfra1 expression. Nonetheless, a couple of genes, namely ID4 and Pax7, have been identified that are expressed almost exclusively in A_s spermatogonia (Aloisio *et al.*, 2014; Oatley *et al.*, 2011a). Both Id4 and Pax7 were shown to make up a subpopulation of Gfra1 positive A_s (Aloisio *et al.*, 2014; Sun *et al.*, 2015). Interestingly, Pax7 was shown to be dispensable for spermatogenesis (Aloisio *et al.*, 2014), while Id4 mutant mice, according to Oatley *et al.*, were subfertile (Oatley *et al.*, 2011a), although an Id4-specific cell ablation rendered mice sterile as shown by Sun an colleagues (Sun *et al.*, 2015). Lineage tracing of Pax7 and Id4 indicate that both cell populations contribute substantially to a testicular homeostasis and regeneration, in addition, Id4 cells show a reconstitutional activity after transplantation (Aloisio *et al.*, 2014; Chan *et al.*, 2014; Sun *et al.*, 2015). More detailed studies are needed to resolve the relationship between Id4, Pax7 and Gfra1 expressing cells to understand the biology of actual stem cells in mouse tetes.

In addition to already mentioned genes, a plethora of other genes have been identified which are implicated in germ stem cell biology. Depending on the focus of the study, some of

the genes where shown to cause spermatogenic impairment due to a stem cell depletion upon loss, eg. Pelo, Rb, Etv5, Foxo1 (Goertz *et al.*, 2011; Hu *et al.*, 2013; Raju *et al.*, 2015; Schlesser *et al.*, 2008), some were found to be expressed in the population of SPCs, eg. LIN28, CDH1 (E-cadherin) (Tokuda *et al.*, 2007; Zheng *et al.*, 2009) or enrich a transplanted population with cells with a stem cell activity, eg. CD9, β1- and α6-integrins (Kanatsu-Shinohara *et al.*, 2004; Shinohara *et al.*, 1999). Even high activity of telomerase reverse transcriptase Tert or production of reactive oxygen species (ROS) are a hallmark of undifferentiated spermatogonia in mouse testes (Morimoto *et al.*, 2013; Pech *et al.*, 2015).

On the other hand, a hallmark of differentiating spermatogonia is considered an expression of c-Kit. c-Kit is a receptor tyrosine kinase (RTK), a ligand of which is expressed by Sertoli cells. C-Kit is expressed on the surface of differentiating A_1-A_4, In and B type spermatogonia (Yoshinaga *et al.*, 1991; Schrans-Stassen *et al.*, 1999), even though its mRNA can be detected in undifferentiated spermatogonia, however, protein is not translated (Busada *et al.*, 2015; Schrans-Stassen *et al.*, 1999). As described before, Gfra1 cells are actual stem cells that give rise to a population of transit amplifying cells, marked by expression of Ngn3. Ngn3 expressing population was found to directly convert into a differentiating c-Kit expressing spermatogonia (Ikami *et al.*, 2015). c-Kit protein translation in Ngn3 expressing cells is initiated by retinoic acid (RA), which is important for spermatogonial differentiation and entry to meiosis (Busada *et al.*, 2015; Ikami *et al.*, 2015). In turn only Ngn3, but not Gfra1 positive cells express a RA receptor Rarγ. Therefore, only Ngn3 cells are primed to differentiate (Ikami *et al.*, 2015). c-Kit expressing cells are considered to be differentiated and do not contain stem cell potential. This notion is supported by the evidence that c-Kit expressing differentiated spermatogonia do not contain reconstitutional activity upon transplantation (Shinohara *et al.*, 2000).

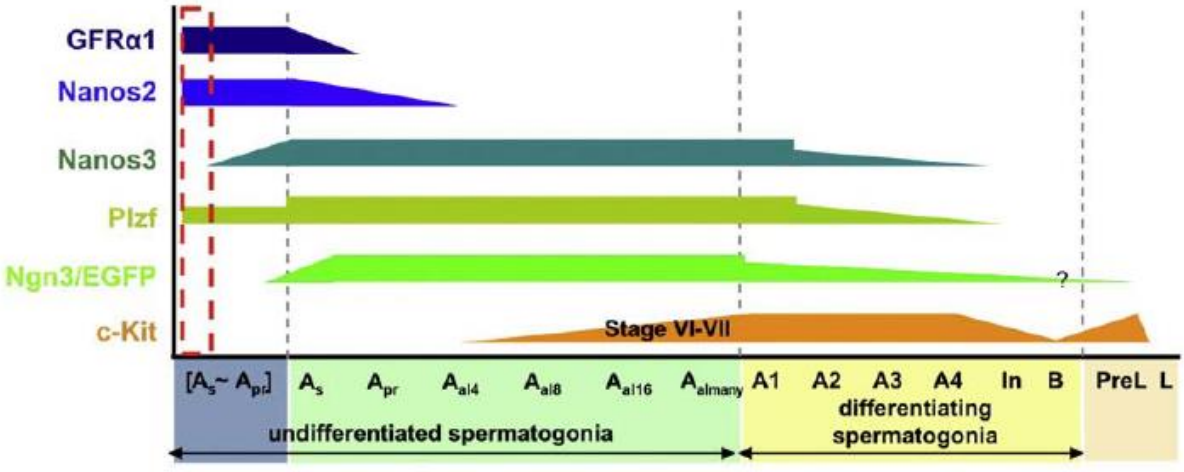

Figure 3. Depiction of expression of GFRa1, Nanos2, Nanos3, PLZF, Ngn3, c-kit in different populations of A-type spermatogonia. Modified from Suzuki *et al.* (2009).

All in all, many genes were found to be expressed in different subpopulations of spermatogonia (Figure 3) and contribute to keeping the balance between self-renewal and differentiation. Spermatogonia were shown to be rather motile and experience fast and stochastic turnover (Klein *et al.*, 2010). I believe that the diversity and heterogeneity of spermatogonial populations in the mouse testes were best described by one of the leading scientists in a field Shosei Yoshida: "…extended and heterogeneous population of cells exhibiting different degrees of self-renewing and differentiating probabilities forms a reversible, flexible, and stochastic stem cell system as a population" (Yoshida, 2012).

EPIGENETIC EVENTS IN DEVELOPING MOUSE GERMLINE

During development embryo experiences two waves of global DNA methylation mark erasure and *de novo* DNA methylation – a process that is collectively called epigenetic reprogramming. First wave of reprogramming occurs in pre-implantation embryo after egg fertilization. Second wave is germline-specific (Lees-Murdock and Walsh, 2008). The germline reprogramming is important to establish a proper parent-of-origin gene expression program and to rest the methylation of transposable elements. Different set of genes – imprinted genes – are methylated depending on their maternal or paternal origin. The outcome of differential gene methylation, and therefore silencing, is a monoallelic gene expression in the offspring of imprinted genes (Lees-Murdock and Walsh, 2008; Sasaki and Matsui, 2008). The caveat of epigenetic reprogramming is a potential transposable element (TE) re-activation due to a DNA methylation loss. The germ line, however, is equipped to deal with TE upregulation and silence them again by establishing new methylation patterns on TE gene promoters. The organism employs small RNA-based defense system coupled with DNA methylation to silence active LINE and LTR type transposons. The former process will be discussed in detail in upcoming chapter.

Dynamics of germline epigenetic reprogramming

DNA is demethylated during primordial germ cell (PGC) migration and proliferation. Removal of DNA methylation marks starts at E8.0. Bulk of DNA methylation is removed by E9.5, DNA become hypomethylated and significantly different than in somatic cells (Seki *et al.*, 2005). However, a substantial amount of DNA methylation at this point is still maintained (Hackett *et al.*, 2013; Hajkova *et al.*, 2002; Lees-Murdock *et al.*, 2003; Li *et al.*, 2004). Interestingly, at the same time, when DNA demethylation is initiated, a repressive mark of dimethylated lysines at position 9 of histone H3 (H3K9me2) is also removed genome-wide.

Almost simultaneously another repressive mark H3K27me3 is upregulated and kept until the phase of *de novo* methylation (Seki *et al.*, 2005). Second wave of demethylation starts at around E12.5 when PGCs reach genital ridges and start forming a gonad. By E14.5 methylation marks are almost completely removed from imprinted genes and transposable elements in male and female germline (Davis *et al.*, 2000; Kafri *et al.*, 1992; Kato *et al.*, 2007; Lane *et al.*, 2003). Therefore, during the phase of epigenetic reprogramming germline experiences changes not only in DNA methylation, but also in chromatin marks. Interestingly, some TEs, especially IAPs (intracisternal A particle), experience only partial DNA demethylation. LINE1 elements are the least resistant to DNA demethylation (Hajkova *et al.*, 2002; Kato *et al.*, 2007; Lees-Murdock *et al.*, 2003). In male germline DNA re-methylation of imprinted genes starts at approximately E14.5-E15.5 and is not finished until a few days after birth (Davis *et al.*, 2000; Li *et al.*, 2004). *De novo* methylation of transposable elements starts at E15.5 at is mostly finished by E17.5 (Lees-Murdock *et al.*, 2003). Methylation at non-promoter and intergenic regions was also addressed. In males DNA methylation dynamics at these regions follows the same trend as the imprinted genes and TEs (Niles *et al.*, 2011). The role of methylation of intergenic, non-promoter regions is not known, however, it is hypothesized that it may be important for gene expression regulation later in adult male germline.

The family of DNA methyltransferases (DNMTs)

Mouse genome encodes five DNMTs: Dnmt1, Dnmt2, Dnmt3a, Dnmt3b, Dnmt3L (Figure 4).

Dnmt1. Dnmt1 is a maintenance methyltransferase, ubiquitously expressed, especially in somatic cells (La Salle *et al.*, 2004). Dnmt1 was shown not to influence *de novo* DNA methylation (Chen *et al.*, 2003; Hsieh, 1999; Lei *et al.*, 1996), while mouse embryonic stem cells (mESCs) deficient of Dnmt11 exhibited lower levels of DNA methylation, which was reduced even to a greater degree upon differentiation (Lei *et al.*, 1996). Dnmt1 expression is also absent in male prospermatogonia undergoing *de novo* DNA methylation (La Salle *et al.*, 2004; Sakai *et al.*, 2001), proving that Dnmt1 is involved only in DNA methylation maintenance in dividing cells. Indeed, Dnmt1 has higher affinity to hemimethylated DNA (Gruenbaum *et al.*, 1982; Okano *et al.*, 1998a) and was found to be associated with a replication fork (Bachman *et al.*, 2001; Leonhardt *et al.*, 1992). Therefore, the main function of this enzyme is to maintain methylation marks on a newly synthesized DNA strand. Mice that are deficient for Dnmt1 were found to die *in utero* (Lei *et al.*, 1996; Li *et al.*, 1992),

showing the importance of maintaining already established methylation patterns in developing embryo.

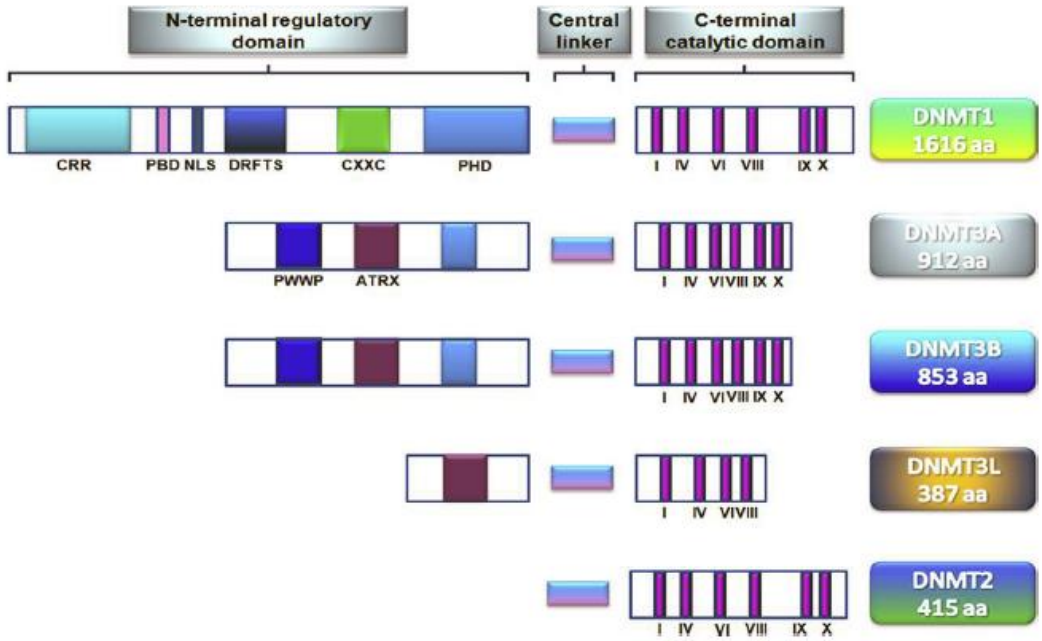

Figure 4. The domain structure comparison of mammalian DNA methyltransferases. Modified from Uysal *et al.* (2015)

Dnmt2. The function of Dnmt2 was puzzling for a while. If compared to full length Dnmt3A or Dnmt3B, it is composed of only C-terminal catalytic domain (Yoder and Bestor, 1998), indicating that the protein still possesses methytransferase activity. Yet it was shown not to contribute to maintenance or *de novo* DNA methylation (Okano *et al.*, 1998b). Dnmt2 was found to be expressed in many mouse tissues (Yoder and Bestor, 1998; Okano *et al.*, 1998b) and later identified as methytrasferase for aspartic acid tRNA (Goll *et al.*, 2006). Therefore, Dnmt2 is the only family member that is not involved in DNA methylation.

Dnmt3a, Dnmt3b and Dnmt3L. Dnmt3a, Dnmt3b and Dnmt3L are involved in *de novo* DNA methylation, where Dnmt3a and Dnmt3b are *de novo* methyltransferases and Dnmt3L is a catalytically inactive co-factor for Dnmt3a and Dnmt3b. Gene coding Dnmt3a produces two transcripts: full length, called Dnmt3a, and truncated one. Truncated version of Dnmt3a, named Dnmt3a2, produces a protein with a shorter N-terminus. Dnmt3a2 expression is initiated from internal promoter, excluding exons 1-6 and introducing exon 7 (Chen *et al.*, 2002). Dnmt3a is expressed at low levels in most of the mouse tissues, while Dnmt3a2 has more restricted expression pattern and is expressed in several tissues, including gonads and mESCs (Chen *et al.*, 2002). Multiple transcripts, coding Dnmt3b, arise from alternative splicing events, involving exons 10, 21, 22. Most of isoforms produced do not have

enzymatic activity due to the absence of crucial motifs present in exons 21 and 22 (Aoki *et al.*, 2001; Chen *et al.*, 2003; Chen *et al.*, 2002; La Salle and Trasler, 2006). Inactive isoforms have different and partially overlapping expression patterns (Chen *et al.*, 2002), however, the function of these truncated, functionally dead proteins is not known. Only a full length protein Dnmt3b and an isoform produced skipping exon 10, named Dnmt3b2, have a characteristic methytrasferase activity (Aoki *et al.*, 2001; Chen *et al.*, 2005b), while both Dnmt3a and Dnmt3a2 were shown to be active (Aoki *et al.*, 2001; Chen *et al.*, 2002; Chen *et al.*, 2005b). Dnmt3a, Dnmt3a2, Dnmt3b and several isoforms of Dnmt3b were found to be expressed in developing embryo male gonad at all stages tested (La Salle *et al.*, 2004; Lees-Murdock *et al.*, 2005). Dnmt3a2 and Dnmt3b2 isoforms were identified as the dominant ones (Lees-Murdock *et al.*, 2005; Sakai *et al.*, 2004), even though Dnmt3b2 expression levels are lower than Dnmt3a2 (La Salle *et al.*, 2004; Sakai *et al.*, 2004). Interestingly, at the protein level Dnmt3a and Dnmt3b production peaked at the stage of DNA *de novo* methylation (Lees-Murdock *et al.*, 2005). Overall, this evidence indicates that Dnmt3a2 and Dnmt3b2 are active methyltransferases, which expression coincide with the phase of epigenetic reprogramming in fetal gonads. Many experiments, however, did not discriminate between different isoforms of Dnmt3a and Dnmt3b, therefore, further on an active methyltransferases irrespective of their isoform will be called Dnmt3a and Dnmt3b, if not stated otherwise.

Dnmt3L coding gene uses tree different promoters, which results in production of full length protein that is expressed in fetal testes, several forms of truncated non-coding transcripts in pachytene spermatocytes and round spermatids, and production of oocyte-specific form of Dnmt3L (O'Doherty *et al.*, 2011; Shovlin *et al.*, 2007). Dnmt3L expression seems to be controlled in a temporal manner. Its transcript was bearly detectable in the fetal testes undergoing DNA demethylation and was highly upregulated during the phase of *de novo* DNA methylation, when Dnmt3a2 and Dnmt3b2 are expressed (La Salle *et al.*, 2004; Sakai *et al.*, 2004). Therefore, it seems that Dnmt3L is the “limiting” factor to start the process of DNA re-methylation.

To note, Dnmt3a, Dnmt3a2, Dnmt3b and several isoforms of Dnmt3b were found to be expressed during spermatogenesis at varying levels depending on the cell type. Nonetheless, expression of Dnmt3’s was detected from A-type spermatogonia to round spermatids (La Salle and Trasler, 2006; Watanabe *et al.*, 2004). According to some studies, the transcript of Dnmt3L after birth was detected only in spermatogonia (Bourc'his and Bestor, 2004; Shovlin *et al.*, 2007), while others detected it also in other type of spermatogenic cells (La Salle *et al.*, 2007). Nonetheless, Dnmt3L postnatal expression commences at very low levels compared to its expression in fetal gonads (La Salle *et al.*,

2004; La Salle *et al.*, 2007). Whether Dnmt3L is expressed at the level of the protein postnatally is also a matter of debate (Liao *et al.*, 2014; Sakai *et al.*, 2004). However, a misregulation of DNMTs in cultured spermatogonia was found to impair their ability to complete spermatogenesis upon transplantation (Takashima *et al.*, 2009), indicated importance of epigenetic events for proper male germ cell development after birth.

Dnmt3L influences on *de novo* DNA methylation

When Dnmt3L was discovered, its sequence and domain structure indicated that Dnmt3L is not an active enzyme. Dnmt3L has shorter C-terminal catalytic domain, missing a few motifs that are present in Dnmt3a and Dnmt3b, additionally, the remaining C-terminal domain does not contain conserved residues required for catalysis and substrate binding (Aapola *et al.*, 2001; Hata *et al.*, 2002), even though it adopts a characteristic fold of methyltransferase domain (Jia *et al.*, 2007). To support this theory, no enzymatic activity of Dnmt3L was ever observed *in vitro* or *in vivo* (Chedin *et al.*, 2002; Chen *et al.*, 2005b; Gowher *et al.*, 2005; Hata *et al.*, 2002). Interestingly, it was shown that Dnmt3a and Dnmt3b, even though possess methyltransferases activity *in vitro* and *in vivo*, it is substantially low (Aoki *et al.*, 2001; Hsieh, 1999). Accumulated evidence – all three Dnmt3 family members were found to be co-expressed in fetal gonads and exhibit similar phenotype upon deletion (discussed later), pointed out that all three proteins may work in concert. Indeed, Dnmt3L was found to directly interact with Dnmt3a and Dnmt3b in *in vitro* assays and *in vivo* (Chen *et al.*, 2005b; Suetake *et al.*, 2004), more importantly, Dnmt3L physically interacted with Dnmt3a2 in fetal testes (Nimura *et al.*, 2006). Additionally, enzymatic activity of Dnmt3a and Dnmt3b increased several fold in the presence of Dnmt3L (Chen *et al.*, 2005b; Gowher *et al.*, 2005; Suetake *et al.*, 2004). It was shown that the affinity to a co-factor S-adenosine L-methionine (SAM), a methyl group donor (Gowher *et al.*, 2005; Kareta *et al.*, 2006), the affinity to a DNA substrate (Gowher *et al.*, 2005) and processivity (Holz-Schietinger and Reich, 2010) was enhanced upon Dnmt3L binding to Dnmt3a or Dnmt3b. Interestingly, the effect of methyltransferases activity stimulation by Dnmt3L is exerted *via* its C-terminal catalytically dead domain, whereas N-terminal domain does not influence substrate methylation (Gowher *et al.*, 2005; Suetake *et al.*, 2004). Dnmt3L with its C-terminal domain interacts with a C-terminal domain of Dnmt3a and Dnmt3b (Chen *et al.*, 2005b; Gowher *et al.*, 2005). It was proposed that this C- to C-domain interaction stabilizes a conformation of a loop present in the active center of *de novo* methyltransferase (Jia *et al.*, 2007). Even though Dnmt3L significantly enhances activity of de novo methyltransferases, it does not seem that this interaction renders any sequence specificity towards DNA substrate. Dnmt3L stimulated

Dnmt3a and Dnmt3b could methylate substrates of various sequence compositions and origins (Chedin *et al.*, 2002; Okano *et al.*, 1998a; Suetake *et al.*, 2004). However, as expected, Dnmt3a and Dnmt3b were found to preferentially methylate cytosine in a CpG context (Aoki *et al.*, 2001).

As noted before, it is not likely that Dnmt3a or Dnmt3b has any sequence preference. Therefore, it is not entirely clear how *de novo* methyltransferases are directed to specific loci in the genome to be methylated. Nonetheless, several features of DNA sequence and chromatin were suggested to play a role in targeting Dnmt3a and Dnmt3b to DNA. Crystal structure of C-terminal domain of Dnmt3L bound to C-terminal domain of Dnmt3a revealed that Dnmt3L and Dnmt3a form a heterotetramer in a ratio 1:1 (Dnmt3L- Dnmt3a- Dnmt3a-Dnmt3L) with two active sites in a complex. According to a modeling of a tetramer bound to a DNA, authors suggested that two cytosines can be methylated simultaneously. In this case both methylated CpG would be separated by one helical turn, which is a distance of about 10 base pairs (Jia *et al.*, 2007). This would suggest that genes or regions targeted for *de novo* methylation could be enriched in CpG nucleotides with periodicity of 10 on average. Indeed, maternally methylated genes were found to contain this signature (Jia *et al.*, 2007). Global analysis revealed that in mouse and human genome CpG sequence has a prevalent periodicity of 8 base pairs, which is especially enriched in a promoter regions of maternally and paternally imprinted genes, LTR and SINE transposable element sequences (Glass *et al.*, 2009). In addition, Chotalia and colleagues implicated that an active transcription through the region to be methylated is crucial to establish DNA methylation marks least at maternally imprinted genes (Chotalia *et al.*, 2009). Moreover, Dnmt3L was shown to interact with all four histones, indicating that Dnmt3L is specifically associated with nucleosomes on DNA. Methylation of lysine 4 in histone H3 abrogated Dnmt3L interaction with nucleosomes (Ooi *et al.*, 2007). Crystallographic analysis confirmed that Dnmt3L particularly binds N-terminal tail of histone H3 when lysine 4 is not methylated (Ooi *et al.*, 2007). In addition, the loss of the N-tail of histone H3 was shown to have a negative impact on DNA methylation (Hu *et al.*, 2009). Therefore, it is possible that a chromatin landscape can also influence *de novo* DNA methylation by marking or creating a permissive environment at certain loci for methylation. It is in agreement with the notion that during the phase of DNA demethylation chromatin experiences extensive remodeling (Seki *et al.*, 2005). To add, Dnmt3a was shown to bind symmetrically methylated arginine of histone H4 (Zhao *et al.*, 2009) and trimethylated lysine 36 on histone H3 (Dhayalan *et al.*, 2010) and methylated DNA upon binding. Furthermore, many transcription factors were found to bind all three Dnmt3's (Hervouet *et al.*, 2009; Pacaud *et al.*, 2014). Even though these studies were not done in a context of *de novo* DNA

methylation in the germline, but rather silencing of specific genes during differentiation, it confirms the importance of chromatin modifications and epigenetic regulation in creating DNA methylation marks.

Significance of DNA methylation in embryo development and germline

The impact of the DNA methylation on embryo and germline development is best seen in Dnmt3a, Dnmt3b and Dnmt3L mutant mice. Dnmt3a deficient animals appeared grossly normal at birth, however, had growth defects and died several weeks later (Okano *et al.*, 1999). Female mutant of Dnmt3a showed deficit in methylation of maternal imprint genes (Hata *et al.*, 2002), which was most likely the cause of perturbed development of these mutant mice. Deletion of *Dnmt3b* resulted in embryonic lethality. Dnmt3b mutant embryos displayed multiple developmental defects and died around mid-gestation. Mice deficient for both methyltransferases resembled a phenotype of Dnmt3b mutant mice. The methylation levels of Dnmt3b and Dnmt3a; Dnmt3b mutant embryos were very similar to the levels of methylation detected at blastocyst stage of wild type embryos. This indicates that Dnmt3b is primarily responsible the first wave of reprogramming occurring after fertilization (Okano *et al.*, 1999). This result is consistent with the Dnmt3b expression pattern. Dnmt3b is a predominant methytransferase expressed at the early stages of embryo development (Okano *et al.*, 1999; Watanabe *et al.*, 2002). To elucidate the importance of Dnmt3a and Dnmt3b in a germline, conditional deletion strategy was employed. Interestingly, Dnmt3b deficient mice, obtained by conditionally ablating Dnmt3b coding gene in fetal testes, appeared normal and were fertile. On the other hand, conditional deletion of *Dnmt3a* gene resulted in male and female sterility (Kaneda *et al.*, 2004). Females though could produce mature oocytes, however, embryos of mutant mothers died before mid-gestation and exhibited gross developmental abnormalities. The impairment of embryo development from Dnmt3a mutant females was associated with failure to establish maternal imprints. All maternally imprinted genes examined were demethylated in the embryos. IAP sequence also showed a decrease in methylation. Males exhibited severe defects in spermatogenesis: very few spermatogonia and no other type of cells were found in the tubules of eleven week-old mice (Kaneda *et al.*, 2004). Mutant spermatogonia were shown to bear unmethylated paternal imprint genes, even though one of them – *Rasgrf1*, retained substantial amount of methylation (Kaneda *et al.*, 2004; Kato *et al.*, 2007). Interestingly, spermatogonia from Dnmt3b conditionally ablated mice also had partial impairment of *Rasgrf1*gene methylation, while other paternal imprinted genes were not affected. To sum up, it appears that Dnmt3a is the main methytransferase required to set maternal and paternal imprints, while some genes may need both Dnmt3a and

Dnmt3b to gain full methylation. The methylation of repetitive elements was also analyzed in Dnmt3a and Dnmt3b conditionally ablated spermatogonia. Methylation analysis indicated SINE B1 elements require Dnmt3a for methylation, whereas major and minor satellite sequences - Dnmt3b. However, LINE1 and IAP TEs are methylated by both *de novo* methyltransferases (Kato *et al.*, 2007). Demethylated minor satellite repeats were also observed in Dnmt3b, but not Dnmt3a mutant mESCs (Okano *et al.*, 1999). Overall, similar results were obtained when studying mESCs deficient of both Dnmt3a and Dnmt3a. Dnmt3a/3b mutant mESCs showed loss of methylation over multiple loci over time, including repeat and imprinted genes (Chen *et al.*, 2003). After introducing *Dnmt3a* or *Dnmt3b* gene in mutant cells the methylation of repeat elements was restored, but Dnmt3b was more efficient in methylating minor satellites, while Dnmt3a in paternal imprint genes (Chen *et al.*, 2003).

Surprisingly, Dnmt3L mutant mice phenotype is similar to Dnmt3a mutant mice phenotype. Dnmt3L deficient females could produce mature oocytes, but embryos of Dnmt3L mutant females did not develop past mid-gestation due to gross developmental defects. The death of the embryos from mutant mothers was attributed to a failure to establish maternal imprints and biallelic expression of maternal imprint genes (Bourc'his *et al.*, 2001; Hata *et al.*, 2002). Interestingly, analysis of several embryos revealed that sometimes a methylation of a maternal imprint gene can happen stochastically and restore monoallelic expression, however, a random methylation of one gene does not save the phenotype of embryos from Dnmt3L mutant mothers (Arnaud *et al.*, 2006). Dnmt3L deficient males were sterile and showed complete loss of germline with time. Spermatogenesis in Dnmt3L deficient animals did not progress beyond pachytene stage. Meiotic cells present in Dnmt3L mutant testes showed abnormal non-homologous and branched asynaptic structures between the chromosomes (Bourc'his and Bestor, 2004; Hata *et al.*, 2006; Webster *et al.*, 2005). Defective cells were eliminated by apoptosis probably due to meiotic check-point activation (Webster *et al.*, 2005). Very few dividing spermatogonia were detected already 3 weeks after birth (Hata *et al.*, 2006). Dnmt3L mutant mice seem to be born with the same number of prospermatogonia as wild type mice, however, the mutant animals may have less actual stem cells, since the defects in germ cell numbers is evident as early as six days after birth (La Salle *et al.*, 2007). Eventually seminiferous tubules of 2-3 month-old mice displayed Sertoli-only phenotype with no germ cells present (Hata *et al.*, 2006). In contrast to the phenotype in females, male sterility was caused by reactivation of transposable elements in meiotic cells. L1 and IAP transcription was elevated (Bourc'his and Bestor, 2004; Hata *et al.*, 2006) due to a loss of DNA methylation at their regulatory regions (Bourc'his and Bestor, 2004; Kato *et al.*, 2007; Webster *et al.*, 2005). Nonetheless, a few paternal imprint genes were also found to be in

hypomethylated state (Bourc'his and Bestor, 2004; Kaneda *et al.*, 2004; Kato *et al.*, 2007; La Salle *et al.*, 2007; Webster *et al.*, 2005), whereas some studies showed that the methylation status of major man minor satellite sequences did not change (Bourc'his and Bestor, 2004), while others implicated Dnmt3L in satellite sequence methylation (Kato *et al.*, 2007). This discrepancy stems from different time point taken into analysis and Dnmt3L is considered to be required for all repeat as well as imprint gene methylation. Furthermore, a global decrease in DNA methylation was also evident in Dnmt3L mutant mice as judged from the methylation analysis of chromosome 4 and X (La Salle *et al.*, 2007). In addition to changes in DNA methylation, changes in chromatin were observed in Dnmt3L deficient animals. Acetylated histone H4, a mark of euchromatin, is usually detected from spermatogonia to preleptotene spermatocytes, whereas in the Dnmt3L mutant mice acetylated histone H4 was also found in leptotene, zygotene and pachytene spermatocytes (Webster *et al.*, 2005). On the other hand, a repressive mark H3K9me2 showed regressed expression pattern. In wild type cells H3K9me2 can be found up to pachytene stage, while in the mutant mice this mark was already lost at the leptotene stage (Webster *et al.*, 2005; Zamudio *et al.*, 2015). Therefore, in Dnmt3L mutant mice during the stages of leptotene to pachytene there is a precocious switch from heterochromatic histone marks to euchromatic ones. It is believed that these changes creates permissive chromatin environment for TE transcription. This hypothesis is corroborated by the fact that even though methylation of TEs is lost during the fetal stages of development, the actual increase in transposon upregulation is not seen before the onset of meiosis (Zamudio *et al.*, 2015). This also holds true not only in Dnmt3L mutants, but also in the other mutants that affect transposon methylation – Miwi2 and Mili (Di Giacomo *et al.*, 2013; Zamudio *et al.*, 2015). In addition to the chromatin changes discussed, an increase in H3K4me3 mark at TE genes in Dnmt3L mutants was observed. This mark of “active” chromatin identifies recombination hot spots during meiosis. Due to an enrichment of H3K4me3 at TE genes, these genomic loci become targets for recombination (Zamudio *et al.*, 2015). Therefore, demethylation of transposable elements not only causes their upregulation, but also results in aberrant synapsis, especially between non-homologous chromosomes due to a repetitive nature of the sequences and leads to meiotic catastrophe. Overall, Dnmt3L is considered to be involved in global *de novo* DNA methylation and is required for silencing transposable elements, imprint establishment and methylation of intergenic and non-promoter regions. Therefore, this places Dnmt3L in the center of all epigenetic events happening in the germline during the phase of *de novo* DNA methylation in embryo.

SMALL RNAs IN MOUSE GERMLINE

Small RNAs are involved in a plethora of biological processes: embryo development, adult stem cell differentiation, genome defense against mobile elements, even memory formation, etc. Small RNAs exert their functions by transcriptional gene silencing (TGS) and post-transcriptional gene silencing (PTGS) mechanisms. By the mode of action, protein binding partners, biogenesis pathways and length and sequence characteristics small RNAs are divided into three groups: microRNAs (miRNAs), endogenous small interfering RNAs (endo-siRNAs) and Piwi-interacting RNAs (piRNAs).

miRNA are generated from a hairpin structure with a terminal loop by processing of RNase III-type proteins – Drosha and Dicer. miRNAs are 21-24nt in size and are bound by Argonaut (Ago) subfamily proteins. Mouse has four Ago proteins – Ago1-4, which bind miRNAs (Kim *et al.*, 2009). By base paring miRNAs guide Ago proteins to their target mRNAs. miRNAs binds at the 3'UTR of their target and base pair *via* the seed sequence (2-7nt at the 5' end of miRNA), while the rest of miRNA usually does not produce perfect complementarity to the target forming bulges. Upon miRNA binding the target mRNA becomes either translationally repressed or is exonucleolotically degraded (Cook and Blelloch, 2013; Kim *et al.*, 2009). Endo-siRNAs biogenesis is Drosha-independent, however, Dicer is important for generating 21-23nt long endo-siRNAs from long dsRNA precursors. In mouse endo-siRNAs are bound by Ago2. In contrast to miRNAs, endo-siRNAs are complementary to their targets along the whole length. Full complementarity with a target results in its cleavage by Ago2 between 10^{th} and 11^{th} nucleotide counting from a 5' end of a bound small RNA (Cook and Blelloch, 2013; Kim *et al.*, 2009). Consistent with this mode of action, in mouse only Ago2 was found to exhibit endonucleolitic slicer activity (Liu *et al.*, 2004).

It has been estimated that approximately one third of human genes are regulated by miRNAs, showing a prevalence of PTGS. While miRNAs are ubiquitously expressed and have a wide range of targets, endo-siRNAs are primarily found in mouse oocytes (Watanabe *et al.*, 2006). The largest source of endo-siRNAs is dsRNAs forming out of transposon transcripts. Therefore, endo-siRNAs evolved to protect female germ lineage from deleterious defects of transposon mobilization (Kim *et al.*, 2009). On the other hand, miRNAs and other miRNA pathway genes like *Dice* or *Drosha* were found to play an important role in PGCs specification and migration, especially by promoting proliferation and survival, as well as orchestrating sex-specific gene expression (Hayashi *et al.*, 2008). In the adult mice miRNA pathway was proven to be indispensable for normal spermatogenesis since loss of *Dicer* or

Drosha results in impaired spermatogenesis and sterility (Papaioannou *et al.*, 2009; Wu *et al.*, 2012). Several different miRNA species or families are involved in meiotic progression and spermiogenesis (reviewed in Cook and Blelloch 2013).

piRNAs make up the third group of small RNAs, identified in a wide range of organisms: human (Aravin *et al.*, 2006; Girard *et al.*, 2006), marsupials (Devor *et al.*, 2008), platypus (Murchison *et al.*, 2008), rooster (Li *et al.*, 2013), rat (Lau *et al.*, 2006), mouse (Grivna *et al.*, 2006a; Watanabe *et al.*, 2006), zebra fish (Chen *et al.*, 2005a), *Drosophila* (Aravin *et al.*, 2003), *Caenorhabditis elegans* (Ruby *et al.*, 2006; Sijen and Plasterk, 2003), planaria (Palakodeti *et al.*, 2008), even *Trypanosoma* (Djikeng *et al.*, 2001) and *Tetrahymena* (Mochizuki *et al.*, 2002). Indeed, piRNAs were shown to be conserved along all animal phyla and found even in sunch organisms like sponges (Grimson *et al.*, 2008). piRNAs were found to be bound by Piwi subfamily of Argonaut proteins, hence named Piwi-interating RNAs. In contrast to miRNAs, which are ubiquitously expressed, piRNAs and Piwi protein expression is germline restricted. piRNAs biogenesis is very distinct from miRNAs: piRNA precursor is a long single stranded RNA, processing is Dicer independent and all piRNAs are 25-32nt long and carry a methylation at their 3' ribose – none of these characteristics are found in other classes of small RNAs (except endo-siRNAs carrying 2'-O-methyl group at their 3' end in flies (Ghildiyal *et al.*, 2008). Functionally, piRNAs evolved to defend the host organism from active mobile element species in the genome. Overall, piRNAs form a specific class of small RNAs with distinct biogenesis and functions in the germline. Our study focused on piRNA and Piwi protein function in male mouse undifferentiated spermatogonial stem cell population. Therefore, piRNA biogenesis and functions will be discussed in detail.

Mouse Piwi proteins

Mouse genome encodes 3 Piwi proteins – Miwi, Mili and Miwi2, each of which has a distinct expression pattern and localization in the cell. Miwi expression starts in primary pachytene spermatocytes and stops when elongating spermatids start forming (Deng and Lin, 2002; Kuramochi-Miyagawa *et al.*, 2001). Mili can be detected in fetal gonads as early as embryonic day 12.5 (E12.5) and the expression lasts until elongating spermatid stage in adult mice (Kuramochi-Miyagawa *et al.*, 2001). Miwi2 protein can be found in fetal gonadocytes (prospermatogonia) at E15.5, while its expression ceases three days after the birth (Aravin *et al.*, 2008).

Mili is a cytoplasmic protein found in granules surrounding nucleus. Usually Mili containing granules are located in a close proximity to mitochondria, in a structure termed intermitochondrial cement (IMC) (Aravin *et al.*, 2009). Mili maintains its perinuclear granular

localization pattern until the stage of round spermatid, when multiple granules "fuse" to form one big granule, called chomatoid body (CB), next to the nucleus (Aravin *et al.*, 2008; Kotaja and Sassone-Corsi, 2007). Miwi also shows a cytoplasmic distribution, which resembles Mili localization. In primary spermatocytes Miwi is organized in a few cytoplasmic foci and later on – in CB (Grivna *et al.*, 2006b). Miwi2 is found both in the cytoplasm and in the nucleus of fetal gonadocytes. In the cytoplasm Miwi2 is localized in perinuclear granules, which are less abundant than Mili positive granules (Aravin *et al.*, 2008). Moreover, Miwi2 containing and Mili containing granules usually reside next to each other or even overlap (Aravin *et al.*, 2009; Shoji *et al.*, 2009). Many piRNA pathway components are found to be distributed in a granular manner around the nucleus and co-localize with Mili, Miwi and/or Miwi2. In electron microscope images these granules look like an electron-dense non-membranous structure around the nucleus, which was named a nuage ("cloud" in French) (Eddy, 1974). Interestingly, Miwi2-containing granules were found to overlap with processing bodies (P-bodies) – a place denoted for RNA metabolism, like mRNA storage or degradation. To note, not all P-bodies in the cell overlap with Miwi2 positive granules. On the other hand, Mili containing granules do not overlap with P-bodies. Therefore, there is an evident compartmentalization of piRNA pathway components (Aravin *et al.*, 2009).

piRNA biogenesis

piRNAs are expressed abundantly in fetal gonadocytes and in postnatal mouse testes. In postnatal mouse testes two populations of piRNAs can be distinguished – pre-pachytene piRNAs and pachytene piRNAs, whose expression switch happens at the pachytene stage of meiosis I (Aravin *et al.*, 2007). As mentioned before, fetal gonadocytes express Mili and Miwi2, while Mili is the only Piwi protein present in the postnatal testes until the pachytene stage when Miwi expression starts. Taken together, obvious differences and diverse requirements exist for the biogenesis of piRNAs during all three noted stages.

piRNA clusters and precursor transcripts

When first piRNAs were discovered, it was assumed that piRNAs were most likely made by Dicer from a dsRNA precursor – in a similar manner to miRNAs and endo-siRNAs (Aravin *et al.*, 2003; Aravin *et al.*, 2001; Djikeng *et al.*, 2001; Kalmykova *et al.*, 2005). However, a few lines of evidence pointed that piRNAs have a very distinct biogenesis pathway. Firstly, when piRNA sequences were mapped to a mouse genome to determine piRNA coding genes, it was noticed that multiple individual piRNAs mapped to a defined set loci, quite often one piRNA not far away from another. In addition to this, piRNAs

exceptionally mapped only to one strand of the locus (single-strand clusters) or, if piRNAs mapped to both strands of the cluster, it was transcribed in a bidirectional non-overlapping manner (double-strand clusters). Secondly, computational prediction and modeling programs did not detect any dsRNA regions or hairpin structures that could potentially form from a piRNA coding cluster transcript (Aravin *et al.*, 2006; Girard *et al.*, 2006; Grivna *et al.*, 2006a; Watanabe *et al.*, 2006). Therefore, these data suggested that piRNA precursor rather is a long, single-stranded RNA, which could not be a suitable substrate for Drosha and Dicer processing. Indeed, piRNA-like long single stranded RNAs were identified which contained transposable element sequences (Ro *et al.*, 2007; Watanabe *et al.*, 2006) and inferred from available expression sequences tags (EST) (Girard *et al.*, 2006). An additional proof that piRNAs are indeed generated in a different pathway than miRNAs and siRNAs came from studies of *Drosophila* piRNA population. Genetic experiments revealed that piRNA production was not hampered in *Dcr-1* and *Dcr-2* (two Dicer genes in flies), *R2D2* and *Loqs* (Dicer co-factors) and *Ago2* mutant flies (Vagin *et al.*, 2006).

Interestingly, it was shown that piRNAs are not well conserved between the species, however, the piRNA coding clusters are. When compared to mouse piRNA clusters, syntenic regions were found in rat and human genomes (Aravin *et al.*, 2006; Girard *et al.*, 2006). In mouse fetal gonadocytes 3399 clusters were identified as producing piRNAs at that developmental stage (Aravin *et al.*, 2008). In postnatal mouse pre-pachytene and pachytene piRNA populations are largely encoded by different loci. Li and colleagues identified 84 pre-pachytene piRNA clusters and 100 pachytene piRNA clusters in mouse genome. Interestingly, 30 piRNA coding clusters were found to give rise to both pre-pachytene and pachytene piRNAs. Furthermore, the expression of some pre-pachytene piRNAs, even though at low levels, was detected also beyond pachytene stage (Li *et al.*, 2013).

RNA Pol II transcribes piRNA clusters, thus piRNA precursor transcript has a poly(A) tail and a 5' cap as most of the cellular mRNAs (Li *et al.*, 2013). So far it is not clear how piRNA precursor is recognized among other mRNAs and fueled into the piRNA biogenesis machinery. A sequence motif recognized by a transcription factor A-Myb was found in a promoter sequence of pachytene, but not pre-pachetene piRNA coding clusters, indicating presence of a developmental control of piRNA expression. Interestingly, A-Myb was found to drive expression not only of piRNA precursors, but also many piRNA pathway genes (Li *et al.*, 2013). In addition, in flies exon 1 of one of the biggest piRNA coding clusters *flam* was found to contain a piRNA trigger sequence (PTS), which fused to a non-coding reporter could drive piRNA production (Homolka *et al.*, 2015). Even though no structural or sequence motifs were identified that could specify PTS, it was proposed that PTS attracts components

of primary piRNA biogenesis machinery (Homolka *et al.*, 2015). It is most likely that similar trigger sequences are also present within mouse piRNA coding clusters which together with transcription factor binding motifs control piRNA expression and possibly directs piRNA precursors to cytoplasmic nuage for further processing. In round spermatids Miwi was shown to interact with testes-specific kinesin Kif17b, which localizes in CB and nucleus providing a possible link for piRNA pathway component shuttling system in and out of the nucleus (Kotaja *et al.*, 2006).

Primary piRNA biogenesis and the *ping-pong* amplification cycle

Most of the knowledge accumulated about piRNA biogenesis pathway is due to an extensive work done using *Drosophila* as a model system. Studies of piRNA pathway in female fly ovaries have elucidated main aspects how piRNAs are produced. Overall, piRNA biogenesis can be divided into two processing events: primary piRNA biogenesis and secondary piRNA biogenesis. Briefly, in flies piRNA precursor is transcribed from a piRNA coding locus as a long single-stranded RNA and transported to the cytoplasm, where primary processing occurs in a perinuclear nuage. A piRNA precursor is sliced into shorter fragments, which are bound by *Drosophila* Piwi and Aubergine (Aub) (Brennecke *et al.*, 2007; Malone *et al.*, 2009), trimmed and methylated at the 3' end (Kawaoka *et al.*, 2011). It is important to note that piRNA precursor contains a lot of repeat derived sequences that are found very commonly in an antisense orientation in regards to transposable elements that piRNAs target (Brennecke *et al.*, 2007). Therefore, primary piRNAs originate from piRNA coding cluster, are often in an antisense orientation and populate Piwi and Aub (Brennecke *et al.*, 2007; Saito *et al.*, 2006; Vagin *et al.*, 2006). It has been noticed that primary piRNAs usually have uridine as their first base (1U). It is postulated that 1U bias results from an affinity of an endonuclease, involved in primary processing, to initiate cleavage events upstream of U. Piwi with bound piRNA is translocated into the nucleus (Malone *et al.*, 2009), while Aub targets a transposon mRNA by complementary pairing with it *via* bound piRNA. Aub is an active slicer, therefore, transposon mRNA is cleaved between 10^{th} and 11^{th} nucleotide counting from a 5' end of bound piRNA (Brennecke *et al.*, 2007; Gunawardane *et al.*, 2007). The cleavage event, firstly, eliminates transposon mRNA and, secondly, a secondary piRNA is generated directly from a cleaved transcript. Secondary piRNA is fed into Ago3. Ago3 bound with secondary sense oriented piRNA can in turn target piRNA precursor transcript to generate more antisense oriented piRNAs (Brennecke *et al.*, 2007; Gunawardane *et al.*, 2007; Li *et al.*, 2009). These cleavage events result in so call *ping-pong* amplification loop, which silence transposons post-transcriptionally by removing their mRNA and expanding the pool of

piRNAs that target them. Due to a nature of a *ping-pong* cycle secondary piRNAs have adenine as 10th nucleotide (10A). Additionally, a pair of piRNAs overlap by 10 nucleotides at their 5' ends - this feature was called a *ping-pong* signature. piRNA biogenesis pathway was found to operate in a similar manner in mouse germs cells, however, there are a few substantial differences.

How primary piRNA biogenesis functions in mice is not well understood. It is proposed that as well as in fruit flies a piRNA containing transcripts are fragmented by endonucleases, loaded into Piwi proteins, trimmed and methylated. There are several genes that are implicated in primary piRNA biogenesis in mice: a putative helicase Mov10L1, putative endonuclease Mael, putative endonuclease MitoPLD, even though mostly these protein functions in piRNA biogenesis were analyzed only in pachytene piRNA production (Castaneda *et al.*, 2014; Watanabe *et al.*, 2011a; Zheng and Wang, 2012; Zheng *et al.*, 2010). The primary processing defines 5' end of the piRNA. In addition, it is quite possible that catalytically competent Piwi proteins themselves are involved in a 5' end formation of piRNA (De Fazio *et al.*, 2011; Reuter *et al.*, 2011). The 3' ends of piRNAs are defined by a 3'-5' trimming event. The evidence that piRNAs are cleaved from a transcript as longer fragments than mature piRNAs and undergo 3'-5' processing came from studies of Tdrkh (Trdr2) mutant mice, where predominant piRNA species are 31-36 nt in length instead of 24-31 nt long (Saxe *et al.*, 2013). After trimming, the 3' end of piRNAs is 2'-O-methylated ensuring piRNA stability and proper function (Lim *et al.*, 2015).

Recently another aspect of primary piRNA biogenesis has been discovered in flies. It was shown that Ago3 cleavage of a target transcript initiates two events: firstly, as expected, a generation of a secondary piRNA bound by Aub and, secondly, a generation of multiple piRNAs in a 5'-3' direction using the 5' cleavage fragment. These piRNAs are made in a phased manner, where generation of 3' end of one piRNA results in a generation of a 5' end of the successive piRNA. Phased piRNAs were found to be fueled mostly into Piwi and possess 1U, a feature of primary piRNAs (Han *et al.*, 2015; Homolka *et al.*, 2015; Mohn *et al.*, 2015). Zucchini (Zuc), an endonuclease involved in primary piRNA pathway in flies, was implicated in generating of these primary piRNAs by cleaving transcript at multiple positions upstream of U (Han *et al.*, 2015; Mohn *et al.*, 2015). Analysis of Mili bound piRNAs in Tdrkh (Trdr2) mutant, where piRNAs are not trimmed after excision from a transcript, showed an existence of phasing in mice (Han *et al.*, 2015; Mohn *et al.*, 2015). Primary production by phasing, also named inchworming, was experimentally validated in a mouse expressing a reporter gene with multiple Mili targeting sites. It was shown that a target slicing by Mili created phased piRNAs that were bound by Mili and Miwi2 (Yang *et al.*, 2016)

(Figure 5). It would be interesting to see whether MitoPLD, a mouse homologue of Zuc, is also involved in this process. Overall, a discovery that piRNAs are produced from a target transcript not only by generating a *ping-pong* pair, but also by utilizing a 5' cleavage fragment (as well as 3' fragment to a certain extent (Homolka *et al.*, 2015) to generate more piRNAs explains the diversity of piRNAs, especially of those that are rare.

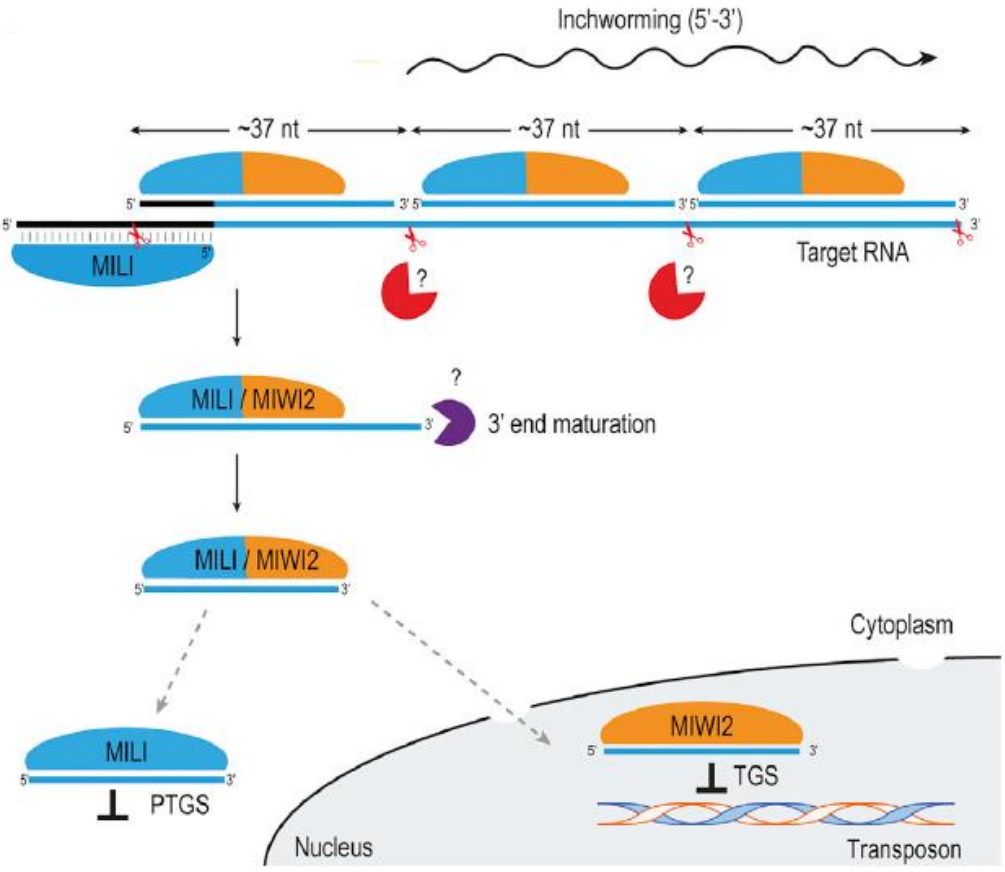

Figure 5. A mechanism of inchworming (phasing) in mouse fetal gonadocytes. Modified from Yang *et al.* (2016).

In mouse a *ping-pong* cycle operates only in fetal gonadocytes where Mili and Miwi2 are expressed. In contrast to a fruit fly, piRNA precursor transcript is not a source for primary processing. In mice transposon mRNA enters a primary processing pathway instead. Transposon mRNA is cleaved and used to derive sense oriented piRNAs which associate with Mili. Mili-piRNA complex targets piRNA precursor transcript and generates secondary antisense oriented piRNA that is bound either by Mili or Miwi2 (Aravin *et al.*, 2008) (Figure 6). Initially it was proposed that both Miwi2 and Mili function in a *ping-pong* amplification loop as slicers (Aravin *et al.*, 2008). Yet it was found that Miwi2 does not contribute to a *ping-pong* cycle (De Fazio *et al.*, 2011) and homotypic Mili:Mili *ping-pong* cycle exsits (De Fazio *et al.*, 2011; Manakov *et al.*, 2015). A finding that is corroborated by the fact Miwi2

does not have a catalytic tetrad required for endonuclease activity of a protein (Nakanishi *et al.*, 2012). In addition to this, a slicer-inactive Mili render a collapse of piRNA production in a *ping-pong* cycle (De Fazio *et al.*, 2011). These data would explain why both Miwi2 and Mili in mouse are highly populated with antisense piRNAs, even though Mili was found to have a bias to bind sense oriented piRNAs, while Miwi2 – antisense piRNAs. In addition to this, Mili and Miwi2 bind piRNAs of different length: Mili was found to bind piRNAs that are 26nt in length on average, while Miwi2 bound piRNAs are ~28nt long (Aravin *et al.*, 2008).

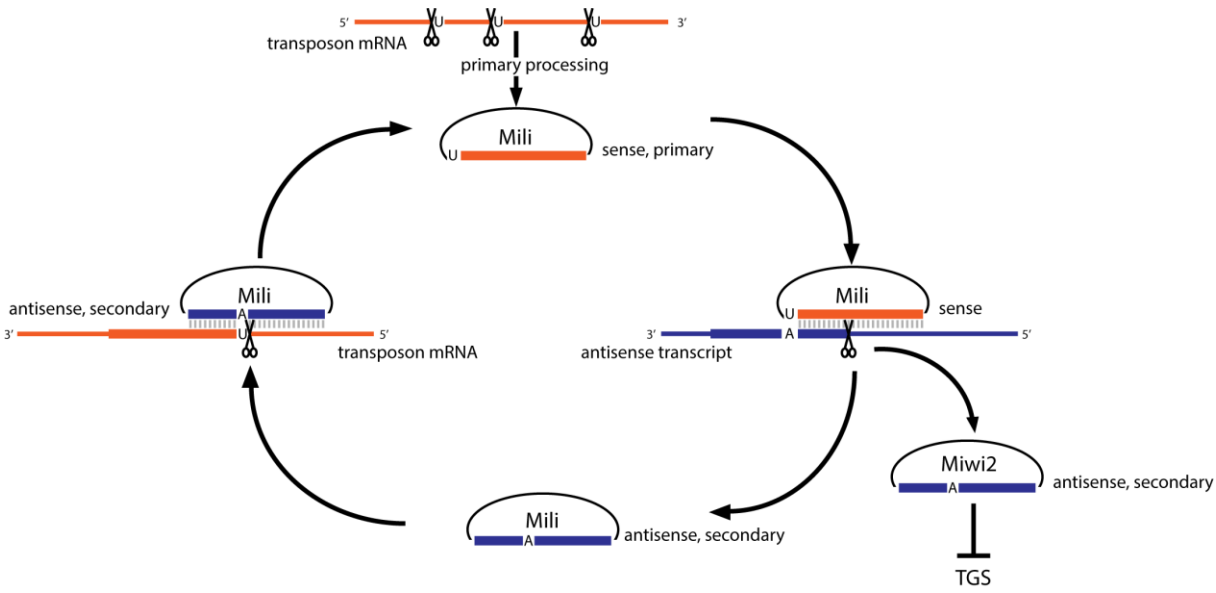

Figure 6. A *ping-pong* cycle in mouse embryonic gonadocytes driven by Mili endonuclease.

In a current piRNA biogenesis model, when Miwi2 is loaded with and antisense piRNA, it is translocated into the nucleus. In the nucleus Miwi2 guides DNA methylation machinery to active TE genes to induce transcriptional silencing by DNA methylation (Aravin *et al.*, 2008) and deposition of a repressive H3K9me3 chromatin mark on most active L1 elements (Pezic *et al.*, 2014). Supporting evidence that Mili initiates generation of secondary piRNAs that results in Miwi2 loading comes from a few observations. Firstly, it was noted that majority of piRNAs were greatly reduced in Mili mutant testes, while Miwi2 deficiency also resulted in downregulation of piRNAs, however, to a lesser degree (Kuramochi-Miyagawa *et al.*, 2008). In addition to this, no piRNAs were found loaded into Miwi2 in the absence of Mili. Moreover, in the absence of Mili, Miwi2 was also found to be re-localized in the cytoplasm (Aravin *et al.*, 2008).

Presently, it is not known how Miwi2 guides DNA methylation of TE sequences in the genome. However, it is clear that piRNA pathway lays upstream of DNR methylation, since a

deletion of Dnmt3L – a co-factor for *de novo* methyltransferases, does not affect piRNA production. Nonetheless, a direct interaction between Miwi2 and Dnmt3L was not found (Aravin *et al.*, 2008). Recently a gene *Morc1*was identified which deficiency phenocopies Mili and Miwi2 mutant phenotype in male mouse testes. In addition to this, Morc1 mutant mice do not show any impairment of piRNA pathway, but LINE1 and IAP TEs were found upregulated. It was shown that Morc1 is responsible for methylation of the regions in the genome that are enriched in TE sequences, but does not impact global DNA methylation like Dnmt3L (Pastor *et al.*, 2014). The data indicates that Morc1 is likely to be involved in transposable element methylation guided by piRNA pathway. It would be interesting to learn whether Morc1 interacts with Miwi2 and/or Dnmt3L.

Mili and Miwi2 are not the only components of piRNA biogenesis pathway in fetal gonadocytes. Many different proteins were shown to co-localize with Mili and/or Miwi2 in perinuclear granules. Mili was found to interact and/or co-localized with a putative helicase MVH (mouse Vasa homologue) (Kuramochi-Miyagawa *et al.*, 2010), Tudor domain containing protein Trdr1 (Vagin *et al.*, 2009), co-chaperone Fkbp6 (Xiol *et al.*, 2012), while Miwi2 – with MVH (Kuramochi-Miyagawa *et al.*, 2010), a putative helicase Mov10L (Vagin *et al.*, 2009), a putative exonuclease Mael (Aravin *et al.*, 2009), Tudor domain containing proteins Trdr2 (Tdrkh) and Trdr9 (Saxe *et al.*, 2013; Shoji *et al.*, 2009; Vagin *et al.*, 2009), an RNA binding protein EXD1 (Yang *et al.*, 2016). Other proteins, whose localization was not specifically associated with Miwi2 or Mili containing granules, but are important for piRNA biogenesis and are found in a nuage are GASZ (Ma *et al.*, 2009), MitoPLD (Watanabe *et al.*, 2011a), HSP90α (Ichiyanagi *et al.*, 2014). All these genes were identified as important players in piRNA biogenesis since the loss of any of them affects primary and/or secondary piRNA processing. For example, mutations in MVH, Mael, Trdr1, Fkbp6, EXD1 result in a great reduction in overall piRNA population, however, the effect is mostly exerted on Miwi2 bound ~28nt piRNAs (Aravin *et al.*, 2009; Yang *et al.*, 2016; Kuramochi-Miyagawa *et al.*, 2010; Vagin *et al.*, 2009; Xiol *et al.*, 2012), implicating these factors in a Miwi2 associated secondary piRNA production and/or Miwi2 loading with piRNAs, as well as stabilizing Miwi2-piRNA complex. Fetal testes deficient of GASZ did not form IMC, in addition to this, Mili was found at a very reduced levels in only 2% of fetal gonadocytes (Ma *et al.*, 2009). This phenotype could potentially eliminate any Mili and therefore Miwi2 associated piRNAs, even though fetal piRNA population was not studied in this mutant. MitoPLD mutant almost absolutely abrogated piRNA population in fetal testes affecting piRNAs derived from transposons and clusters (Watanabe *et al.*, 2011a), indicating that this protein has a prominent role in the initial steps of piRNA biogenesis. Also, in a Mov10L1 mutant neither Mili, nor

Miwi2 were found to be in a piRNA bound state (Zheng *et al.*, 2010). On the other hand, some piRNA pathway mutants – like Trdr9 and HSP90α – have a moderate effect, resulting either in a decrease of antisense piRNAs against specific L1 transposons in case of Trdr9 (Shoji *et al.*, 2009) or overall reduction in piRNA population in HSP90α mutant, yet remaining piRNAs did not show any abnormalities (Ichiyanagi *et al.*, 2014). All these evidence point to a finely ordered and complex, yet still understudied system denoted to defense against transposable elements in the fetal germline.

As mentioned before, after the birth pre-pachytene and pachytene piRNAs are expressed in the male germ cells (Aravin *et al.*, 2007). Pre-pachytene piRNAs are associated with Mili, the only Piwi protein expressed until pachytene stage of germ cell development, while pachytene piRNAs are fueled into both Mili and Miwi. Both Mili and Miwi were shown to possess an endonuclease activity, which is important for their function (De Fazio *et al.*, 2011; Di Giacomo *et al.*, 2013; Reuter *et al.*, 2011). Interestingly, even though Mili and Miwi potentially could be involved in a homotypic or heterotypic *ping-pong* amplification of piRNAs in meiotic cells, no *ping-pong* (Beyret *et al.*, 2012; Di Giacomo *et al.*, 2013; Vourekas *et al.*, 2012) or *ping-pong* signature only in a particular set of piRNAs (eg. targeting LINE1) was found (Goh *et al.*, 2015; Reuter *et al.*, 2011). Indeed, it was shown that secondary piRNA amplification in a *ping-pong* manner is suppressed in meiotic cells (Wasik *et al.*, 2015). Some protein coding mRNAs and lncRNAs that are important for spermatogenesis possess an insertion of a young transposable element. In a piRNA biogenesis factor Rnf17 (Trdr4) mutant mice a *ping-pong* amplification was increased inappropriately targeting aforementioned RNAs (Wasik *et al.*, 2015). In addition, Trdr1 mutant mice also showed abnormal piRNA profile with a substantial increase of cellular mRNAs entering piRNA pathway (Reuter *et al.*, 2009). Thus, in meiotic cells piRNA pathway activity is limited to protect developmentally important RNA species. And hence, the abundance of pre-pachytene and pachytene piRNA population is generated mainly by primary processing of piRNA precursor transcripts. This is corroborated by the fact the most of the pre-pachytene and pachytene piRNAs bound by Mili or Miwi display a 1U bias (Aravin *et al.*, 2006; Aravin *et al.*, 2007; Grivna *et al.*, 2006a; Vourekas *et al.*, 2012). Moreover, Mili and Miwi were found in a complex with large fragments cleaved from a transcript (Nishibu *et al.*, 2012; Vourekas *et al.*, 2012), therefore, it is possible that Mili and Miwi are directly involved in primary biogenesis of piRNAs in meiotic cells.

Many piRNA biogenesis factors were found to localize in IMC and CB in postnatal mouse testes and work in a concert with Mili and Miwi. Some of the piRNA biogenesis factors like GASZ, Mov10L1, Mael, Trdr1, Trdr2 (Tdrkh), Trdr9 are expressed in fetal

gonadocytes, as well as in meiotic cells (Aravin *et al.*, 2009; Chuma *et al.*, 2006; Frost *et al.*, 2010; Ma *et al.*, 2009; Saxe *et al.*, 2013; Shoji *et al.*, 2009; Soper *et al.*, 2008; Vagin *et al.*, 2009; Zheng *et al.*, 2010). However, there are some piRNA pathway components that are specific only to biogenesis and functions of pre-pachytene and pachytene piRNAs, like Rnf17 (Trdr4), Trdr6, Trdr7 (Hosokawa *et al.*, 2007; Pan *et al.*, 2005; Tanaka *et al.*, 2011; Vasileva *et al.*, 2009). Such differences in prenatal and postnatal nuage elements are probably related to different requirements for piRNA biogenesis and functions.

piRNA functions

piRNA pathway evolved to defend the germline against potentially dangerous mobilization of transposable elements (TEs). It has been estimated that 39% of the mouse genome is occupied with active transposable elements and their remnants (Mouse Genome Sequencing *et al.*, 2002). Even though overall transposition events that could cause insertional mutagenesis are rare, newly introduced mutation would be carried to the next generation which is a threat to an individual and species fitness. Moreover, reactivation of TEs is often associated with a loss of fertility in mouse. Almost all up-to-date identified proteins involved in piRNA pathway render male mice sterile if mutated, demonstrating importance of small RNA derived defense against TEs.

As discussed above, all of the three mouse Piwi proteins have distinct expression, localization patterns, as well as a unique role in piRNA biogenesis. Nonetheless, mice deficient of Mili, Miwi or Miwi2 share a lot of common aspects of the mutant phenotype. Miwi2 and Mili deficient mice are sterile due to a meiotic block before the pachytene stage. Appearance of abnormal spermatocytes coincides with the elevated levels of apoptotic cells within the seminiferous tubule (Carmell *et al.*, 2007; Kuramochi-Miyagawa *et al.*, 2004). It is believed that the cell death in meiotic cells is induced by de-repressed TEs. Indeed, LINE1 and IAP transcripts were found in Miwi2 and Mili deficient testes, with IAP showing more modest upregulation in comparison to LINE1 in Miwi2 mutant animals (Aravin *et al.*, 2007; Carmell *et al.*, 2007; Kuramochi-Miyagawa *et al.*, 2008). In line with the evidence that Miwi2 is involved in methylation of TE sequences in the genome, a promoter regions of a specific L1 and IAP elements were found to harbor lower methylation levels in Miwi2 and Mili mutant testes as compared to heterozygous littermates (Kuramochi-Miyagawa *et al.*, 2008). Moreover, it was shown that a decrease in methylation of the respective TEs already happens at the fetal stages (Kuramochi-Miyagawa *et al.*, 2008). More detailed analysis of TE expression in Mili and Miwi2 deficient testes revealed that two families of young and active LINE1 elements (L1-T and L1-Gf) and a family of IAP elements are upregulated in Miwi2

mutant testes (Manakov *et al.*, 2015). Mili also was found to be involved in controlling the expression of aforementioned elements, but in addition to this, 9 more TE families were found to be overexpressed in Mili mutant. DNA methylation analysis yield similar results. Overall, it was concluded that Mili is required for silencing of a bigger group of TE families than Miwi2 (Manakov *et al.*, 2015). Interestingly, piRNA pathway was found to control the methylation of a paternal imprinted gene *Rasgrf1*. A non-coding RNA, which was shown previously to be essential for *Rasgrf1* locus methylation, has a repeat element sequence that is targeted by piRNAs. In the absence of the transcription of *Rasgrf1*-locus related non-coding RNA, DNA methylation does not occur (Watanabe *et al.*, 2011b). These data is in accordance with the model where Miwi2-piRNA complex targets TE transcript in the nucleus and recruit DNA methylation machinery at the site of an active transcription. Indeed, piRNAs that are bound by Mili and Miwi2 in fetal testes are enriched in TE-derived sequences (Aravin *et al.*, 2008; Kuramochi-Miyagawa *et al.*, 2008). Approximately 50% of Mili bound piRNAs are repeat-associated. Most of them are derived from LTR-retrotransposons and LINEs, and less than 10% from SINEs. Similar trend was observed in Miwi2 bound piRNAs (De Fazio *et al.*, 2011).

In postnatal mice pre-pachytene piRNAs, bound by Mili, were found to comprise of mostly unique sequences (84%), while 35% of them correspond to TEs: LTR transposons, LINEs and SINEs. Two largest pre-pachytene piRNA clusters are rich in TE sequences. Since pre-pachytene piRNAs are relatively enriched in transposon sequences, this piRNA population is reminiscent of fetal piRNAs, even though there are less TE-derived piRNAs among pre-pachytene piRNAs and the overall contribution of different TE classes is distinct (Aravin *et al.*, 2007). Nonetheless, it is has been shown that that pre-pachytene piRNAs together with Mili are involved in transposon control (Di Giacomo *et al.*, 2013). Additionally, majority of pre-pachytene piRNAs correspond to genic regions and are in a sense orientation (Aravin *et al.*, 2007). It is not known if these piRNAs have a function.

Pachytene piRNAs are a very diverse group of piRNAs: more than eighty percent of pachytene piRNAs are unique (Aravin *et al.*, 2007), while only approximately 20% of pachytene piRNAs correspond to repetitive elements (Aravin *et al.*, 2006; Reuter *et al.*, 2009). Even though pachytene piRNA population is largely devoid of transposon-derived piRNAs, Miwi-piRNA complex was shown to be important in post-transcriptional transposon silencing in meiotic cells (Goh *et al.*, 2015; Reuter *et al.*, 2011). On the other hand, most of the pachytene piRNAs map only to one position in a genome – a piRNA cluster where it is coded. Therefore, for a long time the function of pachytene piRNAs beyond transposon control was unknown. Recently it was proposed that pachytene piRNAs target cellular mRNAs and

control spermatogenesis process (Goh *et al.*, 2015; Gou *et al.*, 2014; Vourekas *et al.*, 2012; Watanabe *et al.*, 2015; Zhang *et al.*, 2015). Possibly pachytene piRNA targets were not identified for a while due to a fact that the piRNAs do not interact with target mRNA by perfect base-pairing. Maximum of three to four mismatches can occur in nucleotides 12-21 (Gou *et al.*, 2014; Zhang *et al.*, 2015). Pachytene piRNAs and mouse Piwi proteins were implicated is several different aspects of contributing to spermatogenesis. Several research groups identified a couple of hundreds of potential mRNA and lncRNA targets that are thought to be cleaved by Miwi in round spermatids. In wild type mice these genes showed a trend of decreasing expression during a pachytene to round spermatid transition period and, moreover, some of the target mRNAs were found overexpressed in Miwi mutant or catalytically inactive Miwi round spermatids (Goh *et al.*, 2015; Watanabe *et al.*, 2015; Zhang *et al.*, 2015). Interestingly, the target RNA sequence bound by piRNAs was found to contain a repeat element, again associating piRNAs-Piwi to transposon sequence targeting (Watanabe *et al.*, 2015). Furthermore, Miwi was found to interact with deadenilase Caf1 in elongating spermatids and shown induce target mRNA decay. It was estimated that Miwi-piRNA-Caf1 complex could be responsible for elimination approximately 40% of cellular mRNAs at this developmental step (Gou *et al.*, 2014). On the other hand, Miwi was proposed to bind mRNA targets and protect or stabilize them since these mRNAs were found to be downregulated in Miwi deficient post-meiotic spermatogenic cells (Nishibu *et al.*, 2012; Vourekas *et al.*, 2012). It was proposed that the target mRNAs are protected by Miwi and used for translation during later stages of spermatogenesis when transcription is shut. In addition to this, Mili and Miwi were found in a polysome fraction and implicated in a translational control (Grivna *et al.*, 2006b; Unhavaithaya *et al.*, 2009).

As Mili and Miwi2, Miwi deficient animals are also male sterile, however, the arrest occurs at the early round spermatid stage (Deng and Lin, 2002). Since Miwi is implicated in spermiogenesis control, it is likely that the manifested phenotype is caused by misregulated spermiogenesis gene program.

It is interesting to note that most of the piRNA biogenesis pathway mutants nearly perfectly mimic Mili, Miwi2 or Miwi deficiency. MVH, GASZ, Trdr2 (Tdrkh), Trdr9, Mov10L, MitoPLD, Fkbp6, HSP90α, MORC1 male mice are sterile and meiosis is blocked before the pachytene stage. In addition to this, upregulation of LINE1 and/or IAP was also detected in respective mutants (Crackower *et al.*, 2003; Huang *et al.*, 2011; Ichiyanagi *et al.*, 2014; Ma *et al.*, 2009; Pastor *et al.*, 2014; Saxe *et al.*, 2013; Shoji *et al.*, 2009; Tanaka *et al.*, 2000; Watanabe *et al.*, 2011a; Watson *et al.*, 1998; Zheng *et al.*, 2010). On the other hand, a mutant phenotype of some of the piRNA biogenesis components more resembles Miwi

deficiency where spermatogenesis is arrested at the round spermatid stage. Such genes are usually expressed only in postnatal mice like Miwi and include Rnf17 (Trdr4), Trdr5, Trdr6, Trdr7 (Yabuta *et al.*, 2011; Pan *et al.*, 2005; Tanaka *et al.*, 2011; Vasileva *et al.*, 2009).

Piwi proteins and stem cells

The founder of the Piwi family genes is *Drosophila* Piwi protein, which was first discovered as causing male and female sterility in mutant flies (Lin and Spradling, 1997). Soon Piwi homologs were identified in other organisms and silencing a Piwi homolog *prg-1* in *Caenorhabditis elegans* also resulted in germline defects (Cox *et al.*, 1998). Flies deficient of Piwi have very few defectively looking egg chambers and no germline stem cells (GSCs) (Lin and Spradling, 1997). It was determined that in the absence of Piwi all GSCs differentiate without a self-renewing division which causes immediate exhaustion of the stem cells (Cox *et al.*, 1998). However, the defect in the stem cell maintenance is not entirely cell-autonomous. Piwi was found to be expressed in somatic cells and GSCs in the ovary. Deletion of *Piwi* gene in GSCs resulted in slower division rates, while overexpression of Piwi in somatic cells increased GSCs numbers by 4-fold, indicating that somatic cells promote self-renewal divisions of these cells (Cox *et al.*, 2000). In male flies Piwi is important for maintenance of both germline stem cells and somatic stem cells in the testes. Interestingly, in testes Piwi is required for GSCs differentiation (cell-autonomous and non cell-autonomous effect) and self-renewal division of somatic stem cells (Gonzalez *et al.*, 2015). However, when Piwi function in the piRNA pathway was discovered, it was not clear to what extent the sterility caused in flies results from *bona fide* stem cell maintenance phenotype or upregulation of transposable elements in the germline. In fly ovaries Piwi shows nuclear localization (Cox *et al.*, 1998), which is known to be important for its activity in piRNA pathway. Analysis of mutant flies, where Piwi lost its nuclear localization signal, resulted in partial rescue phenotype. The GSCs could self-renew and nearly normal number of egg chambers were produced, however, oogenesis was disturbed due to transposon upregulation (Klenov *et al.*, 2011). Therefore, it is likely that Piwi has two independent roles. On the other hand, nuclear Piwi localization was shown to be important for its functions maintaining male germline (Gonzalez *et al.*, 2015). Nonetheless, Piwi role in the stem cell maintenance in *Drosophila* germline is non-refutable. This is supported by evidence that Piwi proteins have been discovered to be expressed in many organisms, in the stem cells not related to the germline. In most of these cases Piwi is found to be expressed in the somatic stem cells of the low order organisms, which are capable for regeneration, eg. planaria, *Hydra*, sponges (van Wolfswinkel, 2014). In a flat worm planaria Piwi proteins – smedwi-1, smedwi-2, smedwi-3,

are expressed in neoblasts (Palakodeti *et al.*, 2008; Reddien *et al.*, 2005). Neoblasts are adult stem cells that can proliferate and differentiate in any type of cell to replace aged or damaged tissue. Planarian mutants of smedwi-2 and smedwi-3 shown mild defects in neoblast proliferation, but more importantly these stem cells cannot differentiate and replace/regenerate tissue (Palakodeti *et al.*, 2008; Reddien *et al.*, 2005). All in all, accumulated evidence shows that Piwi family proteins are important to maintain germline or somatic stem cells and to assure tissue homeostasis. Whether Piwi proteins have similar role in vertebrates, it is a matter of debate. As discussed earlier, Miwi2 deficient male mice show progressive and complete loss of germ cells over the time (Carmell *et al.*, 2007). The phenotype of total loss of the whole germ lineage is caused by the exhaustion of the stem cell pool. Therefore, it is possible that Miwi2 is involved in the stem cell maintenance. As in the case of *Drosophila* Piwi protein, one may argue that Miwi2 mutant mice lose their germline due to reactivation or transposons. However, spermatogonial stem cells or spermatogonial precursor cells very rarely show upregulation of transposons and mostly piRNA pathway mutants do not affect germ cell maintenance (Di Giacomo *et al.*, 2013; Di Giacomo *et al.*, 2014; Frost *et al.*, 2010; Shoji *et al.*, 2009). It has been established that in piRNA or DNA methylation pathway mutants transposon expression commences during the onset of meiosis (Zamudio *et al.*, 2015). Additionally, spermatogonial precursor cells do not rely only on DNA methylation to repress transposable elements (Di Giacomo *et al.*, 2013). Thus, it is likely that Miwi2 is involved in a germline maintenance since the depletion of the stem cells in the mutant cannot be explained to be caused by transposon de-repression *per se*. There is conflicting evidence whether Mili mutant mice have stem cell deficit or not (Kuramochi-Miyagawa *et al.*, 2004; Unhavaithaya *et al.*, 2009), therefore, more detail characterization and analysis of Mili mutant mice regarding the rate of germ line exhaustion is needed. Whether Miwi2 and/or Mili function in germ line stem cells in mice are dependent on their role in a piRNA pathway, currently it is also not clear. Overall, Piwi proteins have been implicated in germ and somatic stem cell maintenance in numerous organisms like flies, sponges or flat worms. In vertebrates Piwi proteins are mostly expressed in the germline. Whether they have similar roles in defining stem cell functions as in other animals, is an open question.

MATERIALS AND METHODS

Mouse strains

Mili^{Null} (*Mili*$^{-}$) allele is described in Di Giacomo *et al*. (2013).

Mouse harboring *R26*^{ERT2Cre} allele was obtained from Jackson laboratory as a line B6;129 gt(ROSA)26Sortm1(cre/Esr1)Nat/J.

Dnmt3L^{V5} allele was generated using Crisp/Cas9 genome editing technology, where sgRNA, targeting ATG, and oligonucleotide containing 60bp 3' and 5' homology arms, BamHI restriction site and V5 sequence were injected into two-cell stage embryos. Mice were screen by digesting PCR products, amplified by using primers flanking ATG, with BamHI.

Dnmt3L$^{V5\text{-}Myc\text{-}Precission\text{-}Hisx6\text{-}mKO2}$ (*Dnmt3L*^{mKO2}) allele was generated using Crisp/Cas9 genome editing technology, where sgRNA, targeting ATG, and purified DNR fragment containing 709bp 5' and 239bp 3' homology arms and V5-Myc-Precission-Hisx6-mKO2 sequence were injected into two-cell stage embryos. Mice were screen by PCR, amplifying fragments at 3' and 5' insertion site with primers that are outside homology arm and specific to V5 and mKO2 sequences respectively.

For generation of *Dnmt3L*^{Null} (*Dnmt3L*$^{-}$) allele a targeting vector was prepared by Ph. Hublitz from Gene Expression Facility in EMBL Monterotondo. A targeting vector contained exons 1-7, where exon 2 was flanked with *LoxP* sites: one *LoxP* site was inserted 5' of exon 2 and *frt* flanked neomycin resistance cassette with a second *LoxP* site was inserted 3' of exon 2. Targeting vector was linearized using restriction endonuclease NruI (NEB R0192) and used to electroporate A9 mouse embryonic stem cells (mESCs). mESCs that have recombined with electroporated construct were resistant to neomycin treatment, therefore, allowed a successful selection and expansion of 96 clones. DNA extracted from individually mESC-derived clones was digested with BamHI (NEB R0136) and used for screening by Southern blot. A selected probe hybridized to 3' part of intron 7-8, exon 8 and part of intron 8-9 outside the homology arm. A probe was amplified using following primers: Dnmt3l 3' probe Fw 5'ACCAGCATGCATCCTCTTGT; Dnmt3l 3' probe Rv 5'TTCCTCAACAGCAGTCTTCC. In a Southern blot a 8,9kb DNA fragment corresponded to a WT *Dnmt3L* locus. An integration of neomycin resistance cassette with a *loxP* site introduced an additional BamHI site, thus targeted *Dnmt3L* locus corresponded to 6,1kb. A positive mESCs clone, containing recombined *Dnmt3L* locus as identified by Southern blot, was used to prepare cells for injection to mouse embryos at blastocyst stage. Born transgenic animals were screened by Southern blot and mice that were identified by Southern blot and confirmed by PCR genotyping as having targeted *Dnmt3L* locus were cross with mouse line harboring

ubiquitously expressed Deleter-Cre recombinase. A Cre-mediated recombination and excision of exon 2 together with neomycin resistance cassette resulted in a 4,2kb DNA fragment in Southern blots, which corresponds to a *Dnmt3L*^{Null} allele. A Southern blot and PCR genotyping were used to confirm the removal of neomycin resistance cassette together with exon 2. Mice harboring *Dnmt3L*^{Null} allele were used as founders and crossed to C57B1/6N mouse strain before intercrossing heterozygous Dnmt3L$^{Null/+}$ mice to obtain homozygous Dnmt3L deficient animals.

Miwi2^{HA} allele was generated using Crisp/Cas9 genome editing technology, where sgRNA, targeting ATG, and oligonucleotide containing 60bp 3' and 5' homology arms, BamHI restriction site and HA sequence were injected into two-cell stage embryos. Mice were screen by digesting PCR products, amplified by using primers flanking ATG, with BamHI.

Miwi2^{Null} (*Miwi2*$^{-}$) and *Miwi2*^{FL} alleles are described in De Fazio *et al*. (2011).

Miwi2^{Tom} allele is described in Carrieri *et al*., in submission.

Administration of tamoxifen and busulfan

A 10mg/ml tamoxifen (Sigma T5648) solution was prepared in a corn oil (Sigma C8267), leaving tamoxifen to dissolve fully in pre-heated oil at 37^{o}C shaking in a light-protected tube and filtered with 0,22 μm filter. Tamoxifen was administered by intraperitoneal injection in a dose of 75mg/kg every second day until a total of 5 injections per animal were reached.

A 8mg/ml busulfan (Sigma B2635) solution was prepared in pre-heated DMSO (Sigma D2650) to fully dissolve busulfan powder and then diluted 1:1 with PBS to obtain 4mg/ml working solution. Busulfan was administered by a singular intraperitoneal injection in a dose of 10mg/kg.

Germ cell isolation

Adult mouse germ cell isolation

Isolated mouse testes were dealbulginated and digested with collagenase (0,5 mg/ml, Sigma C7657) at 32^{o}C for 10 minutes shaking in 25 ml of DMEM media (Life technologies 41965) supplemented with Pen/Strep (Life technologies 15140), NEAA (Life technologies 11140), sodium pyruvate (Life technologies 11360) and sodium lactate (Sigma L4263) (DMEM+). After digestion seminiferous tubules were left to sediment by gravity and washed with DMEM+. Single cell suspension was prepared by further digesting seminiferous tubules in 5 ml of 0,05% trypsin (Life technologies 25300) at 32^{o}C for 10 minutes shaking. After

digestion trypsin was neutralized by adding 1 ml of FCS (PAN Biotech 3306P131004) and DNase (Sigma DN-25) added to 0,05 mg/ml of final concentration. Cells were spun and resuspended in PBS with 3% FCS. For FACS sorting and analysis germ cells were stained with following antibodies: c-Kit 1:800 (eBioscience 25-1171), CD45-biotin 1:400 (eBioscience 13-0451), CD51-biotin (Biolegend 104104), streptavidin-qDot 1:50 (eBioscience 93-4317), CD9 1:50 (eBioscience 11-009) in PBS with 3% of FCS (PAN Biotech 3306P131004) and 0,01% sodium azide (Sigma 71290). SYTOX blue (Life technologies 934857) was used as a living dye. Cells were sorted/analyzed with an 85 μm nozzle using a FACSAria II SORP (BD Biosciences).

Juvenile mouse germ cell isolation

Isolated mouse testes were dealbulginated and digested with collagenase (0,5 mg/ml, Sigma C7657) at 32^{o}C for 10 minutes shaking in 1ml of DMEM+ media. After digestion seminiferous tubules were collected by centrifugation at 1000 rpm for 5 min. Single cell suspension was prepared by further digesting seminiferous tubules in 1 ml of 0,05% trypsin (Life technologies 25300) and DNase (Sigma DN-25), added to 0,05 mg/ml of final concentration, at 32^{o}C for 8-10 minutes shaking. After digestion trypsin was neutralized by adding 100 μl of FCS. Cells were spun and resuspended in PBS with 3% FCS. For FACS sorting and analysis germ cells were stained with following antibodies: c-Kit 1:800 (eBioscience 25-1171), CD45-biotin 1:400 (eBioscience 13-0451), CD51-biotin (Biolegend 104104), streptavidin-qDot 1:50 (eBioscience 93-4317), CD9 1:50 (eBioscience 11-009) in PBS with 3% of FCS and 0,01% sodium azide. SYTOX blue (Life technologies 934857) was used as a living dye. Cells were sorted/analyzed with an 85μm nozzle using a FACSAria II SORP (BD Biosciences).

Isolation of E16.5 fetal gonadocytes

Isolated fetal testes were placed in a drop of DMEM+ media and gently torn apart to reached more relaxed tissue structure. Further fetal testes were digested in 0,5 ml of 0,25% trypsin (Life technologies 25200056) at 37^{o}C for 8-10 minutes shaking. Trypsin was neutralized with 100 μl of FCS. 10 μl of DNase (dissolved in HBSS) was also added to the media. Cells were collected by centrifugation at 2000 rpm 10 minutes room temperature. After centrifuging cells were resuspended in 100 μl of PBS with 3% of FCS and further cell dissociation was reached by pipetting. Prepared single cell suspension was used for FACS sorting with an 85μm nozzle using a FACSAria II SORP (BD Biosciences). SYTOX blue (Life technologies 934857) was used as a living dye.

While sorting adult and juvenile mice germ cells 10^6 cells' fluorescent activity was recorded. For fetal germ cells 10^5 cells' fluorescent activity was recorded. Recorded

fluorescent events were analyzed using FlowJo program. Adult and juvenile target population was analyzed by excluding cell doublets and $CD45^{pos}$ and $CD51^{pos}$ cells by initially choosing to analyze cells with low side scatter and negative for live cell dye Sytox Blue. Among $CD45^{neg}$ and $CD51^{neg}$ cells, a target population was identified as c-Kit^{neg} and having a live fluorescence of tdTomato (Miwi2-Tom^{pos}) or mKO2 fluorescent proteins (Dnmt3L-$mKO2^{pos}$). Fetal germ cell population was analyzed as having low side scatter and negative for live cell dye Sytox Blue. After excluding cell doublets from analysis, germ cells were identified as showing a live fluorescence of tdTomato (Miwi2-Tom^{pos}) or mKO2 fluorescent proteins (Dnmt3L-$mKO2^{pos}$).

Whole mount immunofluorescence on seminiferous tubules

Isolated mouse testes were dealbulginated and digested at 32^{o}C for 8 minutes shaking in DMEM+ medium (look Materials and Methods, Germ cell isolation) with 0,5 mg/ml collagenase (Sigma C7657) if the testicular weight was normal (≥70mg for an adult mouse) or with 1 mg/ml collagenase if testicular weight was compromised. After digestion seminiferous tubules were left to sediment by gravity and washed with PBS. Tubules were fixed in 4% paraformaldehyde (Sigma P6148) at 4^{o}C for 4 hours. After fixation a few tubules were separated for subsequent steps of immunofluorescence. Tubules were permeabilized and block at the same time in 0.5% Triton-X100 (Sigma T8787), 5% normal donkey serum (Sigma D9663), 1% BSA (Sigma A2153) and 0.1M glycine (Sigma G8898) for 3 hours at room temperature. Primary antibody incubation was done overnight at 4^{o}C or at room temperature in 1% BSA (Sigma A2153) in PBS.

Primary antibody	Dilution
Rabbit monoclonal anti-HA (Cell Signaling 3724)	1:200
Mouse monoclonal anti-V5 (Invitrogen R960-25)	1:100
Rabbit polyclonal anti-PLZF (Santa Cruz Biotechnology sc-22839)	1:100
Mouse monoclonal anti-PLZF (Santa Cruz Biotechnology sc-28319)	1:100
Goat anti-GFRa1 (Neuromics GT15004)	1:50
Goat anti-GFRa1 (R&D Systems AF560)	1:100
Goat anti-c-Kit antibody (R&D Systems AF1356)	1:250

Appropriate donkey anti-mouse AlexaFluor488, donkey anti-rabbit AlexaFluor488, donkey anti-goat AlexaFluor488, donkey anti-rabbit AlexaFluor546, donkey anti-mouse AlexaFluor546 and donkey anti-goat AlexaFluor546 secondary antibodies (Life technologies

A21202, A21206, A11055, A10036, A10036, A11056) were used in a dilution 1:1000 and incubated 1 hour at room temperature in PBS with 1% BSA (Sigma A2153) and 0,1% Triton X-100 (Sigma T8787). DAPI (5 μg/μl) (Life technologies D1306) was used to stain DNA. Samples were mounted with ProLong Gold antifade reagent (Life technologies P36930). Leica TCS SP5 and SP8 confocal microscopes were used to acquire images. After acquisition images were processed with ImageJ and Adobe Photoshop CS5 computer programs. All images corresponding to the same experiment were acquired and processed afterwards applying the same settings.

Immunofluorescence

For immunofluorescence mouse testes were freshly embedded into OCT compound (SAKURA 4583), 8 μm sections were cut, fixed in 4% paraformaldehyde (Sigma P6148) 10 minutes at room temperature and then permeabilized for 10 minutes at room temperature in 0.1% Triton-X100 (Sigma T8787). Subsequently sections were blocked for 30 minutes at room temperature in 10% normal donkey serum (Sigma D9663), 1% BSA (Sigma A2153) and 0.1M glycine (Sigma G8898). Primary antibody incubation was done overnight at 4^{o}C in the blocking buffer.

Primary antibody	Dilution
Mouse monoclonal anti-Mili (R. Pillai)	1:200
Rabbit polyclonal anti-Miwi2 (De Fazio *et al.*, 2011)	1:200
Rabbit monoclonal anti-HA (Cell Signaling 3724)	1:500
Mouse monoclonal anti-V5 (Invitrogen R960-25)	1:200
Rabbit L1 ORF1 (Di Giacomo *et al.*, 2014)	1:500
Rabbit anti-IAP Gag (B. Cullen)	1:500
Rabbit polyclonal anti-gammaH2AX antibody (Bethyl Laboratories IHC-00059)	1:500
Mouse monoclonal anti-gammaH2AX antibody (Abcam ab26350)	1:500
Mouse monoclonal anti-PLZF antibody (Calbiochem OP128)	1:100

Appropriate donkey anti-mouse AlexaFluor488, donkey anti-rabbit AlexaFluor488 and donkey anti-rabbit AlexaFluor546 secondary antibodies (Life technologies A21202, A21206, A10036) were used in a dilution 1:1000. DAPI (5 μg/μl) (Life technologies D1306) was used to stain DNA. Samples were mounted with ProLong Gold antifade reagent (Life technologies P36930). Leica TCS SP5 and SP8 confocal microscopes were used to acquire

images. After acquisition images were processed with ImageJ and Adobe Photoshop CS5 computer programs. All images corresponding to the same experiment were acquired and processed afterwards applying the same settings.

Histology

Testes were fixed in Bouin's fixative (Sigma HT10132) overnight at 4^{o}C and paraffin embedded by dehydrating tissue with an increasing concentration of ethanol (70%, 85%, 95%, 100%) (Sigma 02860) and xylene (Sigma 247642). All testes sections were prepared of 8 μm thickness. Sections then were stained with hematoxylin and eosin by routine methods.

Southern blot

Phenol-chloroform (Sigma 77617) extracted DNA was digested overnight in a solution containing restriction endonuclease (NEB), restriction endonuclease buffer (NEB), 100μg/ml BSA (NEB), 1mM DTT (Sigma 43815), 1mM spermidine (Sigma S2626), 50μg/ml RNase A (Sigma R5250) at temperature suggested by restriction enzyme manufacturer. Digested DNA was resolved on a 0,7% agarose gel in 1x TAE until sufficient resolution of bands of interest was achieved. Then gel was equilibrated and DNA denatured in an alkaline solution (0.4M NaOH (Sigma 30620), 1.5M NaCl (Sigma 31434)) 2x 20min. Blotting was done overnight at room temperature by capillary action in alkaline solution on Hybond™-N+ Nylon Membrane (GE Healthcare Life Sciences RPN203B). After the transfer, the membrane was equilibrated in 2x SSC solution (0.3M NaCl (Sigma 31434), 30mM $Na_3C_6H_5O_7$ (sodium citrate) (Sigma 25116) until pH 7 was reached, air-dried and UV-crosslinked at 254nm, 150mJ/cm^2. Membrane was pre-hybridized for 2 hours at 65^{o}C in hybridization solution (0.5M phosphate buffer pH 7.2 (Na_2HPO_4-ortophosphoric acid) (MERK K32203480; Sigma W290017), 1mM EDTA (AppliChem A1103), 3% BSA (Sigma A2153), 5% SDS (Sigma L4509)) and then incubated with gel-purified, alfa-^{32}P-dCTP labeled, denatured ssDNA probe overnight at 65^{o}C. After extensive washing (40mM phosphate buffer pH 7.2, 1mM EDTA, 5% SDS), membrane was exposed to phosphorimager screen for 1-3 days and read with Fluorescent Image Analysis System FLA-5100 (Fujifilm).

RT-qPCR

Sorted cells where lyzed in 1ml of QIAzol lysis reagent (QIAGEN 79306) and RNA extracted using manufacturer provided protocol. Extracted RNA was disolved in 12μl of DEPC-treated H_2O. 1μl of total RNA was run on Bioanalyzer Pico chip (Agilent

Technologies 5067-1513). RNA that had RIN ≥7.5 was used for reverse transcription (RT) reaction.

Reverse transcription was done using SuperScript II first-strand cDNA synthesis system with random primers (Invitrogen 18064) according to manufacturer‘s recommendations with an 5-10ng of RNA as an input.

0,5µl of reverse transcription reaction was used per one qPCR reaction. qPCR was done using 2x SYBR green I master (Roch 04707516001) in biological and technical triplicates and run on a LightCycler 480 (Roche). An expression level of a target transcrip was normalized to the expression level of GAPDH gene using $2^{-\Delta\Delta Ct}$ method.

PCR program:

Step	Temperature	Time	Cycles
Denaturation	95°C	300s	1x
Denaturation	95°C	10s	45x
Annealing	60°C	15s	
Elongation	72°C	10s	
Denaturation	95°C	5s	1x
Annealing	65°C	60s	1x
Denaturation	95°C	N/A	Continuous
Cooling	40°C	10s	1x

Primers:

GAPDH_Fw	5’ TGTCGTGGAGTCTACTGGTG	126bp
GAPDH_Rv	5’ TTCACACCCATCACAAACAT	
qPCR_Miwi2_Ex11_Fw	5’CTTTCTGAGCTGTCTGAGGAGAG	79bp
qPCR_Miwi2_Ex13_Rv	5’CTCGTCCACTTTTATGATTTTGG	
qPCR_Miwi2_Ex16_Fw	5’AGCGGCTGATATTGCAGATT	287bp or 133bp*
qPCR_Miwi2_Ex18_Rv	5’GCTTCAAGGCATTGTCATCA	

*287bp fragment is amplified in the presence of floxed exon 17. 133bp fragment is amplified in the absence of exon 17.

*On the gel fragments appear by ~100bp higher.

Bisulfite conversion

Whole genome bisulfite sequencing libraries were generated using a post-bisulfite adaptor tagging (PBAT) method as previously described (Miura and Ito, 2015) using 10

cycles of PCR amplification. Three biological replicates were generated per genotype and libraries sequenced using Illumina HiSeq 2000.

Bisulfite sequencing analysis

Bisulfite analysis was performed by R. Barrens (Babraham Institute, Cambridge) as follows. Raw sequence reads were trimmed to remove both poor quality calls and adapters using Trim Galore (v0.4.1, www.bioinformatics.babraham.ac.uk/projects/trim_galore/, Cutadapt version 1.8.1, parameters: --paired). Trimmed reads were aligned to the mouse genome in paired-end mode to be able to use overlapping parts of the reads only once. Alignments were carried out with Bismark v0.14.4 (Krueger and Andrews, 2011) with the following set of parameters: paired-end mode: --pbat.

Reads were then deduplicated with deduplicate_bismark selecting a random alignment for position that was covered more than once. CpG methylation calls were extracted from the deduplicated mapping output ignoring the first 6bp of each read to reduce the methylation bias typically observed in PBAT libraries using the Bismark methylation extractor (v0.14.4) with the following parameters: a) paired-end mode: --ignore 6 --ignore_r2 6; b) single-end mode: --ignore 6.

50 adjacent CpG running window probes were generated and percentage of methylation determined for probes containing at least 5 reads and 3 CpG on the pooled replicate data. For analysis of specific genome features these were defined as follows: Gene bodies (probes overlapping genes), Promoters (probes overlapping 2000bp upstream of genes), CGI promoters (promoters containing or within a CGI), non-CGI promoters (all other promoters). For repetitive elements, Bismark (v0.14.4, using Bowtie 2, default parameters) was used to map all reads from each data set against consensus sequences constructed from Repbase (Jurka *et al.*, 2005). The methylation level was expressed as the mean of individual CG sites. Graphing and statistics were performed using Seqmonk and RStudio.

Repeat analysis

Bisulfite analysis was performed by R. Barrens (Babraham Institute, Cambridge) as follows.

The analysis of repetitive genomic regions in our data was performed by a dual approach. For unique mapping in the genome we excluded any repeats overlapping Gene bodies (probes overlapping genes). For multimapping we used consensus sequence mapping. Annotations for LINE, SINE, ERV1, ERVK and ERVL elements, specified by RepeatMasker were downloaded from the UCSC website and concatenated into repeat class pseudo-genomes

with individual repeat instances padded by 'NNNNN' to prevent reads from aligning over artificially created boundaries. Alignments were performed using Bismark (v0.14.4, using Bowtie 2, default parameters). Graphing and statistics was performed using Seqmonk and RStudio.

Small RNA library generation

Isolated E16.5 fetal testes were homogenized in 1 ml of Qiazol (QIAGEN 79306). Extracted total fetal RNA was used to generate small RNA libraries using NEBNext Multiplex Small RNA Library Prep Set for Illumina (Set 1) (NEB E7300) following manufacturer's instructions with 20 cycles of PCR amplification.

Microarray gene expression analysis

Microarray data was normalized using the Robust Multi-array Average (RMA) expression measure. The linear model was then used to fit the data with the R package, limma. limma powers differential expression analyses for RNA-sequencing and microarray studies (Ritchie *et al.*, 2015). Transcripts with >2 fold, significant ($p<0.05$) expression change were highlighted.

Microarray gene expression analysis was done by M. Morgan.

Small RNA library analysis

Small RNA sequencing analysis was performed by D. Vistios (EMBL-EBI, Cambridge).

RNA-seq analysis

RNA-seq analysis was performed by A. Enright (EMBL-EBI, Cambridge).

Mouse line genotyping

Mili-Null

Genotyping primers:

Mili_Geno_Fw	5'GATTGAACCTTGTGCCTCGTA
Mili_Geno3	5'GCAGGTGTGTGCAACCAGATA
Mili_Geno_Rv	5'GGTTACATGAGACCCTCAAAGG

PCR program:

Step	Temperature	Time	Cycles
Denaturation	94°C	180s	1x
Denaturation	94°C	30s	32x
Annealing	58°C	30s	
Elongation	72°C	30s	
Elongation	72°C	120s	1x
Hold	4°C	Forever	N/A

Expected PCR fragment sizes:

WT – 153bp

$Mili^{Null}$ – 195bp

Miwi2-Null-Flox

Genotyping primers:

Miwi2-KO_Fw2	5'ACTCCATCCCATCTGTGAGAA
Miwi2-LF_Rv	5'TTCCCACCTCTGTACCAGGA
Miwi2-LF_Fw	5'CAGGCAGTGCAGATCTGTTTC

PCR program:

Step	Temperature	Time	Cycles
Denaturation	94°C	180s	1x
Denaturation	94°C	30s	34x
Annealing	56,2°C	30s	
Elongation	72°C	30s	
Elongation	72°C	120s	1x
Hold	4°C	Forever	N/A

Expected PCR fragment sizes:

WT – 111bp

$Miwi2^{Flox}$ – 242bp

$Miwi2^{Null}$ – 280bp

R26ERT2Cre

Genotyping primers:

Rosa_cre_wt_Rv	5'GGAGCGGGAGAAATGGATATG
Rosa_cre_Rv	5'GCGAAGAGTTTGTCCTCAACC
Rosa_cre_wt_Fw	5'AAAGTCGCTCTGAGTTCTTAT

Note: Two PCRs are run: 1) to detect WT allele: primers Rosa_cre_Rv_wt and Rosa_cre_wt; 2) to detect ERT2Cre allele: primers Rosa_cre_Rv and Rosa_cre_wt.

PCR program:

Step	Temperature	Time	Cycles
Denaturation	95^{o}C	180s	1x
Denaturation	95^{o}C	30s	34x
Annealing	57^{o}C	40s	
Elongation	72^{o}C	60s	
Elongation	72^{o}C	300s	1x
Hold	4^{o}C	Forever	N/A

Expected PCR fragment sizes:

WT – 500bp

$R26^{ERT2Cre}$ – 250 bp

Miwi2Tom

Genotyping primers:

Miwi2-Tom_GenoFw1	5'TACTCCCAAACTCCGAGTCAC
Miwi2-Tom_GenoFw2	5'GTGCCTATCAGAAACGCAAGA
Miwi2-Tom_GenoRv2	5'CTCCTAGCCCAGAGTGCCTTTT

PCR program:

Step	Temperature	Time	Cycles
Denaturation	95^{o}C	180s	1x
Denaturation	95^{o}C	30s	34x
Annealing	63^{o}C	30s	
Elongation	72^{o}C	40s	
Elongation	72^{o}C	300s	1x
Hold	4^{o}C	Forever	N/A

Expected PCR fragment sizes:

WT – 329bp

Miwi2^{Tom} – 230bp

HA-Miwi2

Genotyping primers:

Miwi2_ex_Fw2	5'ACAGCCACACCGTCTCTTTT
Miwi2_int1-2_Rv	5'CAGGATAGCCAAAGGAAGGA

PCR program:

Step	**Temperature**	**Time**	**Cycles**
Denaturation	95^{o}C	180s	1x
Denaturation	95^{o}C	30s	45x
Annealing	60^{o}C	30s	
Elongation	72^{o}C	35s	
Elongation	72^{o}C	300s	1x
Hold	4^{o}C	Forever	N/A

Expected PCR fragment sizes:

WT – 207bp

Miwi2^{HA} – 240bp

Dnmt3l-V5

Genotyping primers:

V5-3L_crispr_Fw	5'CATCATCCCAGGCCCTCATA
V5-3L_crispr_Rv	5'TATGGAGCAAGTGGAGGCAA

PCR program:

Step	Temperature	Time	Cycles
Denaturation	94^{o}C	180s	1x
Denaturation	94^{o}C	30s	34x
Annealing	55^{o}C	35s	
Elongation	72^{o}C	40s	
Elongation	72^{o}C	300s	1x
Hold	4^{o}C	Forever	N/A

Expected PCR fragment sizes:

WT – 411bp

Dnmt3l^{V5} – 459bp

Dnmt3l-mKO2

Genotyping primers:

V5-3L_crispr_Fw	5'CATCATCCCAGGCCCTCATA
V5-3L_crispr_Rv	5'TATGGAGCAAGTGGAGGCAA
3L-V5_Rv	5'GGAGAGGGTTAGGGATAGGC

PCR program:

Step	Temperature	Time	Cycles
Denaturation	94^{o}C	180s	1x
Denaturation	94^{o}C	30s	34x
Annealing	60^{o}C	30s	
Elongation	72^{o}C	35s	
Elongation	72^{o}C	300s	1x
Hold	4^{o}C	Forever	N/A

Expected PCR fragment sizes:

WT – 411bp

Dnmt3l^{mKO2} – 262bp

Dnmt3l-Null

Genotyping primers:

3L_Fw1_II	5'TCCTACCCCTACCCCATTTC
3L_Fw2_II	5'GACAGCTCTAGCCCTGATGC
3L_Rv_II	5'CGAGATTAGGGGCTGCAATA

PCR program:

Step	**Temperature**	**Time**	**Cycles**
Denaturation	94^{o}C	180s	1x
Denaturation	94^{o}C	30s	34x
Annealing	55^{o}C	30s	
Elongation	72^{o}C	35s	
Elongation	72^{o}C	300s	1x
Hold	4^{o}C	Forever	N/A

Expected PCR fragment sizes:

WT – 303bp

Dnmt3l^{Null} – 251bp

RESULTS

Generation and validation of mouse alleles

The goal of this study is to understand the impact of germline reprogramming on spermatogonial stem cells. We wished to analyze what impact Mili, Miwi2 and Dnmt3L have on a population of undifferentiated spermatogonia *in vivo* using mouse as a model system. Unfortunately, no reliable antibodies are available for Miwi2 and Dnmt3L. Antibody for Mili was a kind gift from R. Pillai. Therefore, in order to facilitate the research, several different mouse alleles have been created in the lab: *Dnmt3L*^{V5}, *Dnmt3L*$^{V5\text{-}Myc\text{-}Preicision\text{-}Hisx6\text{-}mKO2}$ (*Dnmt3L*^{mKO2}), *Dnmt3L*^{Null}, *Miwi2*^{HA}, *Miwi2*^{Tom}, *Miwi2*^{FL}. Availability of these mouse lines allowed us explore and define the expression of the target proteins and understand their function better by using commercially available reliable antibodies against V5 and HA tags, FACS analysis and other molecular techniques. These tools, together with other alleles – *Mili*^{Null} and *R26*^{ERT2Cre} – available in the lab, permitted us to investigate Miwi2, Mili and Dnmt3L contribution to establishment of spermatogonial stem cell population.

Dnmt3L alleles

Dnmt3L locus encodes several transcripts: male-specific, expressed during embryo development in the germline, female-specific, expressed in oocyte and a few non-coding short transcripts found in meiotic spermatocytes. Male-specific transcript consist of 13 exons, first of which is non-coding and ATG is found in the middle of exon 2. Female specific transcript skips exon 1, but has additional two non-coding exons 1b and 1c. Protein translation in females is initiated from the same ATG in exon 2 (Ooi *et al.*, 2007; Shovlin *et al.*, 2007) (Figure 7). Use of different promoters in male and female most likely stems from the need to control expression of Dnmt3L temporarily since *de novo* DNA methylation is initiated later in females than in males (Sasaki and Matsui, 2008).

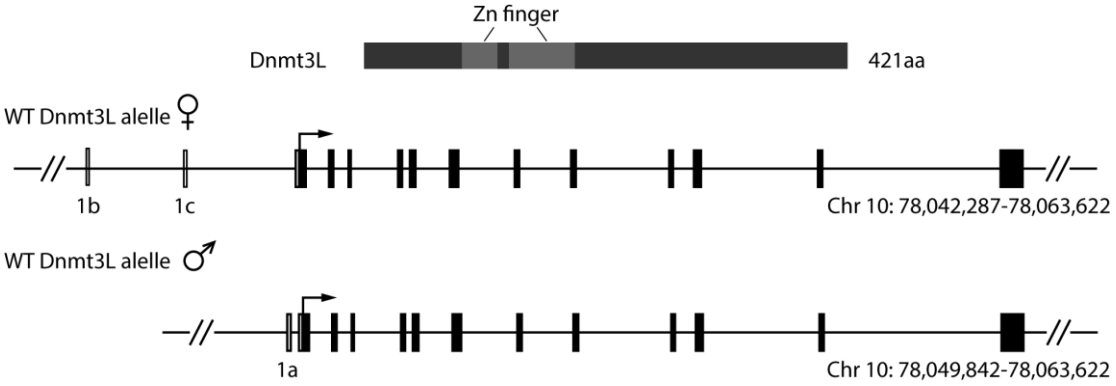

Figure 7. WT Dnmt3L locus showing exons characteristic to female and male transcripts.

Dnmt3L^{V5}. To explore the expression pattern of Dnmt3L a V5-epitope tagged allele was generated. *Dnmt3L^{V5}* allele was created using Crispr/Cas9 gene editing technology (Figure 8 A). (For more details refer to Materials and Methods.) V5-tag was inserted at the N-terminus of Dnmt3L to acquire the expression of a V5-Dnmt3L fusion protein. A successful recombination and V5-sequnce insertion was confirmed by PCR using primers flanking ATG site. In the case of WT Dnmt3L allele a band of 411pb is amplified, while the presence of *Dnmt3L^{V5}* allele is revealed by a 459bp band (Figure 8 B). The expression of V5-Dnmt3L protein was detected by immunofluorescence analysis using anti-V5 antibody in E16.5 fetal gonadocytes, where Dnmt3L is highly expressed (Figure 8 C) (La Salle *et al.*, 2004; Sakai *et al.*, 2004). V5-Dnmt3L was observed to be localized exclusively in the nucleus as expected. Deletion of Dnmt3L coding gene results in meiotic arrest and compromised testicular weight (Bourc'his *et al.*, 2001). To test whether V5-tag interferes with Dnmt3L function, WT and Dnmt3L$^{V5/V5}$ mice testicular cross-sections, stained with hematoxylin and eosin, were analyzed (Figure 8 D). Hematoxylin and eosin stain nucleus and cytoplasm of the cell respectively. A comparison of WT and Dnmt3L$^{V5/V5}$ mice testicular cross-sections did not reveal any histological differences. The testicular weight of Dnmt3L$^{V5/V5}$ mice was also normal (Figure 8 E). Therefore, it can be concluded that an addition of V5-tag at the N-terminus of the Dnmt3L protein generates a functional allele.

Dnmt3L$^{V5\text{-}Myc\text{-}Preicision\text{-}Hisx6\text{-}mKO2}$ (Dnmt3L^{mKO2}).To detect Dnmt3L expression in live cells by flow cytometry a fluorescent protein mKO2 sequence was fused to the N-terminus of Dnmt3L. Additional tags – V5 and Myc, a precision protease cleavage site and six His residues were added upstream of mKO2 sequence. The combination of these tags allows to isolate Dnmt3L by sequential rounds of immunoprecipitation and affinity chromatography purification. *Dnmt3L$^{V5\text{-}Myc\text{-}Preicision\text{-}Hisx6\text{-}mKO2}$* allele was made using Crispr/Cas9 gene editing technology (Figure 9 A). (For more details refer to Materials and Methods.) An insertion of V5-tag, Myc-tag, precision protease cleavage site, six His residues and a fluorescent protein mKO2 sequence at N-terminus of Dnmt3L results in a V5-Myc-Precision-Hisx6-mKO2-Dnmt3L fusion protein. We termed the new allele *Dnmt3L^{mKO2}* allele. To determine if the insertion occurred in the *Dnmt3L* locus, PCR, using 5' external primers and 3' external primers, was performed. A pair of 5' external primers consisted of a forward primer annealing to the 5'UTR outside homology arm and a reverse primer annealing to a V5-tag sequence. A pair of 3' external primers consisted of a forward primer annealing to an mKO2 sequence and a reverse primer annealing to an intron between exon 2 and exon 3 outside homology arm (Figure 9 A). A PCR with a pair of 5' external primers gave a band of 865bp and a PCR with 3' external primers gave a band of 448bp only in Dnmt3L$^{mKO2/+}$ mice as expected, confirming

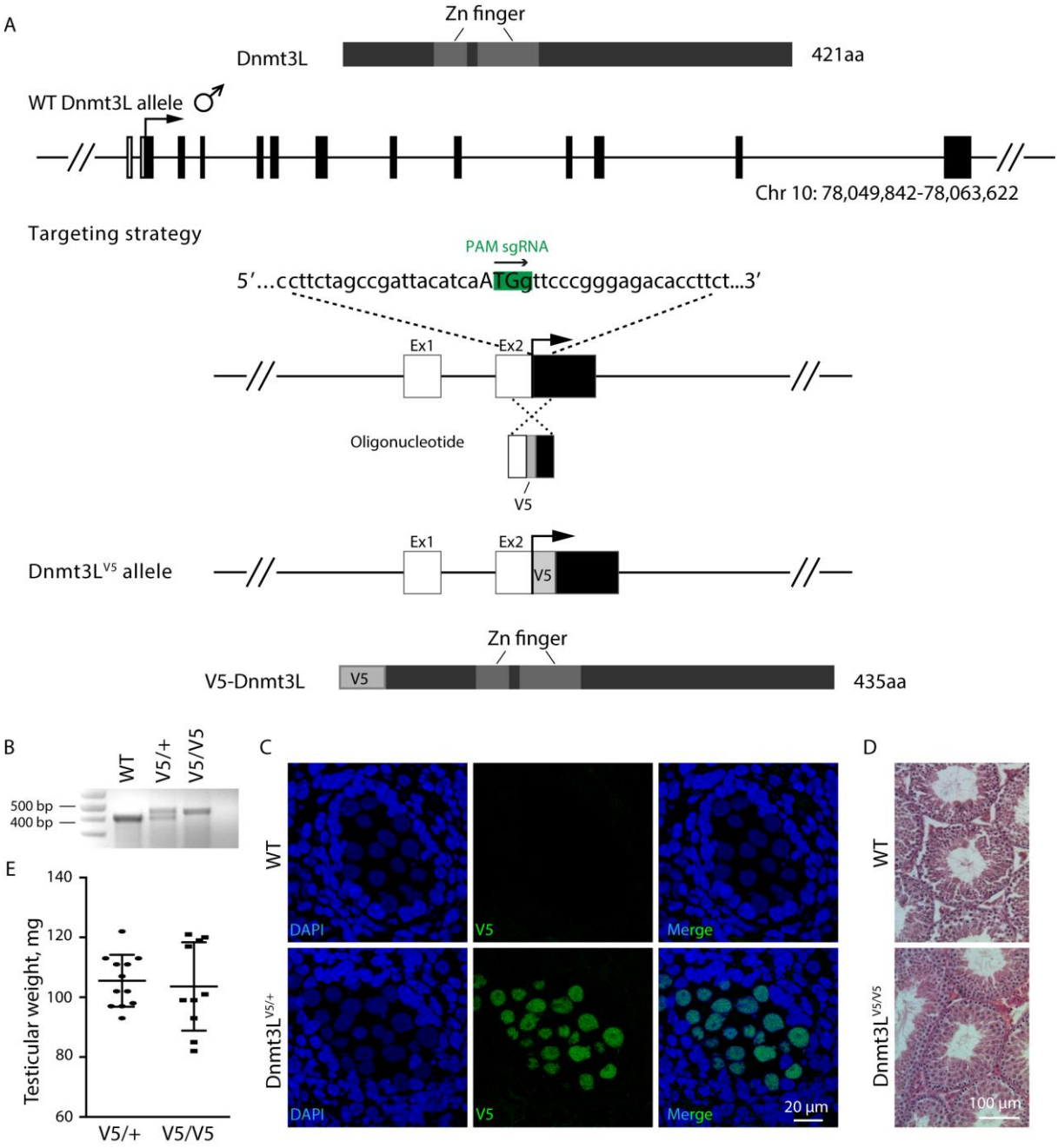

Figure 8. *Dnmt3L^{V5}* allele generation and validation

(A) A targeting strategy for *Dnmt3L^{V5}* allele generation by Crispr/Cas9 gene editing technology. Male-specific transcript is shown.

(B) Validation of a V5-tag insertion into Dnmt3L locus by PCR with primers flanking ATG.

(C) Immunofluorescence analysis with anti-V5 antibody on E16.5 fetal testicular cross-sections of wild type (WT) and Dnmt3L$^{V5/+}$ mice.

(D) Hematoxylin and eosin stained testicular cross-sections of adult wild type (WT) and Dnmt3L$^{V5/V5}$ mice.

(E) Testicular weight of adult Dnmt3L$^{V5/+}$ and Dnmt3L$^{V5/V5}$ mice.

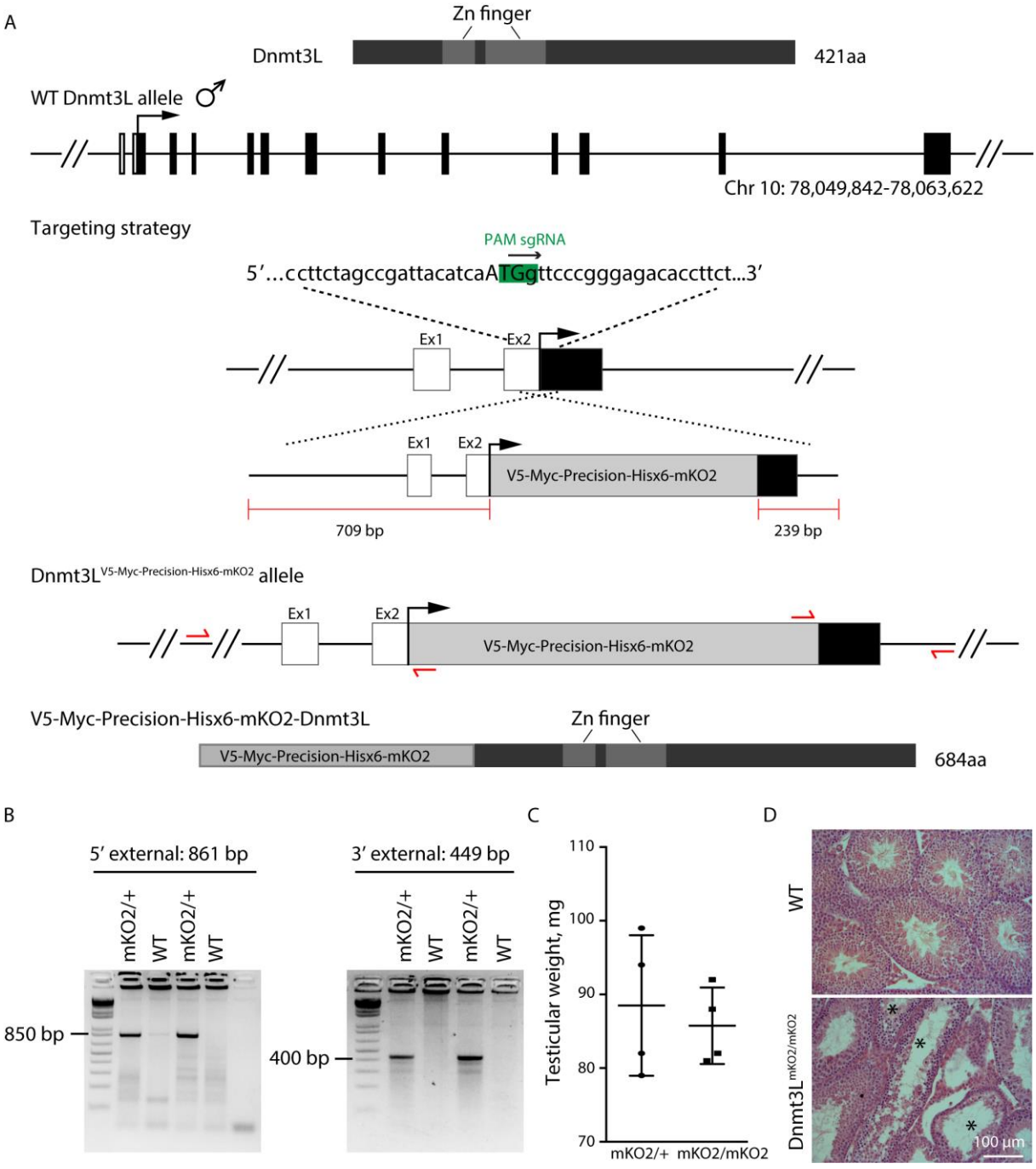

Figure 9. *Dnmt3L*$^{V5\text{-}Myc\text{-}Preicision\text{-}Hisx6\text{-}mKO2}$ (*Dnmt3L*^{mKO2}) allele generation and validation

(A) A targeting strategy for *Dnmt3L*^{mKO2} allele generation by Crispr/Cas9 gene editing technology. Male-specific transcript is shown.

(B) Validation of multi-tag insertion into Dnmt3L locus by PCR. Primers used for PCR are presented as red arrows in *Dnmt3L*^{mKO2} allele depiction.

(C) Testicular weight of Dnmt3L$^{mKO2/+}$ and Dnmt3L$^{mKO2/mKO2}$ mice.

(D) Hematoxylin and eosin stained testicular cross-sections of juvenile wild type (WT) and Dnmt3L$^{mKO2/mKO2}$ mice.

a successful recombination at *Dnmt3L* locus (Figure 9 B). To determine whether added tag to Dnmt3L protein affects its function, homozygous mice Dnmt3L$^{mKO2/mKO2}$ testicular weight was analyzed. A slight decrease in a testicular weight of Dnmt3L$^{mKO2/mKO2}$ mice was observed when compared to heterozygous Dnmt3L$^{mKO2/+}$ littermates (Figure 9 C). When a hematoxylin and eosin stained WT and Dnmt3L$^{mKO2/mKO2}$ testicular cross-sections were analyzed, it was noticed that some of the tubules of Dnmt3L$^{mKO2/mKO2}$ mice had uncompleted spermatogenesis: round and elongated spermatids were missing (tubules marked with asterisk in Figure 9 D). However, the majority of the tubules were normal (Figure 9 D). Therefore, we made a conclusion that a *Dnmt3L^{mKO2}* allele is a hypomorph, because introduced tag partially affects Dnmt3L function. Nonetheless, this allele could be a valuable tool, since Dnmt3L fusion with a fluorescent protein mKO2 allows live imaging or analysis of Dnmt3L expressing cells by flow cytometry in the testis.

Dnmt3L^{Null}. To determine what effect the deficiency of Dnmt3L has on spermatogonial stem cells a *Dnmt3L^{Null}* allele was generated using homologous recombination strategy in embryonic stem cells (ESCs), where the first coding exon (exon 2) was flanked by two *LoxP* sites (Figure 10 A). (For more details refer to Materials and Methods.) This strategy resulted in disrupting Dnmt3L transcript by introducing a shift in an open reading frame. Recombination of *Dnmt3L* allele was confirmed by Southern blot analysis using 3' external probe, where WT *Dnmt3L* allele, digested with BamHI, corresponds to 8,9kb DNA fragment, while successful integration of neomycin resistance cassette with 3' *LoxP* site results in insertion of additional BamHI site, therefore, targeted *Dnmt3L* allele corresponds to 6,1kb DNA fragment (Figure 10 B). When male mice harboring targeted *Dnmt3L* allele were crossed with a mouse line harboring ubiquitously expressed deleter Cre-recombinase, *Dnmt3L^{Null}* allele was generated, which was detected as 4,2kb DNA fragment in Southern blot analysis (Figure 10 B). Male mice, lacking Dnmt3L, have great reduction in testicular weight and meiosis does not progress beyond pachytene stage (Bourc'his and Bestor, 2004; Hata *et al.*, 2006; Webster *et al.*, 2005). This phenotype was recapitulated in Dnmt3L$^{Null/Null}$ mice. The testicular weight of Dnmt3L$^{Null/Null}$ mice was as low as 20-30mg, while Dnmt3L$^{Null/+}$ mice had normal size testes (90-130mg) (Figure 10 C). Hematoxylin and eosin stained Dnmt3L$^{Null/Null}$ mice testicular cross-sections showed that spermatogenesis of Dnmt3L$^{Null/Null}$ mice is highly compromised: spermatogenesis in Dnmt3L$^{Null/Null}$ male mice did not advance further than leptotene-zygotene stage (Figure 10 D). Another hallmark of the loss of Dnmt3L is upregulation of transposable element LINE1 (Bourc'his and Bestor, 2004). As expected, upregulation of LINE1 element was detected in adult male Dnmt3L$^{Null/Null}$ testis, but not in the WT control (Figure 10 E). In conclusion, generated *Dnmt3L^{Null}* allele leads to the loss of

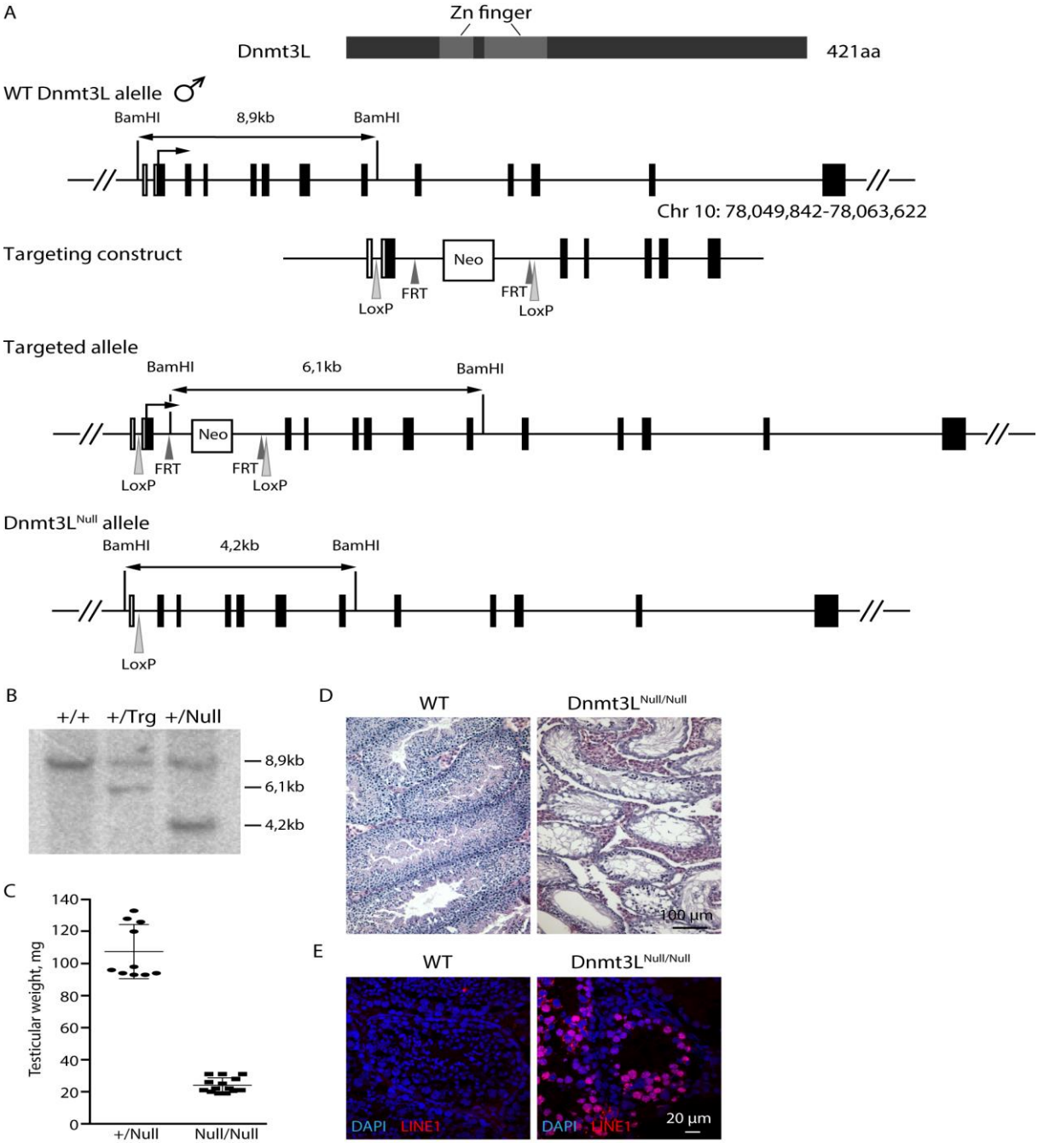

Figure 10. *Dnmt3L*^{Null} allele generation and validation

(A) A targeting strategy for *Dnmt3L*^{Null} allele generation by recombination in mouse embryonic stem cells. Male-specific transcript is shown.

(B) Validation of Dnmt3L locus recombination and successful neomycin cassette and exon 2 deletion by Southern blot.

(C) Testicular weight of adult Dnmt3L$^{Null/+}$ and Dnmt3L$^{Null/Null}$ mice.

(D) Hematoxylin and eosin stained testicular cross-sections of adult wild type (WT) and Dnmt3L$^{Null/Null}$ mice.

(E) Immunofluorescence analysis with anti-LINE1 ORF1p antibody of adult wild type (WT) and Dnmt3L$^{Null/Null}$ mice testicular cross-sections.

Dnmt3L protein, which in turn perfectly phenocopies previously published *Dnmt3L*^{Null} allele (Bourc'his and Bestor, 2004; Hata *et al.*, 2006; Webster *et al.*, 2005). To note, in contrast to males female Dnmt3L$^{Null/Null}$ mice were sub-fertile. They were able to give birth to one or two litters. The reason for such phenotype was not investigated.

Miwi2 alleles

Miwi2^{HA}. To study the function and expression of Miwi2 a HA-tagged Miwi2 allele was generated. *Miwi2^{HA}* allele was created using Crispr/Cas9 gene editing technology (Figure 11 A). (For more details refer to Materials and Methods.) HA-tag was inserted at the N-terminus of Miwi2 to obtain the expression of HA-Miwi2 fusion protein. The insertion of HA-tag was verified by PCR, using primers flanking ATG site. A band of 207bp is amplified if the WT Miwi2 allele is present, while HA-tagged Miwi2 allele gives a band of a size of 240bp (Figure 11 B). Expression of HA-tagged Miwi2 protein was confirmed by immunofluorescence analysis using anti-HA antibody (Figure 11 C). Immunofluorescence was performed on E16.5 fetal gonadocytes where Miwi2 is highly expressed (Aravin *et al.*, 2008). HA-Miwi2 expression pattern was identical to that of Miwi2 – Miwi2 was found to be localized in the cytoplasmic foci surrounding nucleus, as well as in the nucleus. In the cytoplasm Miwi2 positive granules were found to overlap with processing bodies (P-bodies) – a granule associated with RNA metabolism, although not all P-bodies contain Miwi2. Therefore, these distinct perinuclear foci that encompass Miwi2 and P-bodies were termed Pip-bodies (Aravin *et al.*, 2009). It is known that Miwi2 deficiency leads in meiotic arrest and great reduction in testicular weight and size in adult male mice (Carmell *et al.*, 2007). Therefore, in order to find out if HA-tag affects Miwi2 function, immunofluorescence was performed on testicular cross-sections of WT and Miwi2$^{HA/HA}$ adult mice. The sections were stained with DNA binding dye (DAPI) and γH2AX (Figure 11 D). It is established that all types of germ cells found in the testis have a very specific nuclear morphology, while γH2AX helps to stage meiotic cells. Comparison of germ cell composition in WT and Miwi2$^{HA/HA}$ adult mice testicular cross-sections did not reveal any differences. The testicular weight of Miwi2$^{HA/HA}$ adult mice as compared to Miwi2$^{HA/+}$ mice also did not show any impairment (Figure 11 E). To sum up, the targeting strategy resulted in a successful insertion of HA-tag and generation of a fully functional *Miwi2^{HA}* allele.

Miwi2^{FL}. To study Miwi2 function in adult male mice without affecting its function in fetal gonadocytes a *Miwi2^{FL}* allele was created to utilize a conditional deletion strategy. *Miwi2^{FL}* allele is published by De Fazio *et al.* (2011). Briefly, WT *Miwi2* allele was targeted using homologous recombination in embryonic stem cells to insert two *LoxP* sites flanking

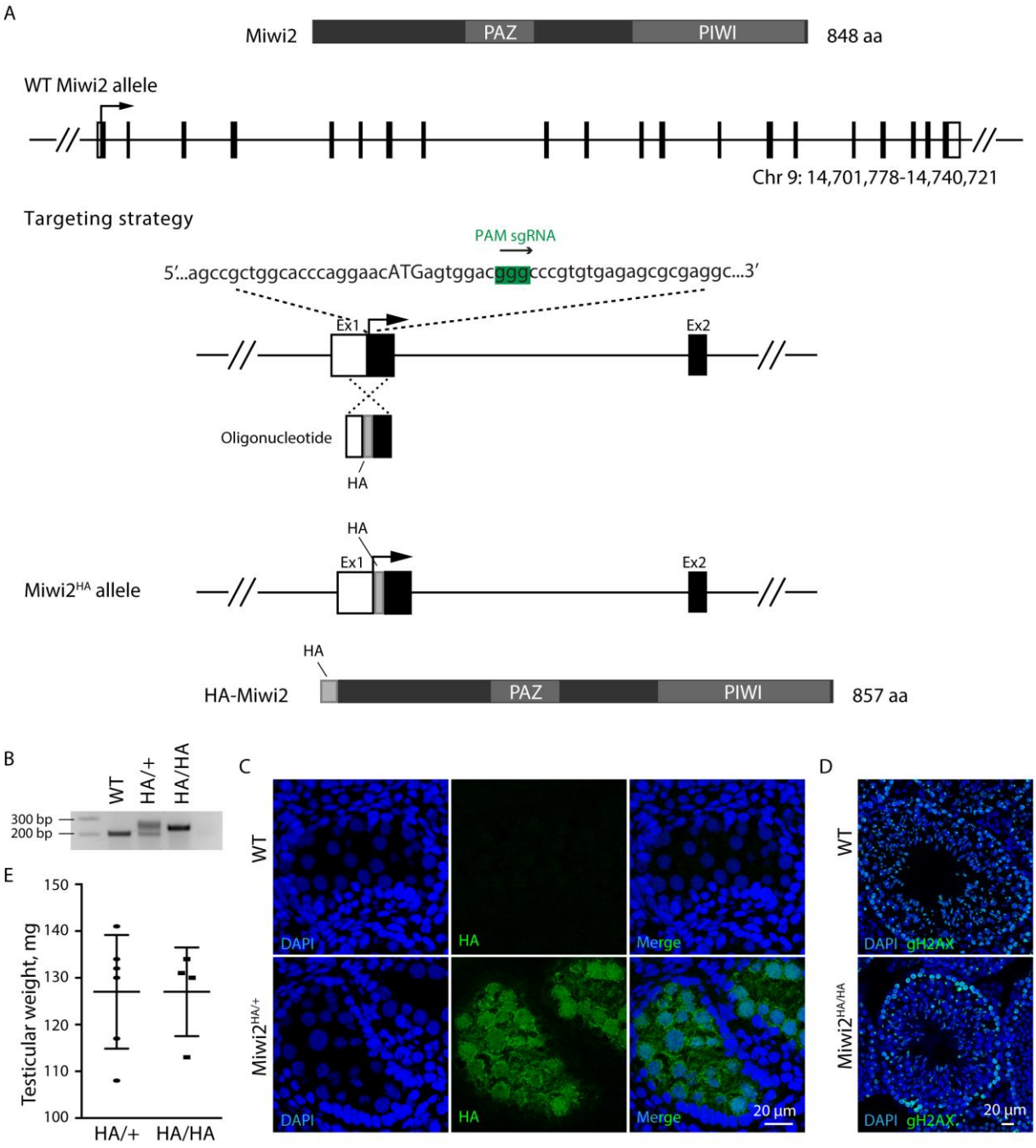

Figure 11. *Miwi2*^{HA} allele generation and validation

(A) A targeting strategy for *Miwi2*^{HA} allele generation by Crisp/Cas9 gene editing technology.

(B) Validation of HA-tag insertion into Miwi2 locus at the site of ATG by PCR.

(C) Immunofluorescence analysis with anti-HA antibody on E16.5 fetal testicular cross-sections of wild type (WT) and Miwi2$^{HA/+}$ mice.

(D) Immunofluorescence analysis with anti-gH2AX antibody of adult wild type (WT) and Miwi2$^{HA/HA}$ mice testicular cross-sections.

(E) Testicular weight of adult Miwi2$^{HA/+}$ and Miwi2$^{HA/HA}$ mice.

exon 17 (Figure 12 A). Exon 17 in Miwi2 is a part of PIWI domain. When mice having *Miwi2*^{FL} allele are crossed to a mouse line that possesses an expression of a Cre-recombinase, exon 17 is excised and *Miwi2*^{FL} allele is converted into *Miwi2*^{Null} allele (Figure 12 A). Deletion of exon 17 results in a shift in an open reading frame in the transcript. As noted before, Miwi2 mutant male mice exhibit testicular atrophy. Spermatogenesis in mutant animals do not progress beyond pachytene stage (Carmell *et al.*, 2007). To validate that our generated *Miwi2*^{Null} allele indeed leads to Miwi2-mutant-characteristic phenotype in Miwi2$^{Null/Null}$ mice, a testicular cross-sections of adult mice were examined. No round or elongated spermatids were observed, furthermore, meiosis was identified to be arrested at the pachytene stage (Figure 12 C). Thus, Miwi2$^{Null/Null}$ mice exhibit exactly the same Miwi2-mutant phenotype as described by Carmell *et al*. (2007).

In this study, mice having *Miwi2*^{FL} allele were used in a combination with *R26*^{ERT2Cre} allele (obtained from Jackson laboratories, for more details refer to Materials and Methods). *R26*^{ERT2Cre} allele produces ubiquitously expressed ERT2Cre recombinase, where Cre-recombinase gene is fused with an estrogen receptor ligand binding domain. Expressed ERT2Cre is localized in the cytoplasm and is inactive. Upon administration of tamoxifen (a receptor antagonist), ERT2Cre is translocated into the nucleus, where DNA flanked by two *LoxP* sites is excised (Feil *et al.*, 1997). Therefore, a mouse homozygous for *Miwi2*^{FL} allele and harboring *R26*^{ERT2Cre} allele (Miwi2$^{FL/FL}$; R26$^{ERT2Cre/+}$) upon tamoxifen administration becomes Miwi2 deficient due to *Miwi2*^{FL} allele conversion into *Miwi2*^{Null} allele.

Miwi2^{tdTom} (Miwi2^{Tom}). In order to determine Miwi2 expression pattern by flow cytometry *Miwi2*^{Tom} allele was generated using homologous recombination technique in embryonic stem cells. (Carrieri *et al*., in submission.) At the site of ATG in exon 1 an artificial intron, tdTomato coding sequence with a strong poly(A) motif and neomycin resistance cassette, flanked by *ftr* sites, were inserted generating a *Miwi2*$^{Tom\text{-}Neo}$ knock-in allele. *Miwi2*$^{Tom\text{-}Neo}$ knock-in mice were crossed with Deleter-Cre expressing mice to remove neomycin resistance cassette. *Miwi2*^{Tom} allele serves as an expressional reporter of Miwi2, since an expression of a fluorescent protein tdTomato is driven my Miwi2 promoter. Functionally, *Miwi2*^{Tom} allele is equal to *Miwi2*^{Null} allele because Miwi2 coding transcript is not produced from *Miwi2*^{Tom} coding locus due to insertion of very strong poly(A) sequence after tdTomato gene, which terminates transcription. Therefore, Miwi2$^{Tom/Tom}$ mice should also have a reduced testicular weight like Miwi2$^{Null/Null}$ mice (Carmell *et al.*, 2007). Indeed, a great decrease in testicular weight of Miwi2$^{Tom/Tom}$ adult male mice was observed as compared to Miwi2$^{Tom/+}$ mice (Figure 12 B). When testicular cross-sections, stained with hematoxylin and eosin, of Miwi2$^{Tom/Tom}$ and Miwi2$^{Null/Null}$ adult male mice were compared,

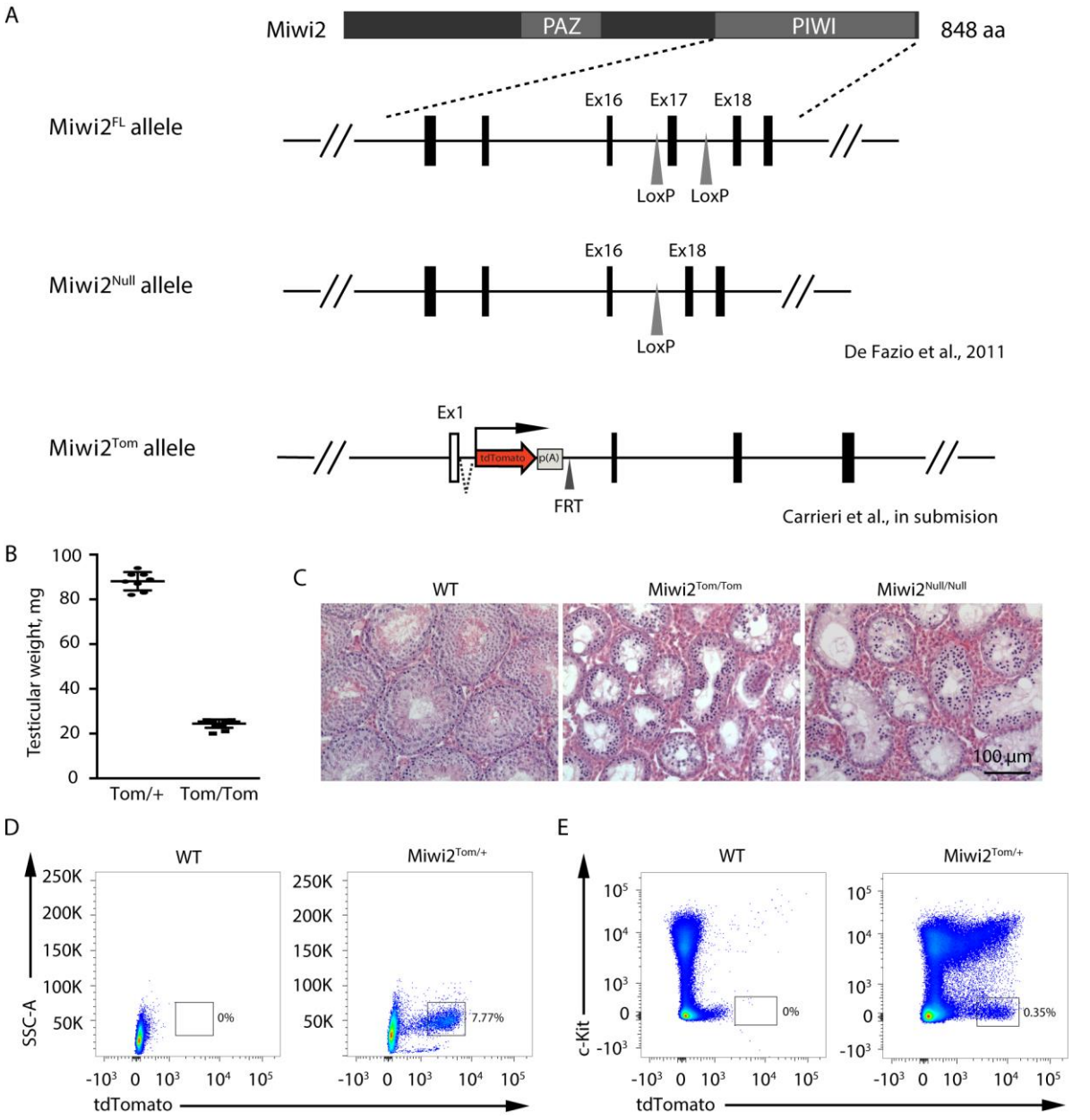

Figure 12. *Miwi2*^{Null} and *Miwi2*^{Tom} allele generation and validation

(A) A targeting strategy for *Miwi2*^{Null} allele and *Miwi2*^{Tom} allele generation.

(B) Testicular weight of adult Miwi2$^{Tom/+}$ and Miwi2$^{Tom/Tom}$ mice.

(C) Hematoxylin and eosin stained wild type (WT), Miwi2$^{Tom/Tom}$ and Miwi2$^{Null/Null}$ adult mice testicular cross-sections.

(D) Flow cytometry analysis of E16.5 fetal testes of wild type (WT) and Miwi2$^{Tom/+}$ mice.

(E) Flow cytometry analysis of adult testes of wild type (WT) and Miwi2$^{Tom/+}$ mice.

identical phenotype was observed. Miwi2$^{Tom/Tom}$ mice exhibited abnormal spermatogenesis, which ceased at the pachytene stage (Figure 12 C). Nontheless, mice having *Miwi2*^{Tom} allele can be used to perform live cell analysis by flow cytometry of the target Miwi2-expressing population in the testes due to the expression of tdTomato fluorescent protein. The expression of Miwi2-Tom protein was confirmed by analyzing a single cell suspension prepared from Miwi2$^{Tom/+}$ E16.5 fetal testes by flow cytometry. Miwi2 is highly expressed in fetal gonadocytes at the embryonic day 16.5 (E16.5) Miwi2 (Aravin *et al.*, 2008). Indeed, a population of Miwi2-Tom^{pos} cells was detected, which makes up approx. 7-8% of total cells in the fetal testes (Figure 12 D). Miwi2 expression was also detected in the adult male mouse testis. A single cell suspension obtained from an adult mouse testis was analyzed by flow cytometry excluding CD45^{pos} and CD51^{pos} somatic cells and looking for Miwi2-Tom^{pos}, c-Kit^{neg} cells – undifferentiated spermatogonial precursor cells that express Miwi2. Indeed, a small population, approx. 0,35% of all testicular cells, of Miwi2-Tom^{pos}, c-Kit^{neg} cells was identified (Figure 12 E). Observed Miwi2-Tom^{pos}, c-Kit^{pos} population (Figure 12 E) was found not to contain Miwi2 transcript (Carrieri *et al*., in submission). Miwi2-Tom^{pos}, c-Kit^{pos} cells are labeled by tdTomato expression because c-Kit^{neg} cells give rise to c-Kit^{pos} cells, where tdTomato is passed from one population to another due to its long half-life. It was found that Miwi2 expression defines a population of transit amplifying cells in the adult testes. Miwi2 expressing cells partially overlap with Gfra1 expressing cells, but Miwi2 is mostly co-expressed with Ngn3. It was shown that Miwi2 expressing cells possess a stem cell activity upon transplantation, additionally, are important for rapid recovery of spermatogenesis after chemically induced damage (Carrieri *et al*., in submission). These characteristics are very reminiscent of Ngn3 expressing cell population in the adult testes (Nakagawa *et al.*, 2007). Therefore, Miwi2 defines a population of spermatogonial precursor cells with regenerative capacity in the adult testes. All in all, *Miwi2*^{Tom} allele is a great tool to study Miwi2 expressing cell biology since it can be used in combination with other alleles, as well as Miwi2$^{Tom/Tom}$ equals Miwi2$^{Null/Null}$ mice, but still allows to visualize, analyze and sort Miwi2 expressing cells.

A primary Mili-independent piRNA biogenesis pathway residually loads Miwi2 empowering partial reprogramming activity

Summary

Miwi2 and Mili are involved in piRNA production and transposon silencing in fetal gonads. It is known that the loss of Miwi2 leads to a complete exhaustion of germline in male mice. Whether the absence of Mili results in the same phenotype, has not been establish yet. In this study we show that Mili is also required for germ cell maintenance, but presents a much weaker phenotype than Miwi2 with only a partial loss of the germ line observed in aged mice. The difference between the two mutant phenotypes could be explained by the fact that in Mili deficient fetal testes a small amount of piRNAs is produced that can mount a residual defense against transposable elements as determined by bisulfite sequencing data. We have determined that piRNAs made in the absence of Mili make up a small pool of piRNAs that are also present in the wild type mice. Mili mutant piRNAs are mainly primary in nature and are most likely bound by Miwi2 since Miwi2 partially retains its nuclear localization in the absence of Mili in mouse fetal gonadocytes. In summary, a primary piRNA biogenesis pathways exist in mouse in the absence of Mili that contribute to both germ line reprogramming and maintenance.

Ein primär Mili-unabhängiger piRNA Biogeneseweg lädt Miwi2 geringfügig und erlaubt partielle Reprogrammierungsaktivität

Zusammenfassung

Miwi2 und Mili sind in der piRNA Produktion und der Stilllegung von Transposons in fötalen Hoden involviert. Es ist bereits bekannt, dass der Verlust von Miwi2 zu einem Totalverlust der Keimbahnzellen in männlichen Mäusen führt. Ob jedoch der Verlust von Mili zu einem ähnlichen Phänotyp führt, wurde bisher noch nicht erforscht. In dieser Studie zeigen wir, dass Mili ebenfalls für die Keimzell-Erhaltung benötigt wird, jedoch einen schwächeren Phänotyp als Miwi2 zeigt, der sich in teilweisem Verlust von Keimzellen in gealterten Mäusen manifestiert. Der Unterschied zwischen den Phänotypen der zwei Mutanten konnte durch die Produktion von kleinen Mengen piRNAs in Mili-defizienten fötalen Hoden erklärt werden. Diese ermöglichen eine Restantwort auf transponierbare Elemente, welche durch Bisulfit-Sequenzierungs Daten demonstriert wird. Wir beschreiben, dass piRNAs, die in Abwesenheit von Mili produziert werden, eine kleine Gruppe piRNAs darstellen, die auch in Wildtyp-Mäusen präsent ist. Diese piRNAs sind hauptsächlich primärer Natur und sehr wahrscheinlich an Miwi2 gebunden, da Miwi2 trotz Abwesenheit von Mili auch weiterhin teilweise eine nukleare Lokalisation in fötalen Hoden aufweist. Zusammenfassend legt diese Studie nahe, dass ein tertiärer piRNA Biogeneseweg in Maushoden existiert, der zu Keimzell-Reprogrammierung und -Erhaltung beiträgt.

A primary Mili-independent piRNA biogenesis pathway residually loads Miwi2 empowering partial reprogramming activity

Mili and Miwi2 are components of piRNA biogenesis pathway, which evolved in animals as a defense mechanism against mobile transposable elements (TEs). In piRNA biogenesis and TE silencing Miwi2 and Mili have distinct functions (Aravin *et al.*, 2008; De Fazio *et al.*, 2011; Kuramochi-Miyagawa *et al.*, 2008). Nonetheless, Miwi2 and Mili deficient mice share nearly identical phenotype (Carmell *et al.*, 2007; Kuramochi-Miyagawa *et al.*, 2004): DNA demethylation of TEs at their regulatory sequences and hence TE de-repression, meiotic arrest at the pachytene stage and male sterility. Additionally, it was shown that that Miwi2-deficient mice manifest with a progressive and complete loss of the germ line with age (Carmell *et al.*, 2007). However, no data is available whether Mili mutant mice exhibit similar phenotype regarding germ cell lineage maintenance. It has been established that Mili functions upstream of Miwi2 in reprogramming gonadocytes during the phase of *de novo* DNA methylation to guide the silencing of distinct transposable elements (Aravin *et al.*, 2008). Therefore, it could be assumed that Mili deficiency should result in the same or more severe germ cell maintenance phenotype compared to Miwi2 deficiency.

Mili deficient male mice display incomplete germ cell loss with age

In this study we sought to determine whether Mili mutant mice exhibit a similar germline maintenance phenotype as Miwi2 mutant mice. To understand whether Mili contributes to the germ line maintenance, $Mili^{Null/+}$ and $Mili^{Null/Null}$ mice were aged. Testes of twelve months old mice were analyzed to evaluate whether any germ cells are present in the seminiferous tubules. To do so, testes from five $Mili^{Null/+}$ and five $Mili^{Null/Null}$ mice were sectioned throughout the whole length of the tissue, the cross-sections were stained with hematoxylin and eosin and Sertoli-only tubules were counted. Even though the testicular weight of Mili mutant animals was significantly lower (Figure 13 A), it was observed that only 50% of the tubules in $Mili^{Null/Null}$ mice are completely devoid of any germ cells (Figure 13 B), while the other half of the tubules in aged mice had at least one type of germ cells present. The representative images of testicular cross-sections of $Mili^{Null/+}$ and $Mili^{Null/Null}$ aged mice are shown in Figure 13 C. To sum up, here we show that, Mili-deficient aged mice partially loose germ cells with age. This finding indicates that Mili and Miwi2 mutant mice are phenotypically distinct in terms of germ line maintenance, which contradicts the current model implicating that Miwi2 function is Mili-dependent.

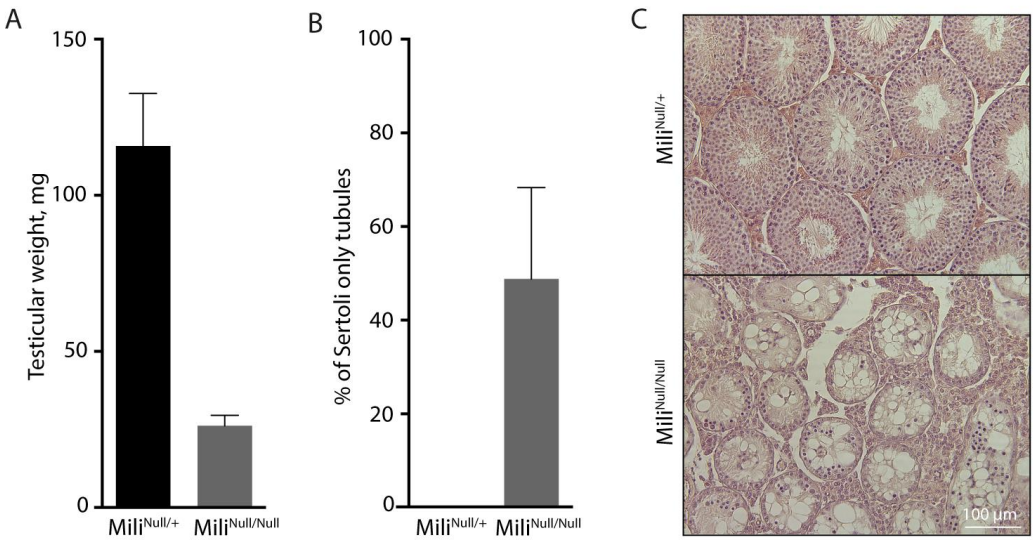

Figure 13. Aged Mili$^{Null/Null}$ mice partially lose germline

(A) Testicular weight of aged Mili$^{Null/+}$ and Mili$^{Null/Null}$ mice.

(B) Percentage of Sertoli-only tubules in aged Mili$^{Null/+}$ and Mili$^{Null/Null}$ mice.

(C) Hematoxylin and eosin stained testicular cross-sections of aged Mili$^{Null/+}$ and Mili$^{Null/Null}$ mice.

Miwi2 deficient spermatogonia have more severe methylation defects

To get insight into the discrepancy of germ cell maintenance between Miwi2- and Mili-deficient mice, we have set to explore the methylation status of undifferentiated spermatogonia in Miwi2 and Mili mutant mice. To this end, CD45^{neg}, CD51^{neg}, c-Kit^{neg}, Miwi2-Tom^{pos}, CD9^{pos} spermatogonia were sorted from 1) Miwi2$^{Tom/+}$ (=CTL), 2) Miwi2$^{Tom/Tom}$ (=Miwi2$^{Null/Null}$) and 3) Mili$^{Null/Null}$; Miwi2$^{Tom/+}$ (=Mili$^{Null/Null}$) juvenile mice. Sorted cells from all three genotypes were subjected to bisulfite conversion and whole genome bisulfite sequencing (WGBS) (in collaboration with R. Barrens and W. Reik, Babraham Institute, Cambridge). Three biological replicates were sequence per genotype analyzed. To quantify differences in methylation differentially methylated regions (DMRs) were defined. A DMR was considered as a region having 50 adjacent CpGs, where a level of methylation was calculated of those CpGs that had at least 5 reads from pooled biological replicates. Firstly, we sought to investigate whether changes in methylation status of different genomic regions could be observed. We have analyzed the level of methylation of different genomic regions: genic and intergenic regions, CGIs and promoters. Analysis revealed a slight decline in methylation in both Mili- and Miwi2-deficient cells when looked genome-

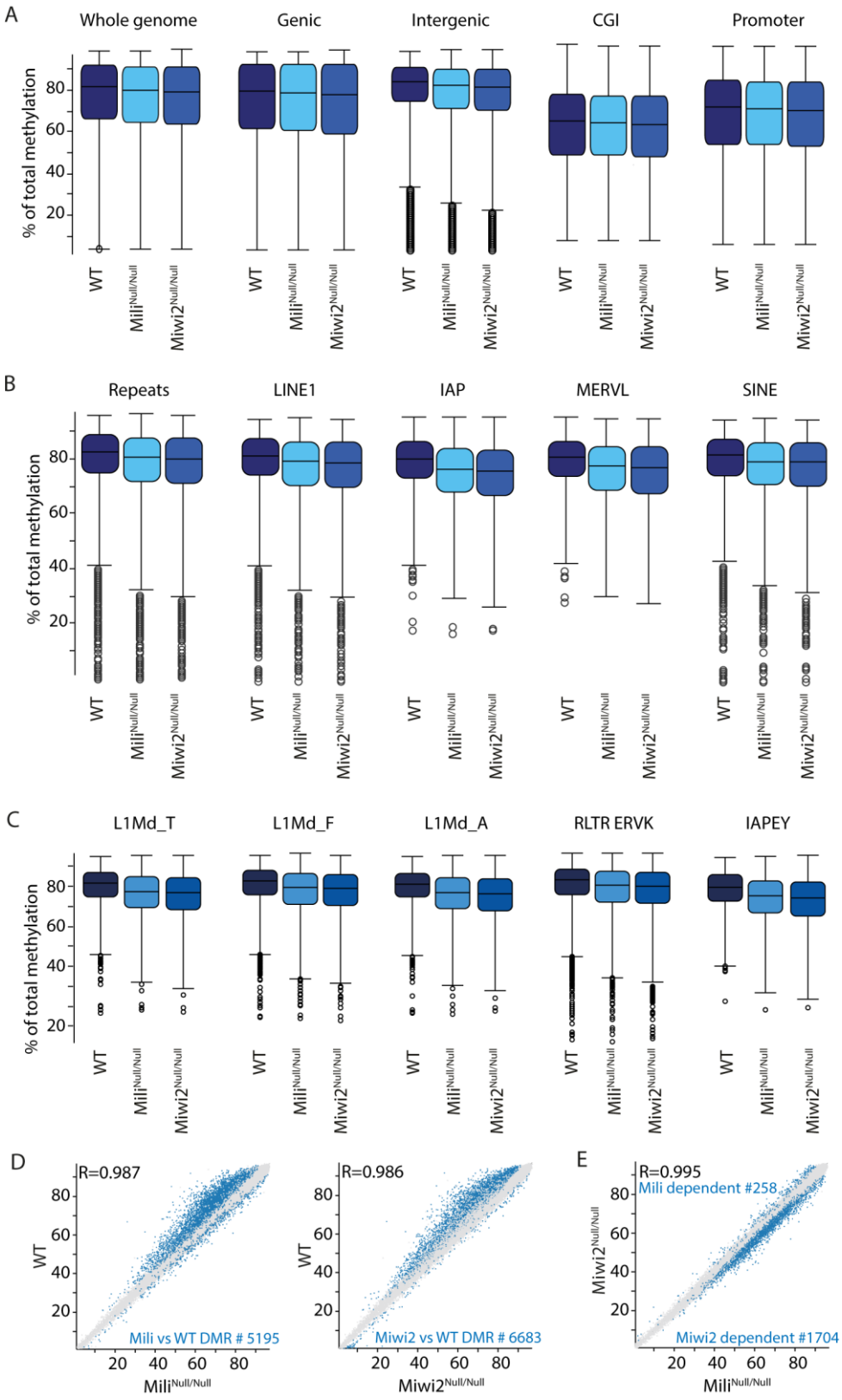

Figure 14. Miwi2$^{Null/Null}$ mice exhibit greater changes in methylation than Mili$^{Null/Null}$ mice

(A) Box plots showing distribution of methylation levels for different genome features between wild type (WT), Mili$^{Null/Null}$ and Miwi2$^{Null/Null}$ mice.

(B) Box plots showing methylation levels of different repeat classes between wild type (WT), Mili$^{Null/Null}$ and Miwi2$^{Null/Null}$ mice.

(C) Box plots showing methylation levels of different repeat elements between wild type (WT), Mili$^{Null/Null}$ and Miwi2$^{Null/Null}$ mice.
(D) Scatter plots showing percentage of methylation between wild type (WT) and Mili$^{Null/Null}$, wild type (WT) and Miwi2$^{Null/Null}$ mice. Blue dots represent significantly differentially methylated regions (DMRs).
(E) Scatter plot showing percentage of methylation between Miwi2$^{Null/Null}$ and Mili$^{Null/Null}$ mice. Blue dots represent significantly differentially methylated regions (DMRs).

wide, however, no differences were found in methylation status of other genic regions in the two mutants as compared to a wild type sample (Figure 14 A). These results are in agreement that Miwi2 or Mili were never reported to be involved in methylation of other sequences in the genome, but transposable elements. Therefore, secondly, we have investigated the methylation of all repeat elements and specifically the methylation of LINE1, IAP, MERVL and SINE elements. We have detected a decrease in methylation in both Mili- and Miwi2-deficient samples in all groups analyzed. In addition, we have noticed a trend where Miwi2 knock-out displayed overall lower methylation levels as compared to Mili mutant sample (Figure 14 B). These results were recapitulated when comparing methylation levels of individual transposons between Miwi2- and Mili-deficient samples (Figure 14 C): both mutants showed a decrease in methylation, however, Miwi2-deficiency seemed to have a slightly greater effect. These data indicated that overall Miwi2-defficient cells experience greater methylation loss. Hence we were interested to see to what extent Mili and Miwi2 contribute to methylation genome-wide. When Mili- and Miwi2-decifient samples were compared to a control sample, it has been revealed that Miwi2 is linked to methylation of 6683 differentially methylated regions (DMRs) in undifferentiated spermatogonia, while Mili – to 5195 DMRs (Figure 14 D). To understand whether identified DMRs are common for Mili and Miwi2, we have compared methylation status of DMRs between the two mutants. We determined that there is a significant overlap between the two samples, but, in addition to this, analysis revealed presence of 1704 Miwi2-dependent DMRs and 258 Mili-dependent DMRs (Figure 14 E). To sum up, these data have shown that Miwi2 mutant mice undifferentiated spermatogonia have more severe methylation defects as compared to Mili deficient cells. These results are in agreement with observed milder Mili knock-out phenotype in germ line maintenance.

Miwi2- and Mili-dependent DMRs are the source of piRNAs

Currently, in the field it is regarded that a function of Miwi2 is completely dependent on Mili, where Mili serves as a solo-catalytic machinery for generating piRNAs in a *ping-pong* cycle and silencing transposable elements, while Miwi2 is an acceptor of primary and secondary piRNAs that guides the methylation of LINE1 and IAP elements in the genome. It is established that losing either of the two proteins results in a failure to establish silencing of these transposable elements by methylation (Aravin *et al.*, 2008; Kuramochi-Miyagawa *et al.*, 2008). However, we have shown that Miwi2 has more severe germ cell loss phenotype and, in addition to this, WGBS analysis on Miwi2 and Mili mutant undifferentiated spermatogonia revealed the existence of the regions in the genome, which methylation are dependent either only on Miwi2 or only on Mili. Thus, firstly we wanted to determine whether in the wild type situation identified loci produce piRNAs that are bound by Mili and Miwi2. To do so, piRNAs, obtained from immunoprecipitation of Mili and Miwi2 ribonucleoprotein (RNPs) complexes in wild type fetal gonadocytes (De Fazio *et al.*, 2011), were mapped to 1704 Miwi2-dependent and 258 Mili-dependent loci, which take up 109,6 kb and 12,8 kb of the genome respectively. Indeed, we have found multiple piRNAs mapping to respective loci from Mili and Miwi2 RNPs. A single peak in plots in Figure 15 A, B represents an accumulative count of reads per locus (normalized to the size of the locus). It is well known that piRNAs that represent transposable elements can map to multiple positions in the genome due to their repetitive nature. In order to avoid piRNAs that could have potentially mapped to other positions in the genome, not only loci in question, we have chosen to analyze only uniquely mapping piRNAs. When unique piRNAs were mapped to 1704 Miwi2-dependent and 258 Mili-dependent loci, a substantial amount of piRNAs were found to originate from the both sets of loci (Figure 15 C, D). Thus, this data confirms that previously identified regions are actual piRNA producing loci.

In mice primary piRNAs are processed from transposable element mRNA and loaded into Mili and Miwi2. piRNA biogenesis machinery has a bias to process transcripts at U-rich positions, therefore, a created 1U bias is a hallmark of primary piRNAs. Primary piRNAs, bound by Mili, enter a *ping-pong* amplification cycle, when secondary piRNAs are made by Mili cleaving piRNA precursor transcript between position 10 and 11 counting from 5' end of bound piRNA. Therefore, a pair of two piRNAs is generated that has a 10nt overlap, where one piRNA has 1U and another 10A bias. This feature was called a *ping-pong* signature (Aravin *et al.*, 2008; De Fazio *et al.*, 2011). Secondary piRNAs that are generated by Mili cleavage event are loaded into Mili and Miwi2. Miwi2 with a bound piRNA is translocated into the nucleus and guides DNA methylation of TE sequences (Aravin *et al.*, 2008). We have

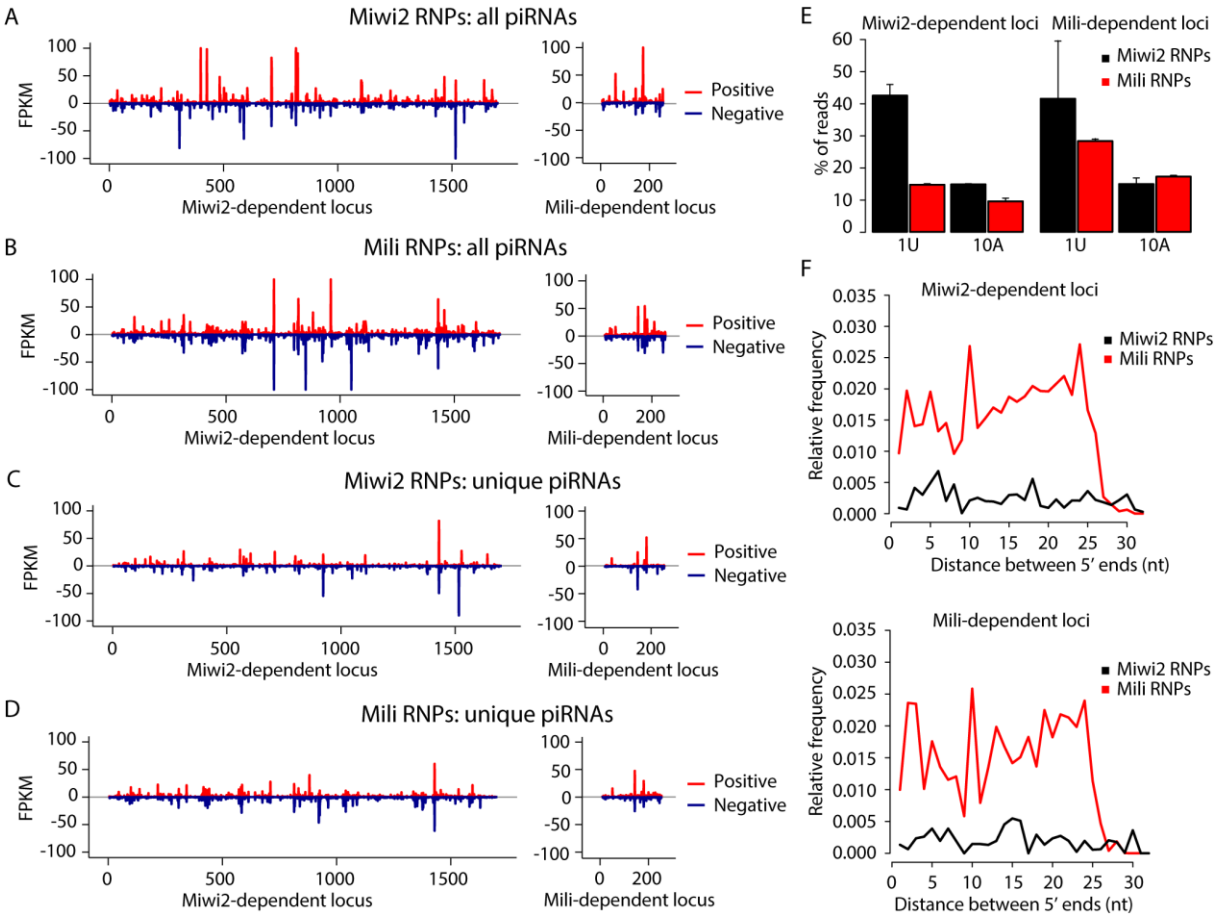

Figure 15. Miwi2- and Mili-dependent loci are piRNA producing loci in wild type fetal testes

(A) Mapping of all piRNAs from Miwi2 RNPs to 1704 Miwi2-dependent and 258 Mili dependent loci. One peak represents one locus.

(B) Mapping of all piRNAs from Mili RNPs to 1704 Miwi2-dependent and 258 Mili dependent loci. One peak represents one locus.

(C) Mapping of unique piRNAs from Miwi2 RNPs to 1704 Miwi2-dependent and 258 Mili dependent loci. One peak represents one locus.

(D) Mapping of unique piRNAs from Mili RNPs to 1704 Miwi2-dependent and 258 Mili dependent loci. One peak represents one locus.

(E) Percentage of piRNAs, which mapped to Miwi2- and Mili-dependent loci, that have U at their first position without A at the tenth position and A at the tenth position without U at the first position.

(F) A *ping-pong* cycle analysis: an overlap between piRNA, which mapped to Miwi2- and Mili-dependent loci, 5’ ends.

analyzed piRNAs that mapped to Miwi2- and Mili-dependent loci and found that Miwi2 RNP piRNAs showed an enrichment in uracil as the first base (1U), while Mili RNP piRNAs showed a weaker enrichment in 1U and only in those piRNAs that mapped to Mili-dependent loci (Figure 15 E). Thus, piRNAs that originate from identified loci are most likely primary in origin, out of which are mostly Miwi2-bound piRNAs. In addition to this, no particular bias was found in piRNAs harboring adenine as tenth nucleotide (10A) (Figure 15 E). We have also looked whether those piRNAs that were found to map to Miwi2-dependent and Mili-dependent loci do overlap by 10nt counting from their 5' end. A *ping-pong* signature analysis did not show a prominent peak over 10nt in any data set analyzed (Figure 15 F). This outcome is in an agreement that no clear 10A bias was found in the piRNA sequence. Overall, these data indicate that loci identified as differentially methylated in Mili and Miwi2 deficient undifferentiated spermatogonia are *bona fide* piRNA producing regions in wild type fetal gonadocytes, where piRNAs originating from these loci are mostly primary in nature, especially those that are bound by Miwi2.

A residual amounts of piRNA is present in Mili$^{Null/Null}$ fetal gonadocytes

In this study we have shown that 1) Mili mutant mice do not possess the same severity of germ cell loss as Miwi2 mutant mice; 2) the absence of Miwi2 results in a greater loss of methylation of repetitive elements as compared to Mili; 3) we have identified of 1704 loci, which methylation depends only on Miwi2. All these data lead to a hypothesis that Miwi2 has a function that extends further than its canonical Mili-limited role in transposon silencing. We sought to address this discrepancy by looking into piRNA production in the absence of Mili. To this end, total small RNA libraries were prepared and sequenced from E16.5 WT and Mili$^{Null/Null}$ fetal testes. miRNAs present in the libraries were used for normalization, since the impairment of piRNA pathway in Mili deficient testes does not affect miRNA levels. The size distribution analysis confirmed that the levels of miRNAs (21-24 nt in length) have remained the same between WT and Mili$^{Null/Null}$ samples (Figure 16 A). In contrast, the levels of piRNAs (26-32 nt in length) in Mili$^{Null/Null}$ fetal testes were highly compromised (Figure 16 A, B). Nonetheless, a residual amount of piRNAs were still present in Mili$^{Null/Null}$ fetal testes, which was calculated to be 17% of the WT sample. When genomic origin of piRNAs in Mili$^{Null/Null}$ sample was analyzed, it was evident that piRNAs against LINE1 element were affected the least, some piRNAs against SINE element and LTR were still present, while IAP piRNAs had the greatest decrease (Figure 16 C). piRNA biology regarding silencing of LINE1 and IAP elements has been investigated the most, therefore, we have focused our attention in analyzing piRNAs made against LINE1 and IAP transposable elements. After

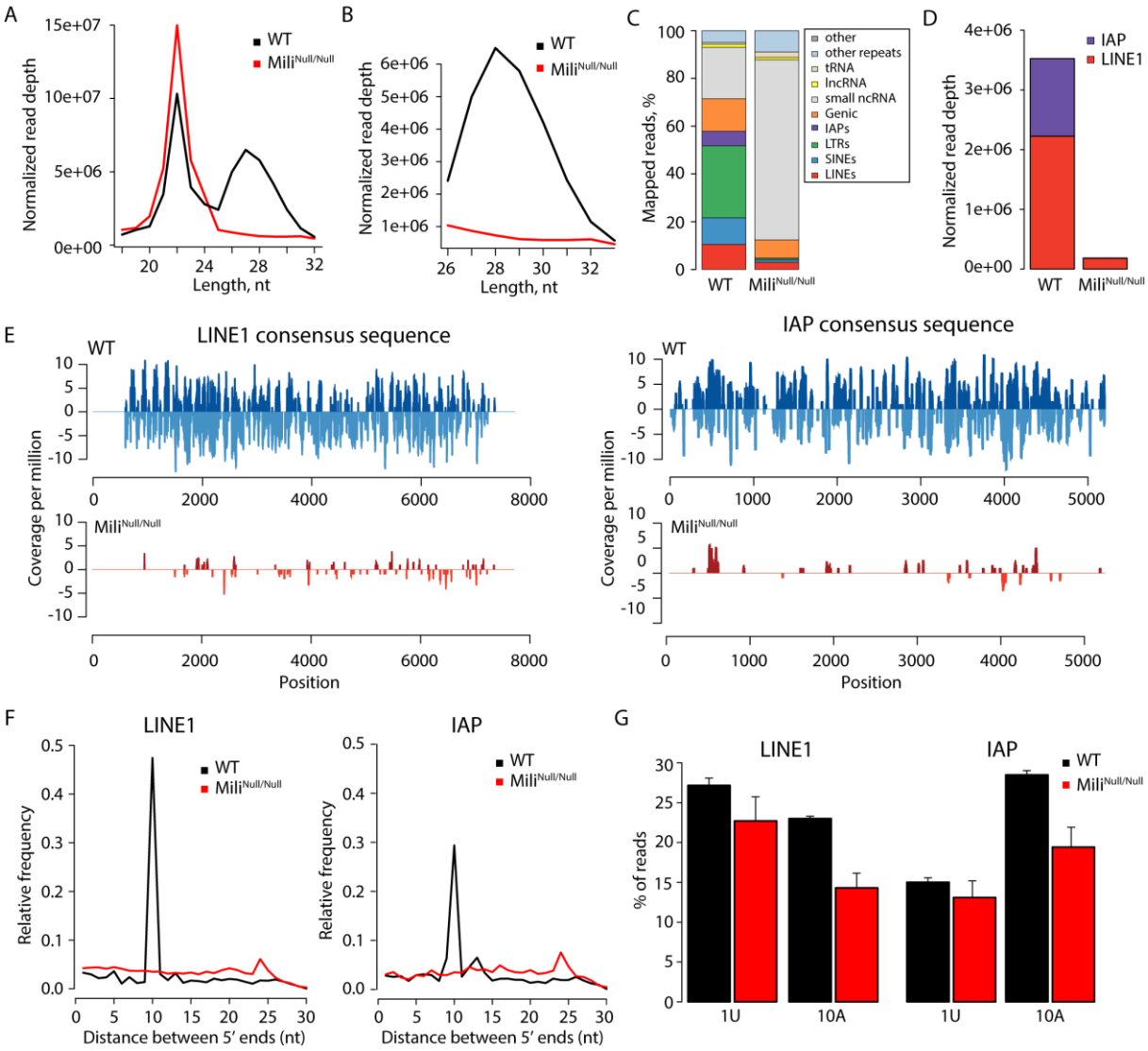

Figure 16. Residual amounts of primary piRNAs are made in the absence of Mili

(A) A size distribution of small RNAs from wild type (WT) and Mili$^{Null/Null}$ E16.5 fetal testes.

(B) A size distribution of piRNAs from wild type (WT) and Mili$^{Null/Null}$ E16.5 fetal testes.

(C) Genomic annotation of piRNAs from wild type (WT) and Mili$^{Null/Null}$ E16.5 fetal testes.

(D) Amount of anti-LINE1 and anti-IAP piRNAs in wild type (WT) and Mili$^{Null/Null}$ E16.5 fetal testes.

(E) piRNAs mapped to LINE1 (left panel) and IAP (right panel) consensus sequence allowing 3 mismatches in wild type (WT) (blue) and Mili$^{Null/Null}$ (red) E16.5 fetal testes.

(F) A *ping-pong* cycle analysis: an overlap between anti-LINE1 (left) and IAP (right) piRNA 5' ends in wild type (WT) and Mili$^{Null/Null}$ E16.5 fetal testes.

(G) Percentage of anti-LINE1 (left) and anti-IAP (right) piRNAs that have U at their first position without A at the tenth position and A at the tenth position without U at the first position in wild type (WT) and Mili$^{Null/Null}$ E16.5 fetal testes.

analyzing IAP and LINE1 piRNAs it was noticed that the expression of LINE1 piRNAs was reduced 12-fold, whereas, the production of IAP piRNAs dropped dramatically and made up only a small proportion of piRNAs (Figure 16 D). Nonetheless, we have confirmed presence of both LINE1 and IAP piRNAs by mapping piRNAs to LINE1 and IAP consensus sequence allowing 3 mismatches (Figure 16 E). Further analysis indicated that, as expected, LINE1 and IAP piRNAs found in Mili-deficient fetal testes were not generated in a *ping-pong* amplification cycle, since no overlap between 5' ends was identified (Figure 16 F). This data is consistent with the decrease in LINE1 and IAP piRNAs species having 10A because most of 10A piRNAs are secondary and made in a *ping-pong* cycle (Figure 16 G). All in all, these data indicate that even in the absence of Mili small amounts of piRNAs are made to defend against transposable elements. Moreover, those piRNAs that are present in Mili$^{Null/Null}$ fetal testes are most likely made only by primary biogenesis.

Mili deficient piRNAs are made from Miwi2-dependent loci

Having discovered the residual production of piRNAs against LINE1 and IAP in the absence of Mili, we sought to find out whether piRNAs that are present in Mili$^{Null/Null}$ fetal testes are cognate to 1704 Miwi2-dependent and 258 Mili-dependent loci that were identified in WGBS analysis. Firstly, we have mapped all piRNAs from WT and Mili$^{Null/Null}$ libraries to aforementioned loci. Indeed, we have discovered that even though overall mapping density is greatly reduced as compared to a wild type sample, there are a significant number of mainly Miwi2-dependent loci that produce piRNA in Mili$^{Null/Null}$ fetal testes (Figure 17 A, B). In this analysis we have noticed that some piRNAs from Mili$^{Null/Null}$ libraries also mapped to Mili-dependent loci. We hypothesized that those piRNAs that mapped to Mili-dependent loci are probably piRNAs that map to multiple positions in the genome, therefore, are not specific to these loci. Thus, we had re-analyzed our data by taking into consideration only uniquely mapping piRNAs. As expected, almost no unique piRNAs were found to map Mili-dependent loci, while Miwi2-dependent loci still showed a significant production of piRNAs, even though overall piRNA mapping density was reduced from both WT and Mili$^{Null/Null}$ libraries (Figure 17 C, D). In addition, it was noticed that some loci in Mili$^{Null/Null}$ sample had even higher number of reads mapping as compared to a WT sample (Figure 2.5 E, F, overproducing loci are indicated by arrows). To have a better overview of the amount of piRNA production still present in Mili knock-out gonadocytes, piRNA density per 1kb was calculated across 1704 Miwi2-dependent and 258 Mili-dependent loci. piRNA density dropped in Mili$^{Null/Null}$ libraries 2-fold and 3-fold across Miwi2-dependent loci counting all

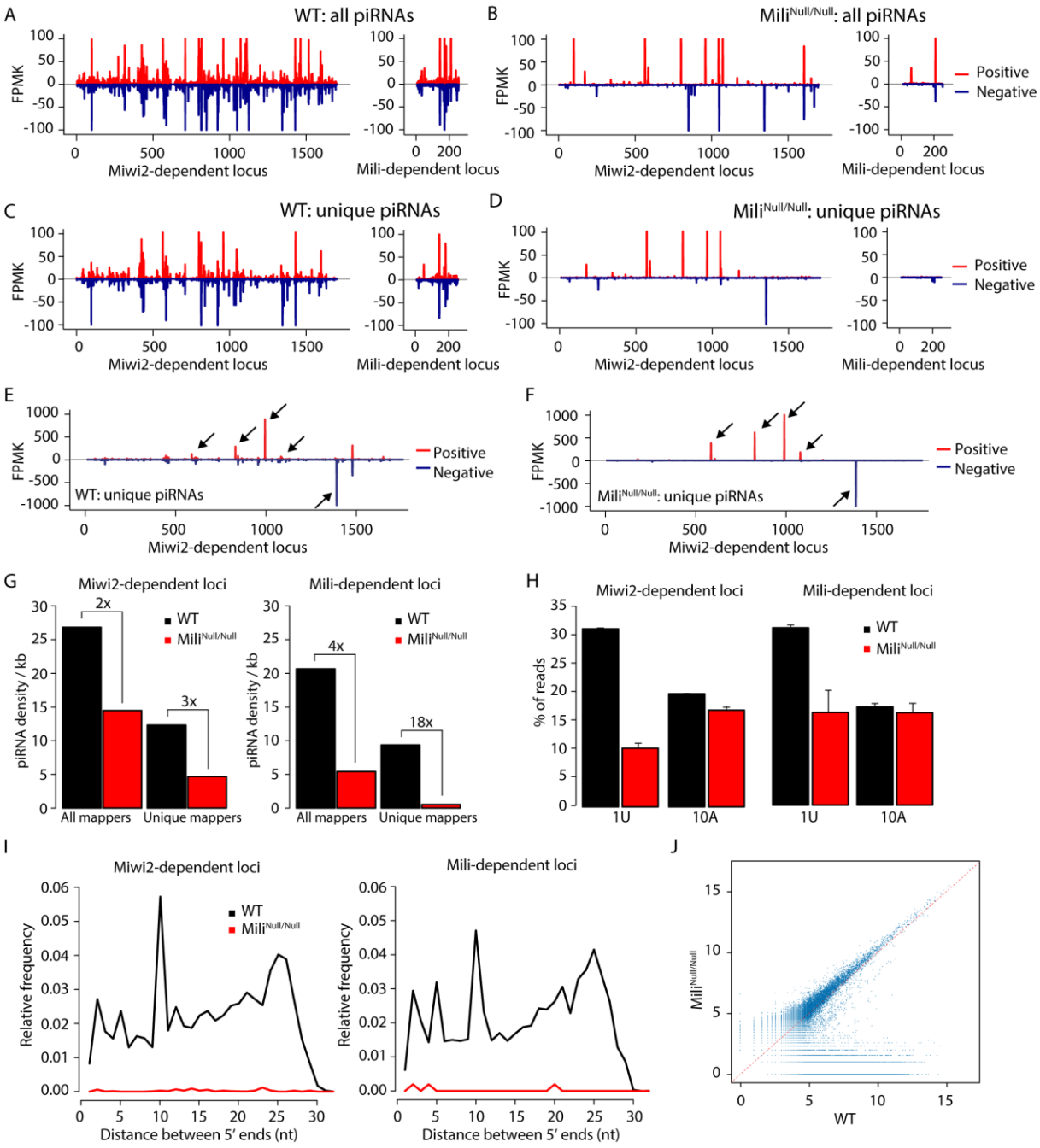

Figure 17. Mili deficient piRNAs are made from Miwi2-dependent loci

(A) Mapping of all piRNAs from wild type (WT) E16.5 fetal testes to 1704 Miwi2-dependent and 258 Mili dependent loci. One peak represents one locus.

(B) Mapping of all piRNAs from Mili$^{Null/Null}$ E16.5 fetal testes to 1704 Miwi2-dependent and 258 Mili dependent loci. One peak represents one locus.

(C) Mapping of unique piRNAs from wild type (WT) E16.5 fetal testes to 1704 Miwi2-dependent and 258 Mili dependent loci. One peak represents one locus.

(D) Mapping of unique piRNAs from Mili$^{Null/Null}$ E16.5 fetal testes to 1704 Miwi2-dependent and 258 Mili dependent loci. One peak represents one locus.

(E) Loci producing most of the piRNAs in wild type (WT) E16.5 fetal testes.

(F) Loci over-producing piRNAs in Mili$^{Null/Null}$ E16.5 fetal testes as compared to the wild type (WT). Over-producing loci are pointed by arrows.
(G) All and unique piRNA density in Miwi2- (left) and Mili-dependent (right) loci in wild type (WT) and Mili$^{Null/Null}$ E16.5 fetal testes.
(H) Percentage of piRNAs, which mapped to Miwi2- and Mili-dependent loci, that have U at their first position without A at the tenth position and A at the tenth position without U at the first position in wild type (WT) and Mili$^{Null/Null}$ E16.5 fetal testes.
(I) A *ping-pong* cycle analysis: an overlap between piRNA, which mapped to Miwi2- and Mili-dependent loci, 5' ends in wild type (WT) and Mili$^{Null/Null}$ E16.5 fetal testes.
(J) piRNA expression analysis between wild type (WT) and Mili$^{Null/Null}$ E16.5 fetal testes.

and unique piRNAs respectively, while the piRNA density in Mili$^{Null/Null}$ libraries reduced 4-fold and 18-fold across Mili-dependent loci counting all and unique piRNAs respectively (Figure 17 G).

To get an insight how Mili knock-out piRNAs are made, we have analyzed 1U and 10A content of the piRNAs that mapped to Miwi2- and Mili-dependent loci. Interestingly, the only evident change in Mili$^{Null/Null}$ piRNAs was a significant decrease of piRNAs that have 1U (Figure 17 H). Moreover, no *ping-pong* signature was detected amongst Mili$^{Null/Null}$ piRNAs. Even though in WT sample some piRNAs had a 5' 10nt overlap (a peak at 10nt) it was not a predominant piRNA species (Figure 17 I). It is possible that not enough piRNAs were taken into analysis to get a clear *ping-pong* signature in WT. Overall, we have confirmed that Mili$^{Null/Null}$ piRNAs are not generated in a *ping-pong* cycle. However, the decrease in 1U piRNAs in Mili$^{Null/Null}$ libraries as compared to a WT sample indicates that some piRNAs could be made in a different way than canonical primary processing, which results in 1U bias. Previously we identified that LINE1 and IAP piRNAs in Mili-deficient fetal testes are likely to be made by primary biogenesis pathway, when piRNAs are processed from transposon mRNA. However, we could not exclude the possibility that other piRNAs are made aberrantly from different sources of RNA. To test this we have analyzed an expression of individual piRNAs that have been annotated in piRNA Bank in the WT and in Mili$^{Null/Null}$ libraries. The expression analysis has revealed that the all piRNAs that are made in Mili deficient fetal testes are also produced in WT fetal testes (Figure 17 J), indicating that in the absence of Mili, piRNA biogenesis machinery is able to produce minimal amounts of piRNAs that would also be made in the wild type situation. To sum up, we have shown that in Mili$^{Null/Null}$ fetal testes piRNAs originate from Miwi2-dependent loci and reflect wild type piRNAs even though greatly reduced in numbers.

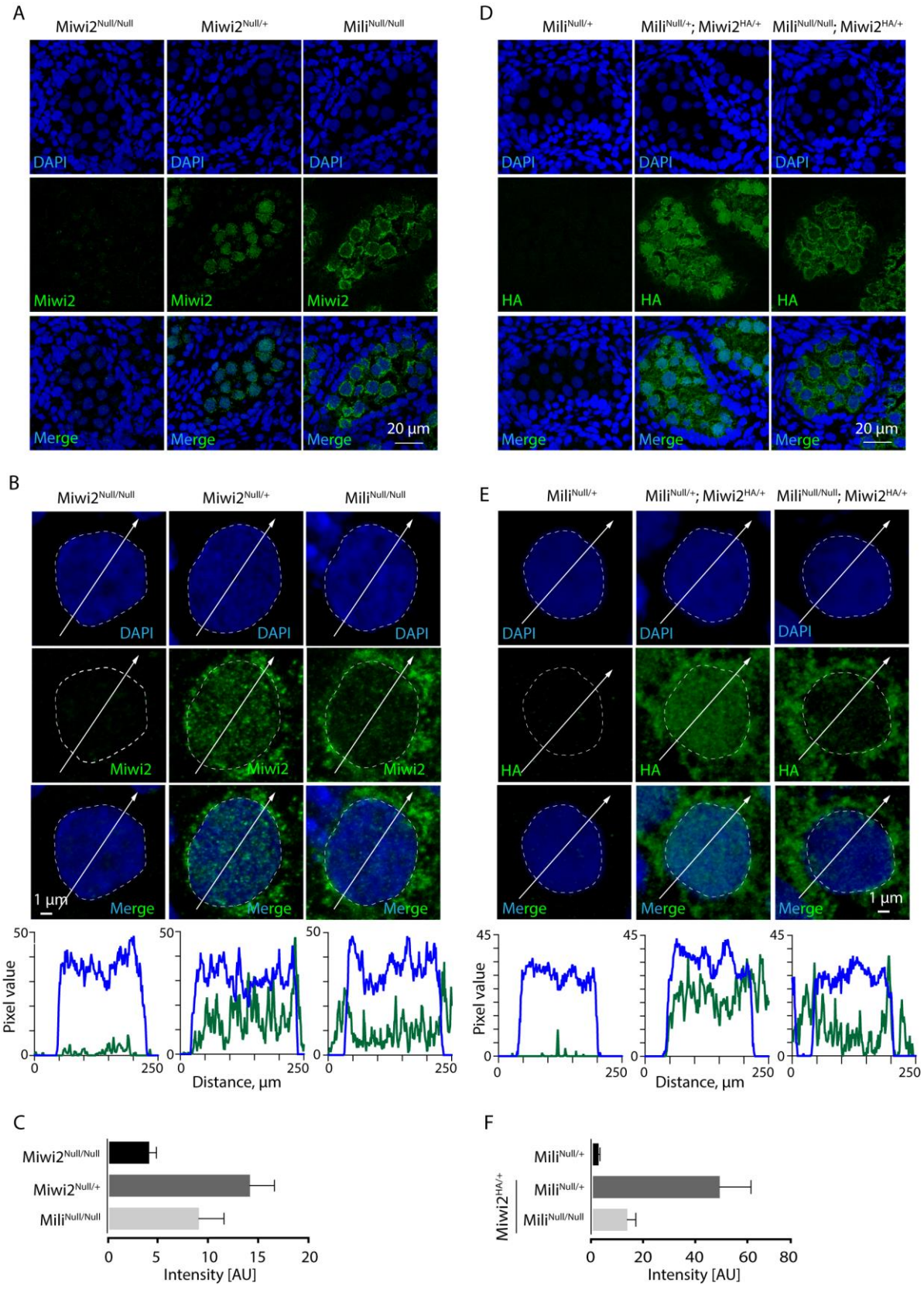

Figure 18. Miwi2 partially retains its nuclear localization in the absence of Mili

(A) Immunofluorescence analysis with anti-Miwi2 antibody on Miwi2$^{Null/Null}$, Miwi2$^{Null/+}$ and Mili$^{Null/Null}$ E16.5-E17.5 fetal testicular cross-sections. A tubule is shown.

(B) Immunofluorescence analysis with anti-Miwi2 antibody on Miwi2$^{Null/Null}$, Miwi2$^{Null/+}$ and Mili$^{Null/Null}$ E16.5-E17.5 fetal testicular cross-sections. A single fetal gonadocyte is shown. Scan-line

profiles (bottom panel) of corresponding genotypes is shown: blue represents DAPI signal, green - Miwi2 signal.

(C) A quantification of anti-Miwi2 fluorescence signal in the nucleus in Miwi2$^{Null/Null}$, Miwi2$^{Null/+}$ and Mili$^{Null/Null}$ E16.5-E17.5 fetal testicular cross-sections.

(D) Immunofluorescence analysis with anti-HA antibody on Mili$^{Null/+}$, Mili$^{Null/+}$; Miwi2$^{HA/+}$ and Mili$^{Null/Null}$; Miwi2$^{HA/+}$ E16.5-E17.5 fetal testicular cross-sections. A tubule is shown.

(E) Immunofluorescence analysis with anti-HA antibody on Mili$^{Null/+}$, Mili$^{Null/+}$; Miwi2$^{HA/+}$ and Mili$^{Null/Null}$; Miwi2$^{HA/+}$ E16.5-E17.5 fetal testicular cross-sections. A single gonadocyte is shown. Scan-line profiles (bottom panel) of corresponding genotypes is shown: blue represents DAPI signal, green - Miwi2 signal.

(F) A quantification of anti-HA fluorescence signal in the nucleus in Mili$^{Null/+}$, Mili$^{Null/+}$; Miwi2$^{HA/+}$ and Mili$^{Null/Null}$; Miwi2$^{HA/+}$ E16.5-E17.5 fetal testicular cross-sections.

Miwi2 partially retains nuclear localization in absence of Mili

Given that some piRNAs are made in the absence of Mili, where at least some of them are against transposable elements, we were hypothesizing that they are most likely to be bound by Miwi2. Therefore, we re-addressed Miwi2's cellular localization in fetal gonadocytes in the absence of Mili. In wild type fetal gonadocytes Miwi2 is found in the nucleus and cytoplasm. In cytoplasm Miwi2 is retained in perinuclear granules, called Pip-bodies, due to their overlap with P-bodies (Aravin *et al.*, 2009). In the absence of Mili, Miwi2 is not loaded with piRNA. PiRNA-free Miwi2 is not licensed to enter the nucleus and is retained in the cytoplasm (Aravin *et al.*, 2008). To research this question, an immunofluorescence was performed on E16.5-E17.5 Miwi2$^{Null/+}$ and Mili$^{Null/Null}$ fetal gonadocytes with antibody recognizing Miwi2. Miwi2$^{Null/Null}$ fetal gonadocytes samples were used as a negative control (Figure 18 A, B). It was noticed that in Miwi2$^{Null/+}$ (=WT) fetal gonadocytes Miwi2 is localized in cytoplasmic granules surrounding the nucleus as well as in the nucleus as has been published previously (Aravin *et al.*, 2008; De Fazio *et al.*, 2011). However, after a careful investigation a few distinctive Miwi2 foci were identified in the nucleus of Mili$^{Null/Null}$ fetal gonadocytes, even though most of the Miwi2 was found relocated in the cytoplasm. (Figure 18 B). Line-scan profiles, which evaluate a relative color intensity of pixels along the line, have confirmed that indeed Miwi2 is present in the nucleus in the absence of Mili (Figure 18 B, bottom panel). Overall quantification of Miwi2 signal intensity in the nucleus was evaluated over three biological replicates, analyzing approximately 150 fetal gonadocytes in total (Figure 18 C). Even though it was evident that Miwi2 retains its nuclear localization in the absence of Mili, quantification showed quite high background staining in the negative control, rendering the results to be less reliable. Therefore, the same

type of analysis was done using *Miwi2*^{HA} allele, where an immunofluorescence was performed on E16.5-E17.5 Mili$^{Null/+}$; Miwi2$^{HA/+}$ and Mili$^{Null/Null}$; Miwi2$^{HA/+}$ fetal gonadocytes with antibody recognizing HA, where Mili$^{Null/+}$ fetal gonadocytes were used as a negative control (Figure 18 D, E). As expected, the same results were recapitulated taking this approach. Quantification of HA-Miwi2 signal intensity in the nucleus has clearly shown that a small, but recognizable portion of Miwi2 is present in the nucleus in the absence of Mili (Figure 18 F). In addition to his, the question of Mili localization in the absence of Miwi2 was addressed. It was confirmed that the loss of Miwi2 does not affect Mili localization (Figure 19 A, B) (Aravin *et al.*, 2008). In summary, Mili localization does not seem to be dependent on Miwi2, yet Miwi2 localization is affected by the loss of Mili, but only partially.

In this study we show that Mili is also required for germ cell maintenance, but presents a weaker phenotype than Miwi2 with only partial loss of the germ line observed in aged mice. It is proposed that Miwi2 function and localization depends on Mili, however, we found that a residual piRNAs biogenesis pathway exists in the absence of Mili that underpins a partial Miwi2 function. Consequently, we identified that a portion of Miwi2 retains its nuclear localization in the absence of Mili in reprogramming fetal gonadocytes. In summary, a primary piRNA biogenesis pathways exist in mouse that contribute to both germ line reprogramming and maintenance.

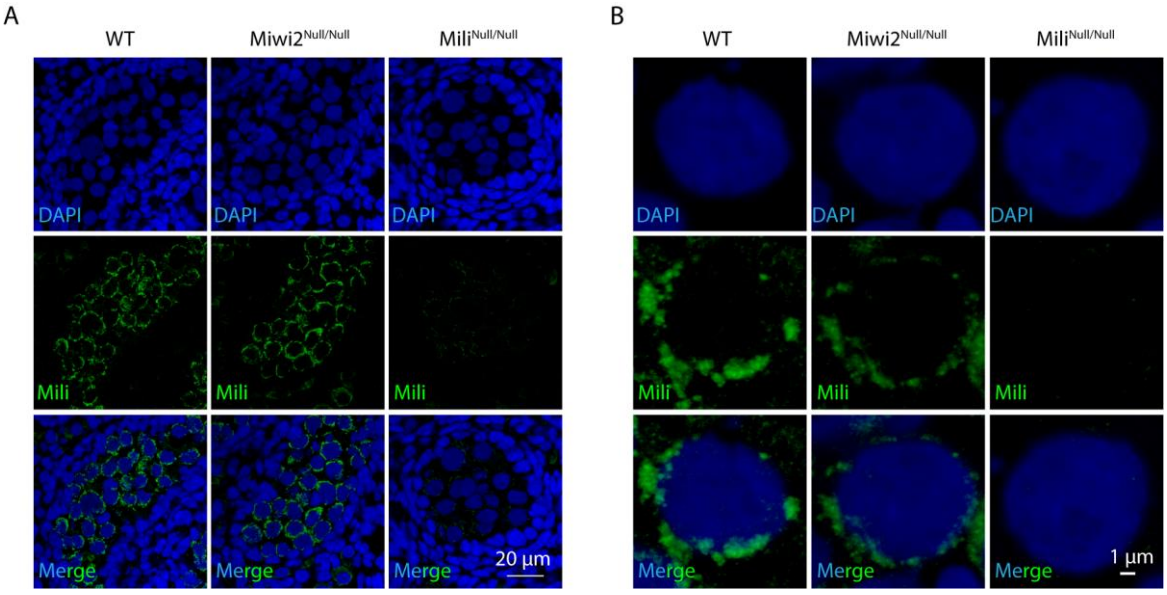

Figure 19. Miwi2 does not influence the localization of Mili

(A) Immunofluorescence analysis with anti-Mili antibody on wild type (WT), Miwi2$^{Null/Null}$ and Mili$^{Null/Null}$ E16.5-E17.5 fetal testicular cross-sections. A tubule is shown.

(B) Immunofluorescence analysis with anti-Mili antibody on wild type (WT), Miwi2$^{Null/Null}$ and Mili$^{Null/Null}$ E16.5-E17.5 fetal testicular cross-sections. A single gonadocyte is shown.

Discussion

Here we have concluded that Mili-deficient mice do not possess an identical phenotype to Miwi2 mutant mice in germline maintenance. The difference between the two phenotypes can be explained by molecular functions of Mili and Miwi2 in piRNA pathway. We have determined that in the absence of Mili a residual amount of primary piRNAs is produced. Additionally, Miwi2 partially retains its nuclear localization in Mili deficient fetal gonadocytes. Therefore, the remaining piRNAs are sufficient to guide Miwi2 to certain loci in the genome. Indeed, the methylation levels in spermatogonia precursor cells were found to be lower in Miwi2 mutant mice than in Mili mutant mice. Thus, in contrast to prevailing piRNA biogenesis model, we have identified a primary piRNA biogenesis pathway that exists in the absence of Mili and results in loading primary piRNAs to Miwi2.

Mili mutant mice partially lose germline

Miwi2-deficient mice were shown to exhibit a progressive germ cell loss (Carmell *et al.*, 2007). Seminiferous tubules of Miwi2 mutant mice at the age of nine months contain almost no germ cells, by the age of twelve month all seminiferous tubules are empty (Carmell *et al.*, 2007; De Fazio *et al.*, 2011). On the other hand, Mili mutant mice at the age of twelve months still retain 50% of seminiferous tubules on average that have at least one type of germ cell present. It was noticed though that this phenotype is prone to variability. Some Mili mutant mice had only 20% of tubules with germ cells, while some as much as 60%. Unhavaithaya and colleagues reported that Mili-deficient mice completely lose germ cells, including spermatogonia by the age of six months (Unhavaithaya *et al.*, 2009). However, in the figures provided of hematoxylin and eosin stained testicular cross-sections of aged Mili mutant mice some spermatogonia were evidently present, as also indicated by the authors. Therefore, their initial statement is not correct. Additionally, in this study if at least one spermatogonium was found in the tubule it was not counted as empty. The most primitive spermatogonia stained with hematoxylin and eosin display rather even nuclear staining, which is slightly darker than somatic Sertoli cells. To locate and recognize these cells requires extensive screening of the basal layer of the seminiferous tubules under the microscope. Moreover, Mili mutant phenotype, as noted, can be rather variable. In this study mice that had high percentage of tubules with germ cells showed rather pronounced appearance of meiotic

cells as well (mainly preleptotene/leptotene). It is not clear how many mice were analyzed in the study of Unhavaithaya and colleagues. All in all, here we performed a comprehensive analysis of aged Mili-deficient mice and determined that Mili is important in spermatogonial stem cell maintenance, but does not cause a complete exhaustion of the stem cell pool.

Mili and Miwi2 contribution to DNA methylation

In mouse embryonic gonadocytes Miwi2, but not Mili is found in the nucleus. Therefore, it is proposed that Miwi2 guides the methylation of TE sequences, while cytoplasmic Mili amplifies piRNAs in a *ping-pong* cycle. A recent study has proposed that Mili influences methylation of more TE families than Miwi2 and that effect of Miwi2 deletion has rather mild loss of DNA methylation (Manakov *et al.,* 2015). Additionally, another study revealed that LTR transposons seemed to be less dependent on Miwi2 than Mili, which is the main difference between the two Piwi proteins (Nagamori *et al.*, 2015). Here we have presented that the loss of Miwi2 has more detrimental effect on methylation in juvenile undifferentiated spermatogonia than the loss of Mili. The discrepancy between the studies could have arisen from different target population analyzed. Manakov and colleagues have purified EpCAM expressing spermatogonia from 10-day-old Miwi2 and Mili mutant mice with 50% reported purity (Manakov *et al.*, 2015; Pezic *et al.*, 2014). Therefore, analyzed population likely contained not only spermatogonia, but also somatic and meiotic cells, since first leptotene spermatocytes are present at postnatal day 10 (Bellve *et al.*, 1977). Furthermore, EpCAM was shown not to be highly enriched in spermatogonia population (Kanatsu-Shinohara *et al.*, 2011), but is strongly expressed in c-Kit^{pos} differentiated spermatogonia (Carrieri and O'Carroll, unpublished data). On the other hand, Nagamori and colleagues used Oct4-GFP transgenic mice to sort spermatogonia from 10-day-old Miwi2 and Mili mutant mice. At this stage of spermatogenesis Oct4 is expressed only in a sub-population of spermatogonia, moreover, it is also present in c-Kit differentiated cells (Li *et al.*, 2015; Ohbo *et al.*, 2003). Here we have acquired highly pure population of undifferentiated spermatogonia from juvenile mice at postnatal day 14 using multi-parametric (CD45^{neg} CD51^{neg} c-Kit^{neg} Miwi2-Tom^{pos} CD9^{pos}) flow cytometry based sorting. Additionally, Manakov and colleagues have reported that Miwi2 is required for repression of three families of transposable elements. However, correlated data between transposon expression levels with the degree of the loss in DNA methylation has shown changes in seven different transposable element families in Miwi2 mutant mice. The same type of correlation analysis was not presented for Mili-deficient mice. Thus, it is plausible that Miwi2 contribution to DNA methylation was underestimated in the study mentioned (Manakov *et al.*, 2015). Nagamori

and colleagues have analyzed methylation levels of 115 transposable elements (22 LINEs and 93 LTRs). A hundred and fifteen TEs were taken into analysis due to their promoter regions being close to a consensus sequence, therefore, such transposons are more likely to be potentially active. Authors have shown that a significant number of LTRs they analyzed were methylated independently of piRNA pathway, which indicates that those transposable elements are non-active remnants and are silence by DNA methylation machinery by "default" (Molaro *et al.*, 2014) and the actual analysis of TE methylation influenced by Mili and Miwi2 must have been less than 115. In our study we took a global DNA methylation analysis approach and presented more comprehensive data for different classes and families of transposable elements as well as different genic regions. This approach allowed us to understand overall contribution of Mili and Miwi2 to DNA methylation, however, such events like piRNA-independent LTR element methylation was not evident. Nonetheless, we wished to understand to what degree Mili and Miwi2 reinforce DNA methylation. We found that Miwi2 loss has greater impact on transposable element methylation in comparison to Mili mutant. Nagamori *et al*. (2015) indicated that Miwi2 is more important for methylation of LINE than LTR elements and overall number of TEs affected was less than in Mili mutant, even though the loss of methylation of LTR elements was claimed to be affected in a similar manner in both Mili and Miwi2 deficient cells. In our study we did not see such a great difference between LINE and LTR transposon methylation in Miwi2 mutant (possibly due to a more global approach). However, analyzing transposon expression data obtained from sorted juvenile spermatogonia, we identified more upregulated IAPs (LTR type transposons) than LINEs (data not shown). This result is also in accordance with immunofluorescence studies (Figure 25 D) (Di Giacomo *et al.*, 2013). Nagamori and colleagues data could be skewed due to a limited number of TEs analyzed, out of which some were piRNA methylation independent. Nonetheless, we have found that Mili and Miwi2 both equally contribute to methylation of many different DMRs (Figure 14 D, E). Interestingly, we have identified 1704 loci which methylation is dependent on Miwi2 and 258 loci which methylation is dependent on Mili. Currently it is not clear how Mili exerts its effect on DNA methylation that would be Miwi2-independent, since Miwi2 is the only nuclear Piwi protein in fetal gonadocytes at the time of *de novo* DNA methylation (Aravin *et al.*, 2008). On the other hand, the fact that Miwi2 is responsible for methylation of 1704 loci, which methylation apparently is Mili-independent, suggests that Miwi2 function in the piRNA pathway does not fully depend on Mili as previously thought.

Primary Mili-independent piRNA biogenesis pathway loads Miwi2 priming for partial reprogramming activity

Current piRNA biogenesis model in mice claims that Mili initiates piRNA production from transposon mRNA. Mili bound with transposon-derived piRNA further on targets piRNA precursor transcript to generate antisense secondary piRNA. Antisense secondary piRNAs are bound by Mili and Miwi2. When Miwi2 is loaded with piRNA, it is translocated into the nucleus, while Mili functions in a *ping-pong* cycle to amplify piRNA in abundance by targeting transposon mRNA and then again piRNA precursor transcript. Therefore, in this model the relationship between Mili and Miwi2 is almost linear: Mili generates piRNAs, Miwi2 "accepts" antisense piRNAs generated by Mili cleavage events. It was shown that in the absence of Mili neither Mili nor Miwi2 are loaded with piRNAs, moreover, Miwi2 is retained in the cytoplasm (Aravin *et al.*, 2008). However, the data obtained in our study indicates that Miwi2 has Mili-independent functions as well, which were discovered analyzing Mili-deficient fetal testes. We have shown that piRNA pathway does not completely collapse in the absence of Mili. A residual amount of piRNAs are still made in Mili-deficient mice, which could have been easily missed in previous studies due to a low abundance. We hypothesize that Mili-mutant piRNAs are made by primary processing and are loaded in Miwi2 since primary processing pathway should not be affected by the loss of Mili. Overall, it is not well understood how Miwi2 is loaded with piRNAs even in the presence of Mili. It was shown that the proper assembly of pi-bodies and Pip-bodies and their components is important for secondary piRNA production and Miwi2 loading (Aravin *et al.*, 2009; Yang *et al.*, 2016; Kuramochi-Miyagawa *et al.*, 2010; Shoji *et al.*, 2009; Xiol *et al.*, 2012). In the absence of Mili, many nuage components are mislocalized (Aravin *et al.*, 2009; Shoji *et al.*, 2009; Vagin *et al.*, 2009), however, it is possible that some piRNA pathway components, in spite of not being "concentrated" in perinuclear granules, can assemble and execute their primary function, even though very inefficiently. The hypothesis that Mili-mutant piRNAs are mostly made by primary processing is confirmed by the fact that most of the piRNAs that map to Miwi2-dependent (and therefore Mili-independent) loci show a pronounced 1U bias and dot not show a *ping-pong* signature in unperturbed testes. 1U bias is reduced in Mili-mutant piRNAs that map to Miwi2-dependent loci, however, this outcome could be skewed by the low abundance of these piRNAs. Despite the low abundance, a significant amount of piRNAs derived against transposable elements were identified. The least affected group by Mili deletion was LINE1-derived piRNAs, while IAP-derived piRNAs were greatly reduced. Interestingly, both antisense and sense LINE1 piRNA were found, while IAP-derived piRNAs were mostly in sense orientation (Figure 16 E). The *pong-pong*

amplification does not function in Mili mutant testes (Figure 16 F), and Miwi2 is not catalytically active (De Fazio *et al.*, 2011; Nakanishi *et al.*, 2012), therefore, it is possible that both primary transcript and transposon mRNA enter primary processing. In this way some transposon mRNAs are cleave and neutralized to make piRNAs. Also, piRNAs cleaved from precursor transcript are antisense and can guide DNA methylation of transposable elements. Indeed, Miwi2 was found to partially retain its nuclear localization in absence of Mili. Miwi2 presence in the nucleus in Mili mutant fetal gonadocytes was confirmed using two independent antibodies – against Miwi2 and against HA. Reliable antibodies against HA have been developed, therefore, this gives us confidence that our produced results related to Miwi2 localization in the absence of Mili are solid. Thus, a minimal defense against transposable elements is mounted post-transcriptionally and transcriptionally, which correlates with the bisulfite sequencing data showing that the loss of Mili does not impact DNA methylation as much as Miwi2 loss does. Overall, in the absence of Mili, the piRNA pathway seems to function the same way as in the wild type testes, just in a very limited capacity. We did not detect non-typical piRNA species, when piRNAs that are made in Mili mutant were compared with piRNAs that are found in the wild type testes. For this comparison piRNAs that are annotated in piRNA bank (Sai Lakshmi and Agrawal, 2008) were used. We do not rule out the possibility that other cellular transcripts can enter piRNA pathway and more stringent analysis will be performed. However, piRNA annotation did not show an increase in piRNA species derived from genic regions in Mili-deficient fetal testes (Figure 16 C).

To summarize, we have shown that Mili-mutant mice do not lose germline in the same manner as Miwi2-mutant mice do. Both Mili and Miwi2 are involved in the piRNA pathway, where Miwi2 function was implied to depend on Mili. Thus, the phenotype discovered raised a question how Miwi2 being downstream of Mili can have more severe testicular phenotype. Here we show that the difference between the two phenotypes can be explained by rudimentary primary piRNA production pathway that loads piRNAs into Miwi2, which enables Miwi2 function independently of Mili. In the absence of Mili most of the piRNA production is ceased, however, Miwi2 still retains partial nuclear localization and reprogramming activity. This correlates with the fact that some piRNAs are still being made in Mili mutant testes, even if very inefficiently. Thus, all piRNA pathway components are required for robust transposon activity suppression. However, in the absence of Mili and piRNA amplification by *ping-pong*, primary piRNA pathway can minimally contribute to *de novo* DNA methylation as long as there is a nuclear Piwi protein.

Embryonic germ cell reprogramming is essential for establishment of the spermatogonial precursor cell gene expression program

Summary

Miwi2 and Dnmt3L are involved in *de novo* DNA methylation in fetal gonads. Miwi2 and Dnmt3L mutant mice exhibit a depletion of germline with age. Dnmt3L mutant mice completely lose germ cells within a two-month period, while Miwi2 mutant mice exhibit Sertoli-only phenotype at nine-month of age. The phenotype of both reprogramming mutants indicates Miwi2 and Dnmt3L's possible role in germline maintenance. In this study we have shown that the main role of Miwi2 and Dnmt3L in establishing and maintaining the population of undifferentiated spermatogonia precursor cell population in the adult is executed through their role in reprogramming fetal gonadocytes. We have observed that even though Miwi2- and Dnmt3L-deficient spermatogonial precursor cells exhibit transposon de-repression, no apparent loss these cells can be associated with DNA damage. We hypothesize that actively transcribed TE containing locus generates hybrid transcripts triggering abnormal gene expression program in spermatogonia stem cells, which leads to a great reduction in the numbers of actual GFRa1^{pos} stem cells observed n Miwi2 and Dnmt3L mutant testis. Overall, this study shows the importance of germ cell reprograming in establishing a healthy, functional stem cell population in the adult tissue.

Reprogrammierung von embryonalen Keimzellen ist essentiell für die Etablierung eines Spermatogonien-Vorläufer Genexpressions-Programm

Zusammenfassung

Miwi2 und Dnmt3L sind in der *de novo* DNA Methylierung DNA in fötalen Hoden involviert. Männliche Miwi2 und Dnmt3L knockout Mäuse zeigen einen Verlust der männlichen Keimbahn im Alter. Die Dnmt3L knockout Mäuse verlieren die Keimzellen dabei innerhalb von zwei Monaten, während die Miwi2 Mutanten mit neun Monaten ein Sertoli-only Syndrom aufweisen. Beide Phänotypen weisen daher auf eine Funktion von Miwi2 und Dnmt3L in der Erhaltung der Keimbahn hin. In dieser Studie haben wir gezeigt, dass die primäre Rolle von Miwi2 und Dnmt3L in der Etablierung und Erhaltung der adulten Population undifferenzierter spermatogonialer Stammzellen in ihrer Funktion während der fötalen Reprogrammierung von Gonadozyten begründet liegt. Wir konnten demonstrieren, dass trotz deutlicher Transposon-Aktivierung in Miwi2- und Dnmt3L-defizienten Spermatogonien Vorläuferzellen der Verlust dieser Zellen nicht mit DNA Schäden korreliert werden kann. Wir stellen daher die Hypothese auf, dass ein aktiv transkribierter Transposonlocus zur Expression von hybriden Transkripten führt, die ein verändertes Genexpressions-Programm in spermatogonialen Stammzellen induzieren. Dieses wiederum würde zu einer deutlichen Reduktion an undifferenzierten GFRa1^{pos} Stammzellen im Hoden führen, wie wir sie in Miwi2 und Dnmt3L knockout Hoden beobachten. Zusammengenommen zeigt diese Studie die Bedeutung der fötalen Keimzellen-Reprogrammierung für die Etablierung einer funktionellen Stammzellpopulation in adulten Gewebe.

Embryonic germ cell reprogramming is essential for establishment of the spermatogonial precursor cell gene expression program

Miwi2 and Dnmt3L expression in the adult mouse testes

In the absence of Miwi2 or Dnmt3L male mice completely lose their germ line over time. Therefore, it is evident that Miwi2 and Dnmt3L are directly or indirectly involved in the spermatogonial stem cell maintenance. It is known that both Miwi2 and Dnmt3L are highly expressed in fetal gonadocytes during the phase of *de novo* DNA methylation of germ line reprogramming. However, we have hypothesized that Miwi2 and Dnmt3L could also be expressed in the compartment of undifferentiated spermatogonial stem cells in adult male mice. To answer this question two new alleles were generated in the lab – $Miwi2^{HA}$ and $Dnmt3L^{V5}$ (Figure 11 and Figure 8), using Crispr/Cas9 gene editing technology.

Seminiferous tubules of $Miwi2^{HA/+}$ and $Dnmt3L^{V5/+}$ adult mice were used for whole mount immunofluorescence analysis (Figure 20 B and C). Immunofluorescence analysis revealed that HA-Miwi2 expression 100% co-insides with the expression of PLZF (Figure 20 A). PLZF is a transcription factor that is expressed in a population of spermatogonial precursor cells (SPCs). A population of spermatogonial precursor cells is comprised of spermatogonial stem cells, a population which expresses GFRa1, and transit amplifying undifferentiated spermatogonia, which express Ngn3. HA-Miwi2 expression partially overlapped with GFRa1 expression pattern. Approximately 50% of A_s $GFRa1^{pos}$ spermatogonial stem cells were found to express HA-Miwi2. The percentage of overlap in A_{pr} and A_{al4} $GFRa1^{pos}$ spermatogonia was 38% and 50% respectively (Figure 20 C). Thus, about half of the $GFRa1^{pos}$ spermatogonia are also positive for HA-Miwi2. On the other hand, A_s spermatogonia that would express only HA-Miwi2, but not GFRa1 was rather rear, whereas this number increased in A_{pr} and A_{al4} spermatogonial populations (Figure 20 C). Interestingly, two distinct staining patterns regarding HA-Miwi2 localization were observed. Some HA-Miwi2 expressing cells showed strong cytoplasmic localization (Figure 20 D, upper panel), while in some cells HA-Miwi2 was predominantly nuclear (Figure 20 C, lower panel). A "transitional" phenotype where HA-Miwi2 was expressed rather strongly in both nucleus and cytoplasm was also observed. The relevance of such differences in a cellular localization is not known. Additionally, all HA-Miwi2 expressing cells we found to be c-Kit negative (Figure 3.1 A). To sum up, these data indicate that Miwi2 is expressed in the population of SPCs and likely transit amplifying cells in the adult mouse testis. There are no antibodies available raised against Ngn3, therefore it was not possible to test if HA-Miwi2 expressing cells indeed constitute a population of transit amplifying cells like Ngn3. However, judging

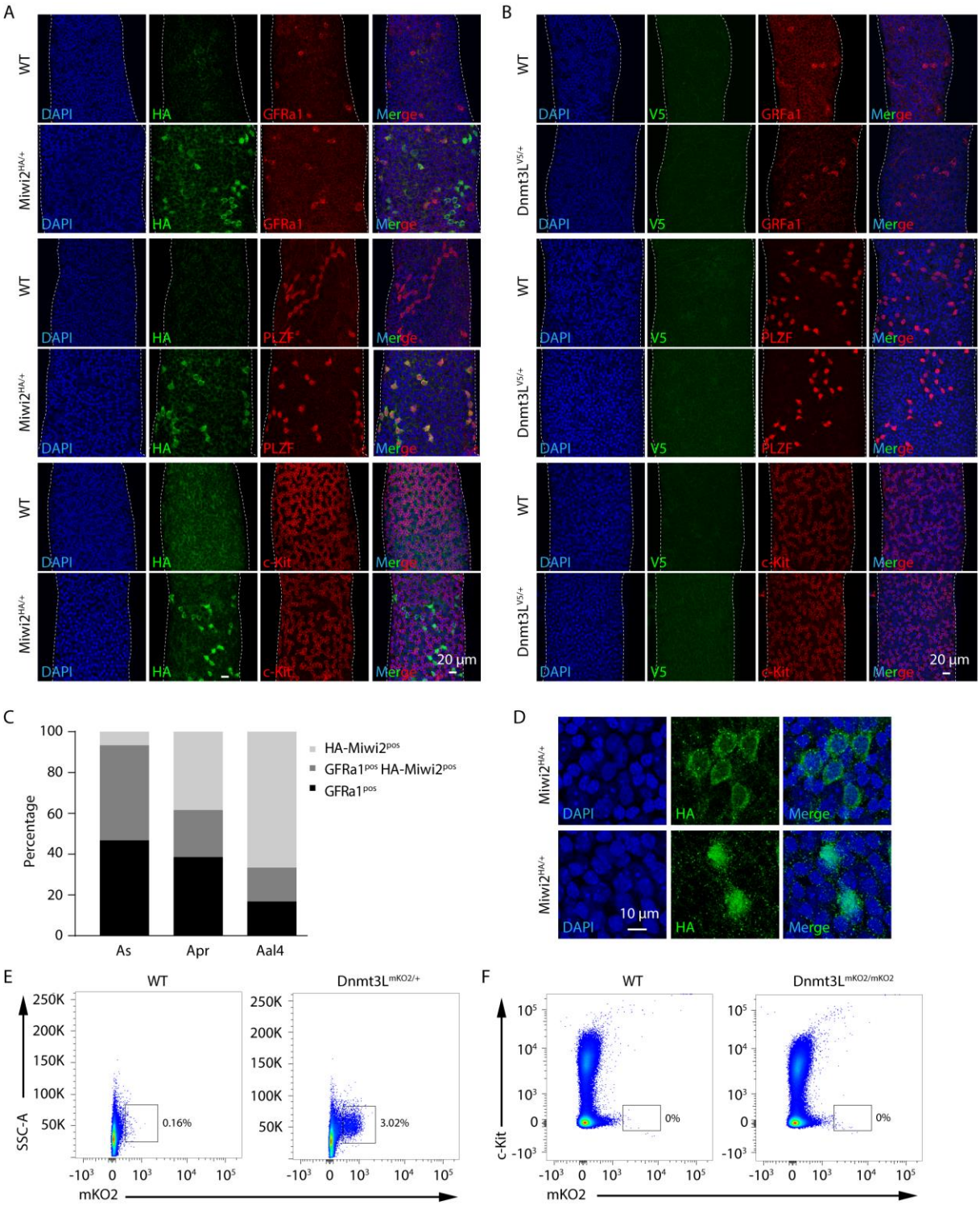

Figure 20. Miwi2, but not Dnmt3L is expressed in the adult mouse testes

(A) Whole mount immunofluorescence analysis with anti-HA antibody of wild type (WT) and Miwi2$^{HA/+}$ seminiferous tubules from adult mice.

(B) Whole mount immunofluorescence analysis with anti-V5 antibody of wild type (WT) and Dnmt3L$^{V5/+}$ seminiferous tubules from adult mice.

(C) Enumeration of GFRa1^{pos}, GFRa1^{pos}; HA-Miwi2^{pos} and HA-Miwi2^{pos} A_s, A_{pr} and A_{al4} spermatogonia in Miwi2$^{HA/+}$ mice.

(D) An example of nuclear and cytoplasmic localization of HA-Miwi2 in spermatogonia. Whole mount immunofluorescence analysis with anti-HA antibody of Miwi2$^{HA/+}$ seminiferous tubules from adult mice.

(E) Flow cytometry analysis of E16.5 fetal testes from wild type (WT) and Dnmt3L$^{mKO2/+}$ mice.

(F) Flow cytometry analysis of testes from adult wild type (WT) and Dnmt3L$^{mKO2/+}$ mice.

from the fact that HA-Miwi2 expression completely overlaps with PLZF and partially with Gfra1 makes such a hypothesis very likely. Additionally, Miwi2-Tom expressing population was shown to overlap with Ngn3 greatly (Carrieri *et al*., in submission). On the other hand, Dnmt3L expression was not detected in the adult seminiferous tubules judging from the absence of fluorescent signal from staining with anti-V5 antibody (Figure 20 A).

To double confirm that Dnmt3L is not expressed in the adult mouse testes another allele for Dnmt3L – *Dnmt3L*$^{V5\text{-}Myc\text{-}Precision\text{-}Hisx6\text{-}mKO2}$ (*Dnmt3L*^{mKO2}), was generated in the lab using Crispr/Cas9 gene editing technology (Figure 9). As described in before, analysis of homozygous Dnmt3L$^{mKO2/mKO2}$ male mice indicated that *Dnmt3L*^{mKO2} allele is hypomorphic (Figure 9 C, D). Therefore, we have checked whether mKO2-Dnmt3L expression can be detected in fetal testes, where Dnmt3L protein is highly expressed (La Salle *et al.*, 2004; Sakai *et al.*, 2004). A single cell suspension was prepared from Dnmt3L$^{mKO2/+}$ E16.5 fetal testes and analyzed by flow cytometry. Indeed, the expression of mKO2-Dnmt3L in fetal testes was identified (Figure 20 E). Subsequently, Dnmt3L$^{mKO2/mKO2}$ adult male mouse testes were used to make a single cell suspension, where cells were stained with CD45, CD51 and c-Kit antibodies and analyzed by flow cytometry. CD45 and CD51 antibodies were used to discriminate somatic cells in the testis, while c-Kit expression was used to discriminate differentiating spermatogonial stem cells. Analysis of CD45^{neg}, CD51^{neg}, c-Kit^{neg} population showed no expression of mKO2-Dnmt3L in the adult mouse testis (Figure 20 F). Overall, we conclude that Dnmt3L is not expressed in the adult mouse testes.

Miwi2 is not required for testicular homeostasis maintenance or regeneration

After finding that Miwi2 is expressed in the adult testes we wanted to investigate if Miwi2 has a role in the population of spermatogonial precursor cells where it is expressed. We have decided to take a conditional deletion approach to study the impact of Miwi2 deletion only on the adult spermatogonial precursor cell population without affecting Miwi2 function in fetal gonadocytes. To this end we have used an inducible knock-out mouse line for Miwi2: Miwi2$^{Tom/FL}$; R26$^{ERT2Cre/+}$ (Miwi2^{iKO} or experimental group). Miwi2$^{Tom/+}$; R26$^{ERT2Cre/+}$ (Miwi2^{CTL}) mice were used as a control group. This strategy allowed us to induced Miwi2

deletion in the adult male mice by injecting them with tamoxifen. Miwi2^{iKO} mice that are not treated with tamoxifen exhibit normal testicular morphology and are fertile. Only after tamoxifen injection *Miwi2^{FL}* allele is converted to *Miwi2^{Null}* allele and mice become Miwi2 deficient since *Miwi2^{Tom}* allele is a null allele *per se*. Therefore, after tamoxifen injection Miwi2$^{Tom/FL}$ mice functionally become Miwi2$^{Null/Null}$ mice. In addition, the presence of *Miwi2^{Tom}* allele allowed us to sort Miwi2-deficient cells using flow cytometry. In summary, this inducible Miwi2^{iKO} mouse line allowed us to uncouple Miwi2 function in fetal gonadocytes and adult mouse testes, as well as analyze Miwi2 expressing deficient spermatogonial precursor cells.

To understand the role of Miwi2 in a population of undifferentiated spermatogonia in the adult mouse testes, a cohort of Miwi2^{iKO} (experimental group) and Miwi2^{CTL} (control group) adult mice were injected with tamoxifen in a dose of 75mg/kg 5 times over a period of 9 days to induce the conversion of *Miwi2^{FL}* allele to *Miwi2^{Null}* allele (Figure 21 A). Miwi2-Tom expressing spermatogonia were sorted from tamoxifen treated Miwi2^{iKO} and Miwi2^{CTL} mice two weeks after tamoxifen administration (Figure 21 B) – a period which corresponds to 2-3 division cycles of these cells counting from the fist tamoxifen administration (Hara *et al.*, 2014). A gating strategy used for sorting CD45^{neg}, CD51^{neg}, c-Kit^{neg}, Miwi2-Tom^{pos}, CD9^{pos} undifferentiated spermatogonia is shown in Figure 21 B. CD9 is highly expressed in undifferentiated spermatogonia (Kanatsu-Shinohara *et al.*, 2004), therefore, it was used as an additional marker to reach better sorting efficiency.

A full conversion of *Miwi2^{FL}* allele to *Miwi2^{Null}* allele was confirmed by RT-qPCR (Figure 21 C) and genotyping of genomic DNA (Figure 21 D). For RT-qPCR sorted CD45^{neg}, CD51^{neg}, c-Kit^{neg}, Miwi2-Tom^{pos}, CD9^{pos} cells were used for RNA extraction and later for cDNA synthesis. For RT-qPCR three sets of primers where used: primers to detect GAPDH transcript, primers spanning Miwi2 exons 11 to 13 and exons 16 to 17. Expression levels of GAPDH detected by RT-qPCR were used for the normalization of expression levels of Miwi2 transcript. Primers spanning exons 11 to 13 were used as a control to detect Miwi2 transcript in the samples. In the third set of primers a forward primer annealed to exon 16, while reverse primer annealed to exon 17. In the experimental samples where *Miwi2^{FL}* allele is converted into *Miwi2^{Null}* allele and exon 17 is deleted and no amplification was observed, while primer set exon11-13 showed Miwi2 transcript being present, however, at approximately 50% less than in control sample (Figure 21 C). This indicates that a transcript that is made from *Miwi2^{Null}* allele, which does not have exon 17, is probably not stable and not likely to produce a protein. Additionally, *Miwi2^{Tom}* allele does not produce Miwi2 coding transcript as discussed above. Thus, only transcript that is being analyzed in this RT-qPCR assay is the one

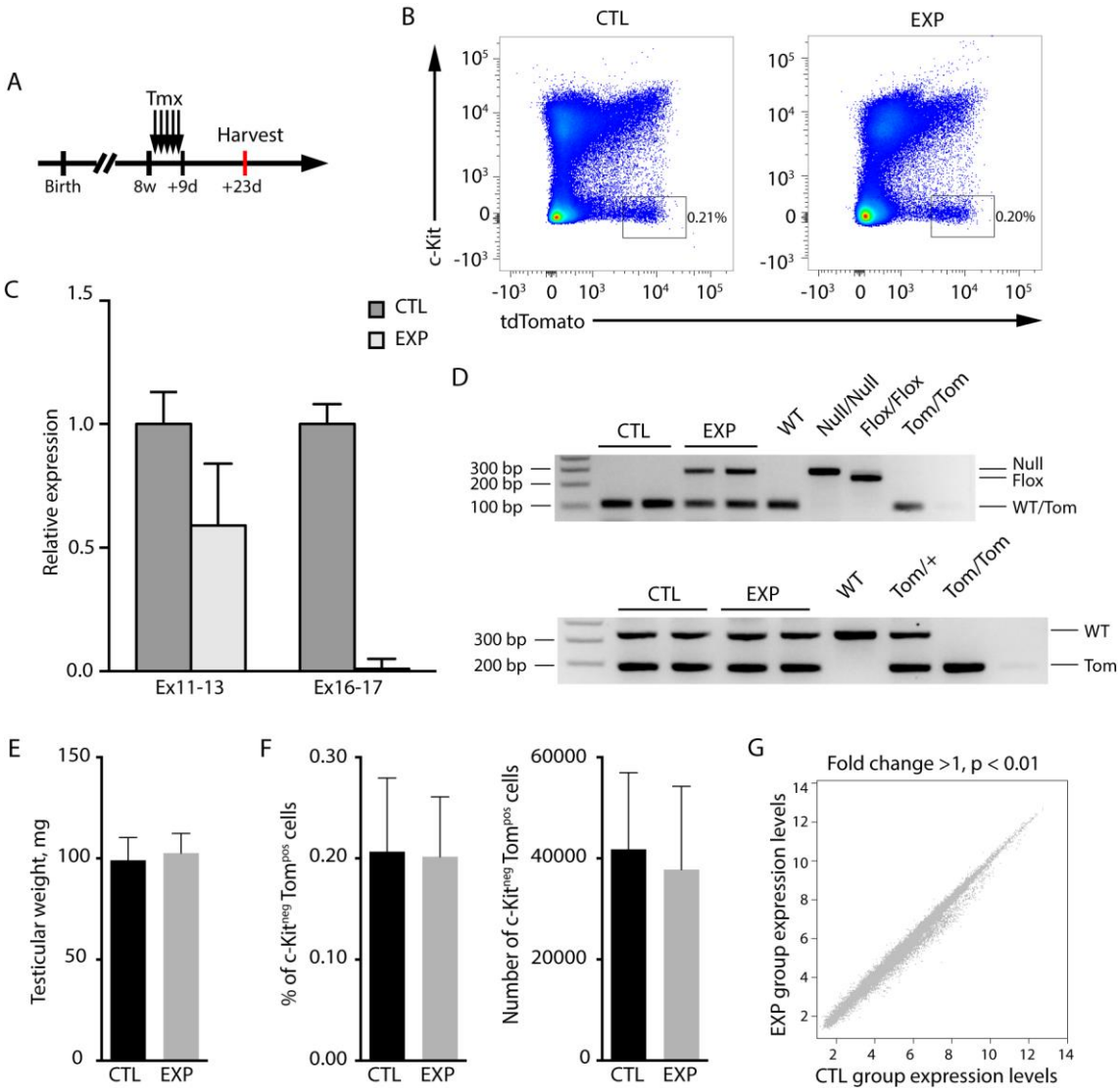

Figure 21. Acute deletion of Miwi2 does not impair spermatogenesis

(A) A time line for inducible Miwi2 allele deletion and mice analysis.

(B) A gating strategy for sorting Miwi2-expressing undifferentiated spermatogonia by flow cytometry. Gate shown: Sytox blue^{neg} CD45^{neg} CD51^{neg}.

(C) Expression of Miwi2 transcript in control and experimental animal groups treated with tamoxifen by RT-qPCR analysis.

(D) Genotype analysis of control and experimental mice after tamoxifen treatment. Detection of *Miwi2*^{Null} (top panel) and *Miwi2*^{Tom} (bottom panel) alleles.

(E) Testicular weight of control and experimental mice after tamoxifen treatment.

(F) Percentage and number of c-Kit^{neg} Miwi2-Tom^{pos} cells in control and experimental mice after tamoxifen treatment.

(G) Gene expression comparison of c-Kit^{neg} Miwi2-Tom^{pos} cells from control and experimental tamoxifen treated mice.

produced from *Miwi2*^{Null} allele. To confirm *Miwi2*^{FL} allele conversion into *Miwi2*^{Null} allele by genotyping CD45^{neg}, CD51^{neg}, c-Kit^{pos}, Miwi2-Tom^{pos} cells were sorted for genomic DNA extraction. In this case c-Kit^{pos} cells would have the same genotype as c-Kit^{neg} cells since c-Kit^{neg} cells are precursors of c-Kit^{pos} cells. For genotyping a set of primers were used that could differentiate *Miwi2*^{FL}, *Miwi2*^{Null} and WT *Miwi2* alleles (for more details refer to Materials and Methods). Indeed, a band corresponding to *Miwi2*^{Null} allele was detected in experimental group samples (Figure 21 D, upper panel). The presence of *Miwi2*^{Tom} allele in the samples was also confirmed by genotyping (Figure 21 D, bottom panel). In summary, the selected regime of tamoxifen administration results in a full conversion of *Miwi2*^{FL} allele into *Miwi2*^{Null} allele.

Analysis of the data revealed that the acute deletion of Miwi2 did not have any impact on spermatogonial precursor cell population where it is expressed. Two weeks after Miwi2 deletion testicular weight of control and experimental animal groups was the same (Figure 21 E), as well as numbers or percentage of Miwi2 expressing undifferentiated spermatogonia (Figure 21 F). Sorted CD45^{neg}, CD51^{neg}, c-Kit^{neg}, Miwi2-Tom^{pos}, CD9^{pos} spermatogonial precursor cells were subjected to gene expression analysis by Affymetrics microarrays. No differences in gene expression were found comparing Miwi2-competent and Miwi2-defficient cells (Figure 21 G). To conclude, acute Miwi2 deletion does not impair spermatogenesis of adult male mice.

To test whether a long-term deletion of Miwi2 has an impact on testicular homeostasis, a cohort of Miwi2^{iKO} and Miwi2^{CTL} mice were injected with tamoxifen as before to induce the conversion of *Miwi2*^{FL} allele to *Miwi2*^{Null} allele. After tamoxifen administration animals' testicular weight was analyzed six and twelve months thereafter (Figure 22 A). No significant differences were observed when testicular weight of control and experimental group mice was compared (Figure 22 B). Four testes from each group were sectioned throughout the whole length of the tissue, stained with hematoxylin and eosin and number of fully spermatogenic tubules counted. Histological analysis did not reveal any differences between control and experimental animal groups (Figure 22 C). Representative microscope images of hematoxylin and eosin stained testes cross-sections are shown in Figure 22 D. These data concluded that Miwi2 function is not required for the maintenance of testicular homeostasis.

It is well know that spermatogonial precursor cells not only maintain tissue homeostasis, but are also actively involved in stress responses and regeneration in the tissue. Thus, secondly, we wanted to apply a standard busulfan, DNA alkylating agent, inflicted damage and regeneration protocol to evaluate whether Miwi2 plays a role in a testicular

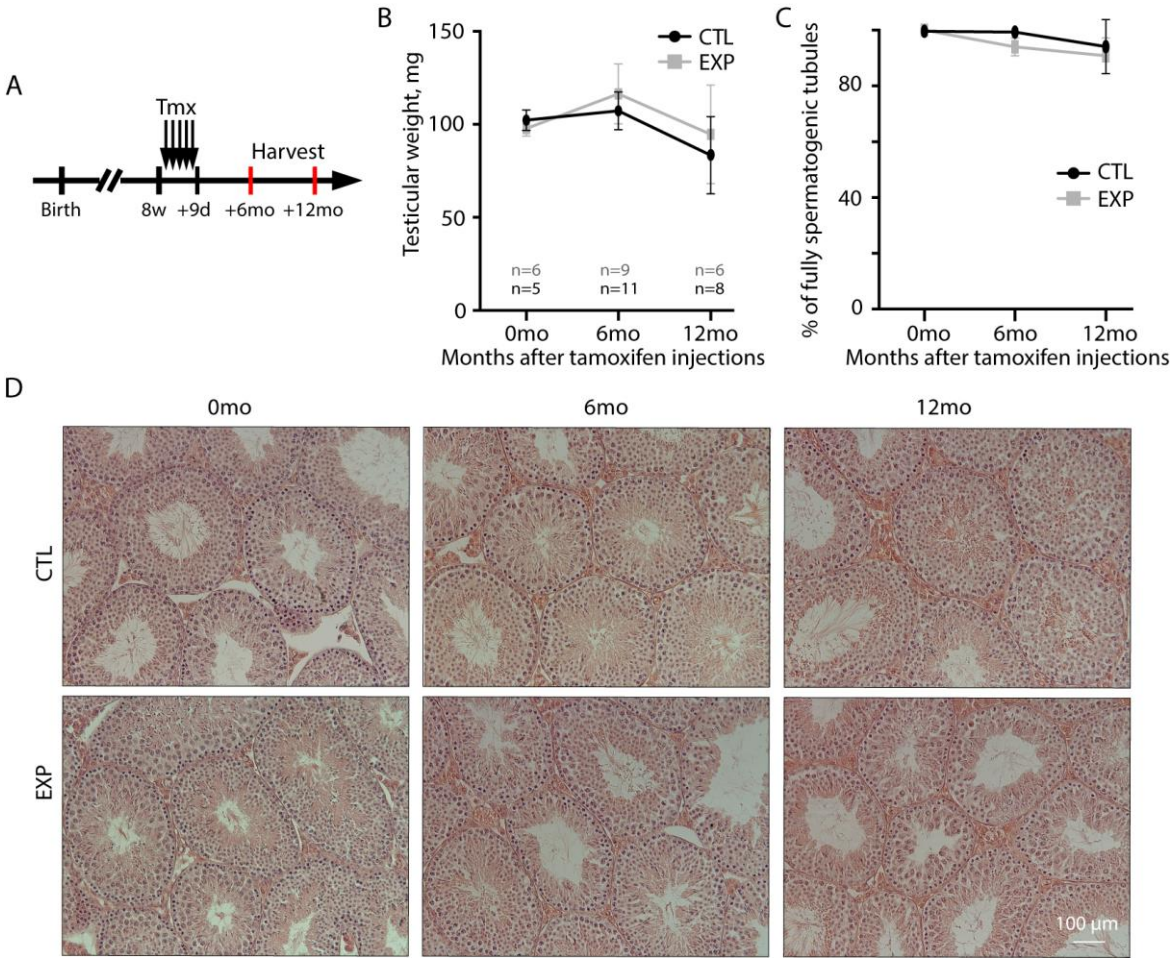

Figure 22. Miwi2 is not required for testicular homeostasis

(A) A time line for inducible Miwi2 allele deletion and mice analysis.

(B) Testicular weight of control and experimental mice treated with tamoxifen.

(C) Percentage of fully spermatogenic tubules in testes of control and experimental mice treated with tamoxifen.

(D) Hematoxylin and eosin stained testicular cross-sections of control and experimental mice treated with tamoxifen.

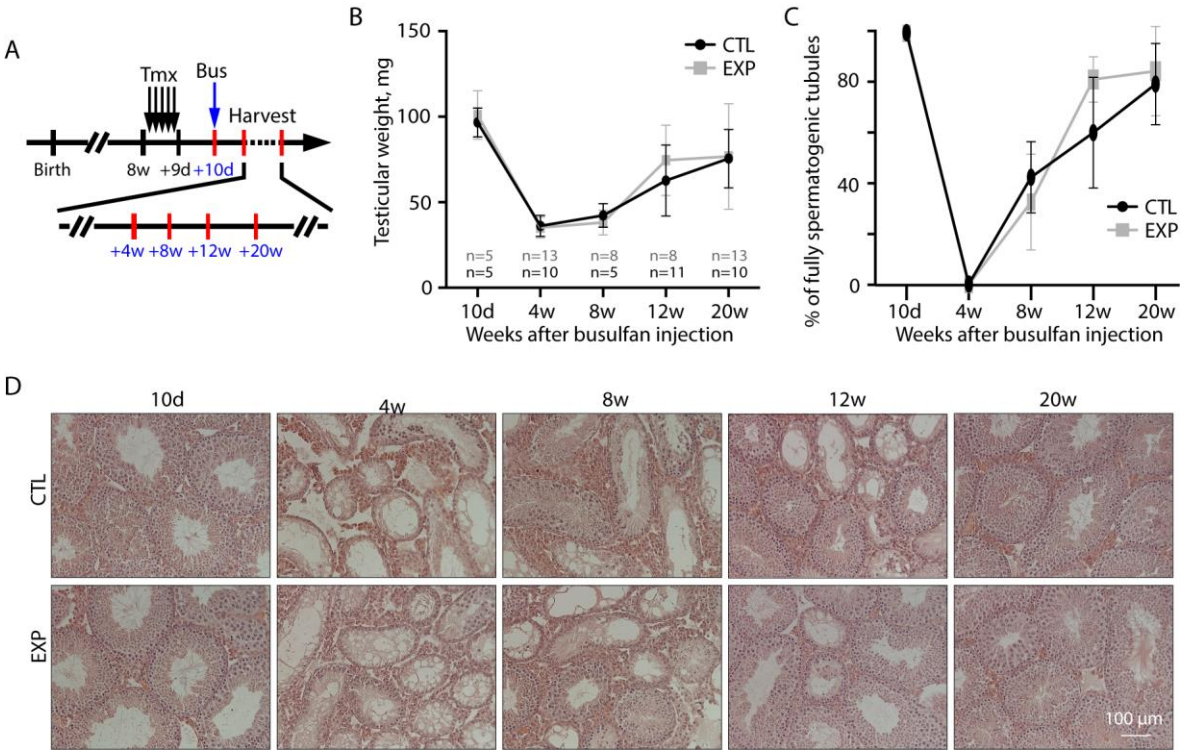

Figure 23. Miwi2 is not required for testicular regeneration after chemically induced damage

(A) A time line for inducible Miwi2 allele deletion and damage infliction and mice analysis.

(B) Testicular weight of control and experimental mice treated with tamoxifen and busulfan.

(C) Percentage of fully spermatogenic tubules in testes of control and experimental mice treated with tamoxifen and busulfan.

(D) Hematoxylin and eosin stained testicular cross-sections of control and experimental mice treated with tamoxifen and busulfan.

regeneration. Mice treatment with busulfan has been proven to be extremely toxic to germ cells, especially spermatogonia. A dose of 10mg/kg has been shown to induce a sub-acute damage (Bucci and Meistrich, 1987), allowing recovery of the testicular tissue when remaining spermatogonial stem cells enter into the cell cycle. A cohort of Miwi2^{iKO} and Miwi2^{CTL} mice were injected with tamoxifen as before to induce the conversion of *Miwi2*^{FL} allele to *Miwi2*^{Null} allele and left to recover for 10 days. After the recovery mice were subjected to a single dose injection of busulfan of 10mg/kg. To evaluate a regenerative capacity of testes in this damage and regeneration model, a testicular weight was evaluated 4 weeks, 8 weeks, 12 weeks, 20 weeks after busulfan administration of control and experimental animal groups (Figure 23 A). This analysis did not show any differences in testicular weight comparing the two groups (Figure 23 B). Four weeks after busulfan administration testes appeared to be completely empty due to elimination of a full wave of spermatogenesis which takes to complete approximately 4-5 weeks in mouse (Oakberg,

1956). From that point upwards testicular weight increased gradually with a full recovery 20 weeks later. Histological analysis of testicular cross-sections, stained with hematoxylin and eosin, counting the number of fully spermatogenic tubules has proven that the recovery rate of $Miwi2^{iKO}$ and $Miwi2^{CTL}$ mice was identical (Figure 23 C). Representative microscope images of hematoxylin and eosin stained testes cross-sections are shown in Figure 23 D. Overall, this experimental data indicate that Miwi2 is also not required for testicular regeneration upon injury.

Undifferentiated spermatogonia from reprogramming mutants experience DNA methylation defects

Miwi2 deficient mice exhibit a progressive stem cell loss – a phenotype associated with a stem cell dysfunction (Carmell *et al.*, 2007). In addition to this, Dnmt3L-deficient mice display the same phenotype, however, more severe: losing germ line more rapidly than Miwi2 (Hata *et al.*, 2006). Taking into account that Miwi2 was proven not to have any apparent function in the adult testicular tissue, where it is expressed, and Dnmt3L expression was not detected in the adult mice, the only possibility how Miwi2 and Dnmt3L support the establishment and maintenance of adult spermatogonial stem cell population is through their role in reprogramming gonadocytes. Therefore, we have decided to investigate Miwi2 and Dnmt3L, two reprogramming mutants, to get an insight into the relationship between early events in gonad development and adult stem cell biology.

The end result of the reprogramming process is completely established DNA methylation patterns. Thus, we have decided to look at the methylation status of undifferentiated spermatogonial precursor cells in Miwi2 and Dnmt3L deficient mice. Miwi2 mutant mouse line was generated using homozygous $Miwi2^{Tom/Tom}$ mice, since $Miwi2^{Tom/Tom}$ animals are functionally equal to $Miwi2^{Null/Null}$ animals. Dnmt3L mutant animals were obtained by intercrossing $Dnmt3L^{Null/+}$ mice.

To investigate the methylation status of undifferentiated spermatogonia, $CD45^{neg}$, $CD51^{neg}$, c-Kit^{neg}, Miwi2-Tom^{pos}, $CD9^{pos}$ cells were sorted from 1) $Miwi2^{Tom/+}$ (=CTL), 2) $Miwi2^{Tom/Tom}$ (=$Miwi2^{Null/Null}$) and 3) $Dnmt3L^{Null/Null}$; $Miwi2^{Tom/+}$ (=$Dnmt3L^{Null/Null}$) juvenile mice. As described above, Miwi2 is found to be expressed in a population of undifferentiated spermatogonial precursor cells, therefore, using $Miwi2^{Tom}$ reporter mouse line allowed us to investigate undifferentiated spermatogonia in Miwi2 and Dnmt3L mutant backgrounds. Sorted cells were used to extract DNA, which was subjected to bisulfite conversion and libraries generation (in collaboration with R. Barrens and W. Reik, Babraham Institute, Cambridge). Three biological replicates were used per genotype analyzed. Data received from

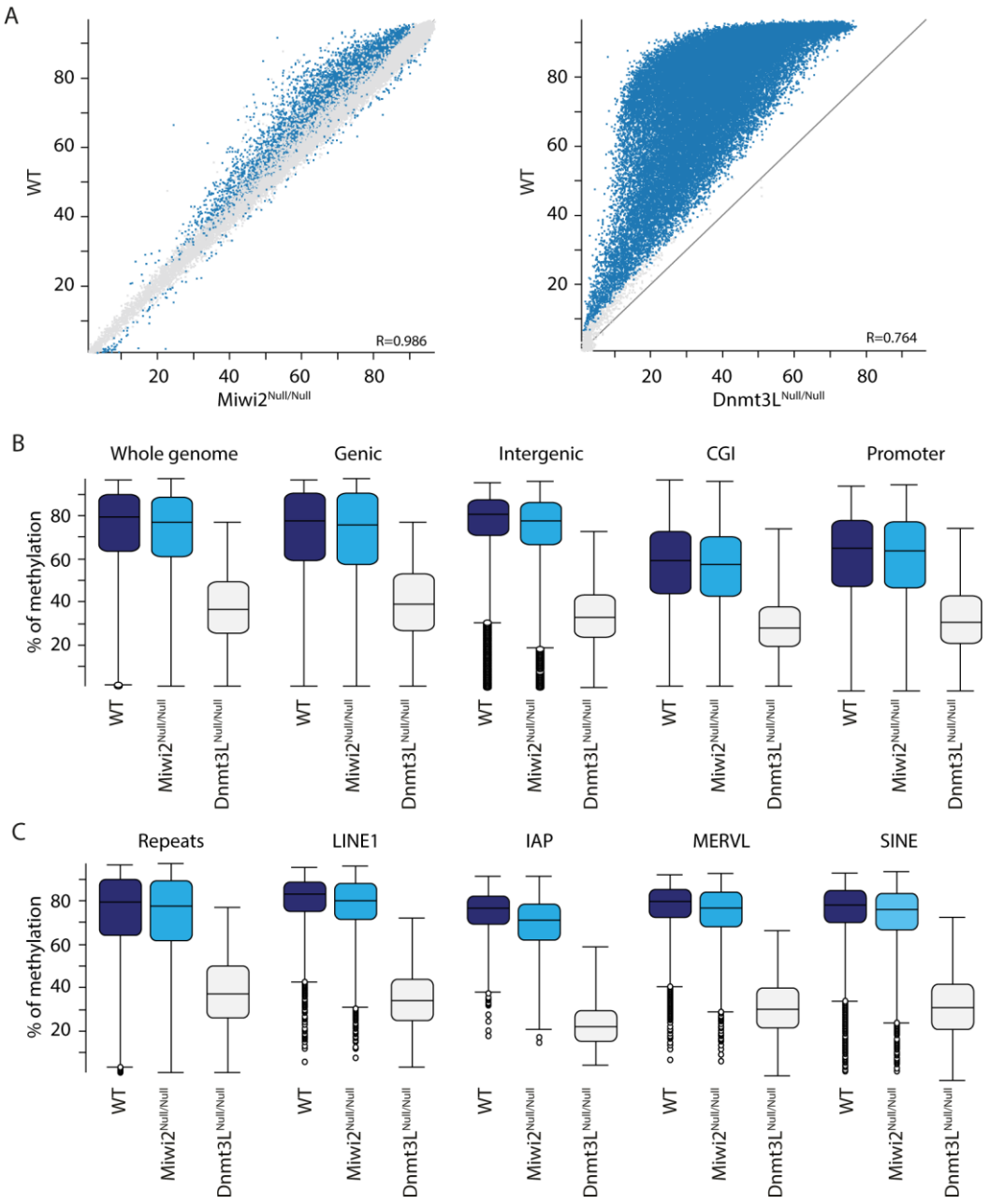

Figure 24. DNA methylation changes in Miwi2$^{Null/Null}$ and Dnmt3L$^{Null/Null}$ undifferentiated spermatogonia

(A) Scatter plots showing percentage of methylation between wild type (WT) and Miwi2$^{Null/Null}$ and wild type (WT) and Dnmt3L$^{Null/Null}$ mice. Blue dots represent significantly differentially methylated regions (DMRs).

(B) Box plots showing distribution of methylation levels for different genome features between wild type (WT), Miwi2$^{Null/Null}$ and Dnmt3L$^{Null/Null}$ mice.

(C) Box plots showing methylation levels of different repeat classes between wild type (WT), Miwi2$^{Null/Null}$ and Dnmt3L$^{Null/Null}$ mice.

whole genome bisulfite sequencing (WGBS) was used to analyze the changes in methylome in corresponding mutants comparing them to a wild type (WT) sample. To quantify the differences in methylation differentially methylated regions (DMRs) were compared amongst the samples. DMRS were defined as having 50 adjacent CpGs, where the level of methylation was determined for those CpGs that had at least 5 reads from pooled three replicates. It is known that Dnmt3L is involved in global DNA methylation events (La Salle *et al.*, 2007; Webster *et al.*, 2005), while Miwi2 has a role in transposable element gene silencing and methylation of at least one imprinted gene (Carmell *et al.*, 2007; Kuramochi-Miyagawa *et al.*, 2008; Watanabe *et al.*, 2011b). Thus, firstly, the level of methylation was analyzed globally across the genome. The comparison of control and Miwi2$^{Null/Null}$ samples revealed that the loss of Miwi2 indeed resulted in the loss of methylation of several thousand DMRs. However, as expected, the loss of Dnmt3L affected methylation of almost all DMRs investigated (Figure 24 A). Next we wished to analyze what impact Miwi2 and Dnmt3L deficiency has on the status of methylation of different genomic regions. We have looked and compared the levels of methylation in control, Miwi2$^{Null/Null}$ and Dnmt3L$^{Null/Null}$ samples regarding methylation of the whole genome, genic and intergenic regions, CGIs and promoters. When whole genome was taken into comparison Miwi2$^{Null/Null}$ samples showed only a moderate decrease in methylation, while there were no changes detected in methylation of specific genic regions as compared to the control. On the other hand, Dnmt3L$^{Null/Null}$ samples had a great reduction in methylation as compared to both control and Miwi2$^{Null/Null}$ across all the genomic regions tested (Figure 24 B). Secondly, we sought to investigate what effect the loss of Miwi2 and Dnmt3L has on the methylation status of repetitive elements. To this end we explored the level of methylation of all repetitive elements in total, and LINE1 elements, IAP and MERVL elements and SINE elements separately. We detected that Miwi2 deficiency significantly affected methylation of all the repeat groups analyzed. In addition to this, Dnmt3L deficiency lead to a dramatic loss of methylation of all groups as compared to the WT or Miwi2$^{Null/Null}$ samples (Figure 24 C). To sum up, WGBS data has shown that undifferentiated spermatogonia from Dnmt3L mutant mice suffer from a greater loss of methylation than Miwi2 mutant mice, however, repetitive element sequences in the genome are were significantly affected in both genotypes.

Upregulation of transposable elements in spermatogonial precursor cells

Haven detected changes in methylation levels of transposable elements (TEs), we wanted to know whether demethylation of TEs genes corresponds to the loss of transcriptional repression. To answer this question, CD45^{neg}, CD51^{neg}, c-Kit^{neg}, Miwi2-

Tom^{pos}, CD9^{pos} undifferentiated spermatogonia were sorted from 1) Miwi2$^{Tom/+}$ (=CTL), 2) Miwi2$^{Tom/Tom}$ (=Miwi2$^{Null/Null}$) and 3) Dnmt3L$^{Null/Null}$; Miwi2$^{Tom/+}$ (=Dnmt3L$^{Null/Null}$) juvenile mice, total RNA extracted from sorted cells and subjected to strand specific RNA sequencing. Three biological replicates were sequenced per genotype. Transposon expression in Miwi2- and Dnmt3L-deficient cells was analyzed by comparing them to a control (CTL) sample. The comparison revealed an upregulation of 17 TEs in Miwi2$^{Null/Null}$ sample and 20 TEs in Dnmt3L$^{Null/Null}$ sample as compared to the control (Figure 25 A). Most of the upregulated TEs in Miwi2 and Dnmt3L mutants belong to LTR class of transposons (88% and 90% in Miwi2 and Dnmt3L deficient cells respectively). The family of IAP elements was the most enriched. Additionally, two LINE1 type of transposons were found to be upregulated in both mutants as well. When TEs expression profile was compared between Miwi2 and Dnmt3L mutants, the expression of only 3 transposable elements were found to be different (Figure 25 B). Interestingly, all three were found upregulated in Miwi2 and Dnmt3L-deficient samples when compared to the control. The possible outcome of this differential expression is that the TEs in question must be upregulated to a different degree in Miwi2 than in Dnmt3L mutant cells. In addition, we have compared repeat element expression data amongst all three genotypes (Figure 25 C). This type of analysis revealed that the changes in TE upregulation in both mutants are nearly the same: the same group of TEs is upregulated to a similar extent in Miwi2 deficient and Dnmt3L deficient mice.

To confirm results obtained by analyzing TE expression data, testis cross-sections of WT, Miwi2$^{Null/Null}$ (Miwi2$^{Tom/Tom}$) and Dnmt3L$^{Null/Null}$ animals were stained for PLZF, LINE1 ORF1p and IAP Gag protein expression (Figure 25 D). PLZF is expressed in the population of spermatogonial precursor cells, which includes a population of GFRa1 expressing stem cells and transit amplifying cells. Therefore, this allowed us to have a broad view of transposon upregulation in undifferentiated spermatogonia. Approximately a hundred PLZF-expressing spermatogonia were analyzed per genotype. LINE1 ORF1p protein expression was not detected in PLZF positive cells neither in Miwi2$^{Null/Null}$ or Dnmt3L$^{Null/Null}$ mice testes. On the other hand, almost all PLZF-expressing Miwi2$^{Null/Null}$ and Dnmt3L$^{Null/Null}$ spermatogonia had high levels of IAP Gag protein expression (Figure 25 E, bottom and middle panels). These data are in a concordance with the data obtained from transposable element RNA sequencing analysis showing that biggest group of upregulated transposons is IAPs.

It is known that one of the hallmarks of testicular phenotype in Miwi2 and Dnmt3L mutant mice is upregulation of transposable elements in meiotic cells, which causes extensive DNA damage. Therefore, we sought to find out whether transposon de-repression could be accounted for the loss of the spermatogonia stem cells in these animals. To test this, testis

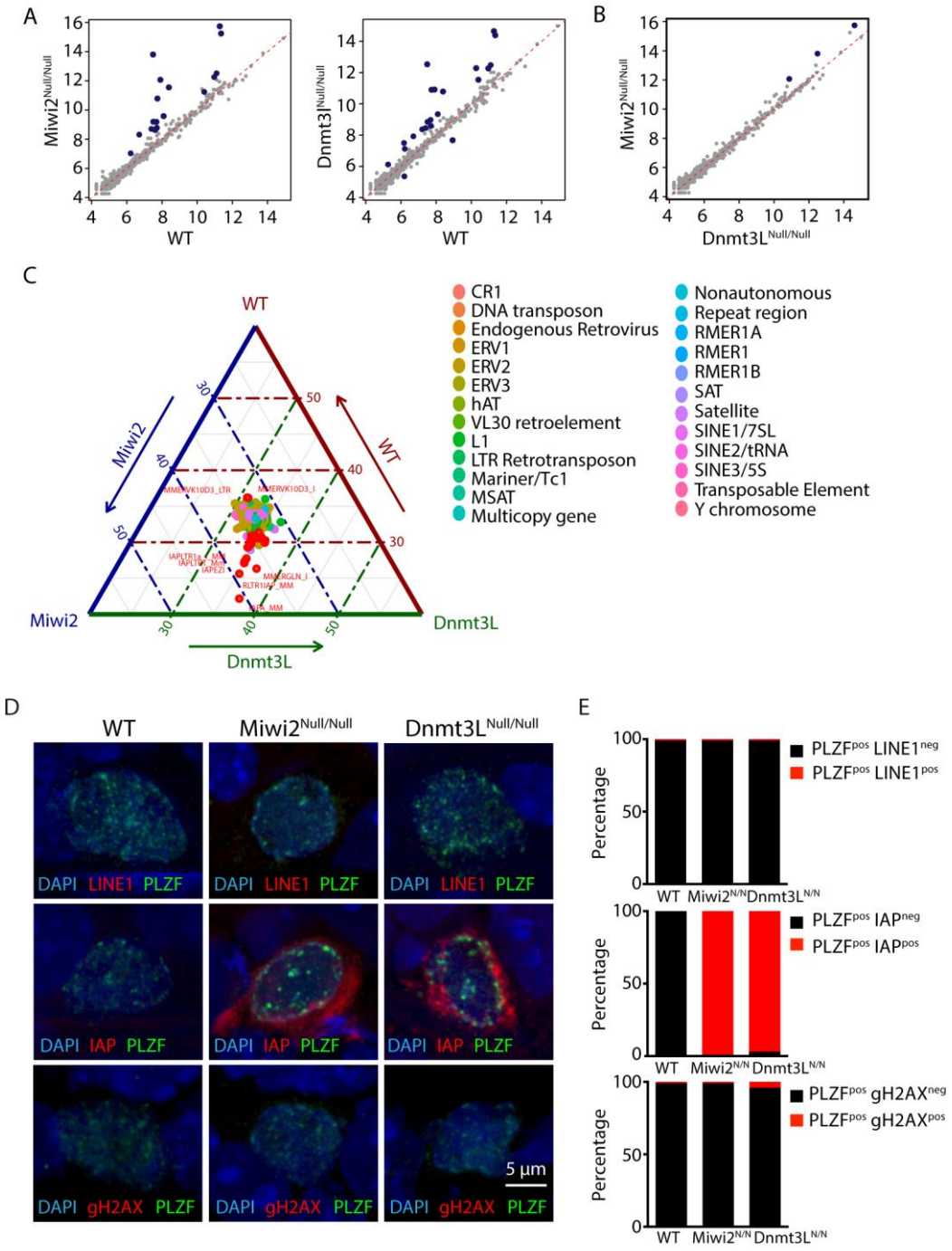

Figure 25. Transposable elements are upregulated in Miwi2- and Dnmt3L-deficient sermatogonial percursor cells

(A) Transposable element gene expression comparison between wild type (WT) and Miwi2$^{Null/Null}$ and wild type (WT) and Dnmt3L$^{Null/Null}$ SPCs.

(B) Transposable element gene expression comparison between Miwi2$^{Null/Null}$ and Dnmt3L$^{Null/Null}$ SPCs.

(C) A three-way comparison of transposable element gene expression between wild type (WT), Miwi2$^{Null/Null}$ and Dnmt3L$^{Null/Null}$ SPCs.

(D) Immunofluorescence analysis with anti-LINE1 OFR1p (top panel), anti-IAP Gag (middle panel), anti-γH2AX (bottom panel) and anti-PLZF antibodies in wild type (WT), Miwi2$^{Null/Null}$ (Miwi2$^{Tom/Tom}$) and Dnmt3L$^{Null/Null}$ SPCs.
(E) Enumeration of LINE^{neg} and LINE^{pos} PLZF^{pos} SPCs (top panel), IAP^{neg} and IAP^{pos} PLZF^{pos} SPCs (middle panel) and γH2AX^{neg} and γH2AX^{pos} PLZF^{pos} SPCs (bottom panel).

cross-sections of WT, Miwi2$^{Null/Null}$ and Dnmt3L$^{Null/Null}$ animals were stained for PLZF and γH2AX as a marker of DNA damage (Figure 25 D). Approximately a hundred PLZF-expressing cells were analyzed per genotype. Interestingly, no detectable accumulation of DNA damage was observed in Miwi2- and Dnmt3L-deficient PLZF^{pos} spermatogonia (Figure 325 E, bottom panel). Even though previous experiment revealed a high expression of IAP Gag protein, it has not been found in the nucleus where transposition events take place (Figure 25 D). Thus, the loss of spermatogonial precursor cells in Miwi2 and Dnmt3L mutant mice cannot be readily explained by the accumulation of DNA damage caused by IAP de-repression. Moreover, a similar level of transposon deregulation was observed in both Miwi2 and Dnmt3L mutant mice. This finding cannot explain why Dnmt3L deficient mice lose germ line much faster than Miwi2 deficient mice.

Aberrant gene expression program is activated in reprogramming mutants

Changes in the gene expression pattern could be another reason why Miwi2- and Dnmt3L mutant mice exhibit complete germ cell loss. Thus, we wanted to investigate if undifferentiated spermatogonial stem cells (c-Kit^{neg}, Miwi2-Tom^{pos}, CD9^{pos}), isolated from reprograming mutants as described above, have abnormal coding gene expression patterns. To do so, the gene expression pattern was compared between control and Miwi2$^{Null/Null}$, control and Dnmt3L$^{Null/Null}$ samples. (Figure 26 A). The analysis revealed that overall Miwi2 had fewer changes in the coding gene expression taking into account both upregulated and downregulated genes. Interestingly, we noticed that the top most significantly upregulated genes were common for both Miwi2 and Dnmt3L mutant samples (Figure 26 A). Therefore, we wished to understand to what degree the deregulation of coding gene expression is distinct or similar between the two mutants. A gene expression comparison amongst Miwi2$^{Null/Null}$ and Dnmt3L$^{Null/Null}$ samples showed that there is a significant number of genes that are specifically misregulated in either Miwi2$^{Null/Null}$ and Dnmt3L$^{Null/Null}$ samples (Figure 26 B). Nonetheless, we were intrigued by the fact that Miwi2 and Dnmt3L mutant did show some degree of similarity considering their different role in germline maintenance. One way to explain these results is to look for a common denominator between the mutants that could potentially drive described changes. As mentioned before, transposon de-repression is similar

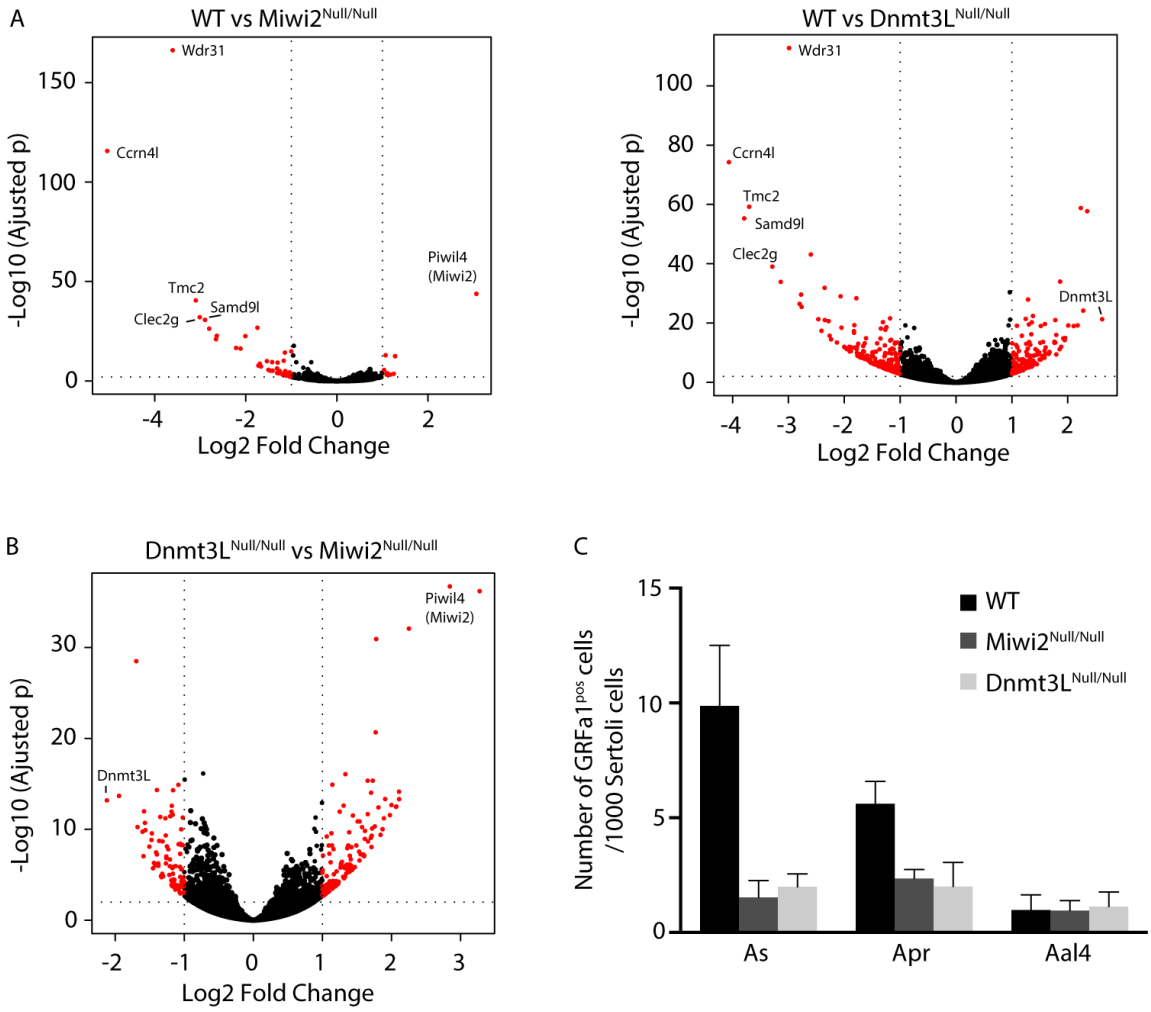

Figure 26. Gene expression changes in Miwi2 and Dnmt3L deficient SPCs result in a loss of GFRa1^{pos} cells

(A) Gene expression comparison between wild type (WT) and Miwi2$^{Null/Null}$ and wild type (WT) and Dnmt3L$^{Null/Null}$ SPCs.

(B) Gene expression comparison between Miwi2$^{Null/Null}$ and Dnmt3L$^{Null/Null}$ SPCs.

(C) Enumeration of GFRa1^{pos} spermatogonia in wild type (WT), Miwi2$^{Null/Null}$ and Dnmt3L$^{Null/Null}$ mice.

between the two reprogramming mutants. Even though it has been ruled out as causing a direct DNA damage to spermatogonial precursor cells, we wish to explore whether transposon expression *per se* can affect the expression of other genes located in proximity. In future, we will analyze if hybrid transcripts between transposons and coding genes are present in reprogramming mutants undifferentiated spermatogonial stem cells. The emergence of hybrid transcripts would at least in part explain gene expression changes.

Knowing that undifferentiated spermatogonial stem cells have an altered gene expression program, we sought explore what the biological outcome this brings. We sought to investigate the composition of the stem cell compartment where GFRa1 is expressed. To achieve this, whole mount anti-GRFa1 immunofluorescence staining was performed on the seminiferous tubules of 1) Miwi2$^{Tom/+}$ (=CTL), 2) Miwi2$^{Tom/Tom}$ (=Miwi2$^{Null/Null}$) and 3) Dnmt3L$^{Null/Null}$ adult mice. Approximately 30 representative images were taken of a seminiferous tubule for each of six animals in each genotype group. The number of GFRa1-experssing cells was counted, which was then normalized to the number of Sertoli cells (Sertoli cells are the somatic support cells for spermatogonia stem cells). As described previously, GFRa1 cells comprise a stem cell compartment, where GRFa1 cells are found as single cells and are called A_{single} (A_s). When they divide, either two A_s cells are made or cytokinesis is not completed and cells stay interconnected *via* cytoplasmic bridge and form a two-cell cyst, called A_{paired} (A_{pr}). A_{pr} cells divide and form a chain of 4 cells, called $A_{aligned-4}$ (A_{al4}).

When number of GRFa1-expressing cells was evaluated, it became evident that there is a 5-6,5-fold reduction of A_s and 2,4-2,8-fold reduction of A_{pr} GRFa1-expressing spermatogonial stem cells in Dnmt3L and Miwi2 mutants (Figure 26 C). Therefore, there is a significant decrease in actual stem cells in the seminiferous tubules of the respective animals.

To conclude, in this study we have shown that a group of repetitive elements is de-repressed in Miwi2- and Dnmt3L-deficient undifferentiated spermatogonial precursor cells due to a loss of methylation, however, it did not result in an apparent DNA damage of these cells. Nonetheless, we hypothesis that active TE genes are responsible for triggering abnormal gene expression program in spermatogonia stem cells due to emergence of a hybdrid TE-driven transcripts. Consequently, these changes lead to a great reduction in the numbers of actual stem cells in the testis.

Discussion

Miwi2 and Dnmt3L are expressed during the window of *de novo* DNA methylation in fetal gonadocytes. Both are responsible for methylation of transposable element sequences in the genome, while Dnmt3L is also linked to global DNA methylation. Dnmt3L and Miwi2 mutant male mice exhibit very similar phenotype with a characteristic progressive germ cells loss, even though Dnmt3L phenotype is more severe. In this study we have shown that Dnmt3L is not expressed in the adult mice testes, while Miwi2, even though expressed in the population of spermatogonial precursor cells, does not have a role in testicular homeostasis or regeneration as proved by inducible knock-out experiments. Therefore, we have shown that a failure to re-establish DNA methylation marks in fetal gonadocytes in Dnmt3L and Miwi2 mutants results in de-repression of transposable elements, which affects gene expression in undifferentiated spermatogonia. The collapse of a proper gene expression program leads to a loss of actual stem cells in Miwi2 and Dnmt3L mutant testes.

Miwi2 expression and function in the adult testes

Miwi2 expression commences at around embryonic day 15.5 (E15.5) (Aravin *et al.*, 2008). Once embryonic *de novo* DNA methylation is finished in the germline around the time of birth, Miwi2 expression was found to decrease sharply and the protein was not detectable a few days after birth (Aravin *et al.*, 2008). We have found that Miwi2 expression does not cease after the birth. HA-Miwi2 was found to be expressed in the adult male testes in a population of spermatogonial precursor cells with a partial overlap with GFRa1 expressing stem cells (Figure 20 A, C). Using *Miwi2*^{Tom} allele we have defined that Miwi2 expressing cell population makes up 0,35% of all germ cells in the adult testes (Figure 12 E), which results in 35 000-40 000 Miwi2-Tom^{pos} cells per testis. Among millions of germ cells in the testis, Miwi2 expressing cell population is difficult to detect without using an expression reporter allele like *Miwi2*^{Tom} or a HA-tagged Miwi2 that would allow identification of Miwi2 expressing cells by flow cytometry or immunofluorescence, since reliable Miwi2 antibodies are not commercially available. HA-Miwi2 was found to be expressed in the spermatogonial precursor cells (SPCs). Judging from the complete overlapping expression pattern with PLZF and partial overlap with GFRa1, HA-Miwi2 expressing cells likely equates a population defined by Ngn3. Indeed, analysis of Miwi2-Tom^{pos} cells showed that this population has a

reconstitutional activity upon transplantation, contributes to testicular regeneration after chemically induced damage and overlaps with Ngn3 expressing cells (Carrieri *et al.*, in submission). Therefore, Miwi2 marks a population of cells in the adult testes that have a regenerative capacity. Experiments presented in this study using inducible knock-out approach failed to reveal any molecular function of Miwi2 in the adult testes. This lead to a conclusion that even though Miwi2 is expressed in SPCs in adult testes it serves only as a marker of a particular cell population. Interestingly, HA-Miwi2 was found to be predominantly localized in cytoplasm or nucleus, or both in spermatogonia where it is expressed. The significance of such cellular distribution is not known and awaits further examination. However, it was noticed that in most cases HA-Miwi2 was localized in the nucleus if its expression coincided with GFRa1, while the cells that were positive for HA-Miwi2, but negative for GFRa1 were most likely to show a cytoplasmic Miwi2 expression pattern (data not shown). It could be speculated that different cellular localization of Miwi2 indicates different states of SPCs regarding their potential to differentiate or self-renew. However, this assumption is not supported by any experimental evidence and needs to be investigated further.

The aim of this study was to elucidate how Miwi2 contributes to maintenance and establishment of adult spermatogonial stem cell population. It is known that loss of Miwi2 results in male mice sterility due to a meiotic block, which happens as a result of transposon upregulation and cell death by apoptosis (Carmell *et al.*, 2007). This testicular phenotype results due to a failure to silence transposons by DNA methylation during fetal testes development. As discussed above, Miwi2 expression was detected in adult testes, thus, it was necessary to uncouple Miwi2 function in fetal gonadocytes and adult SPCs to understand whether Miwi2 has a role in adult testes beyond its involvement in reprogramming. To achieve this we have used inducible knock-out approach, where Miwi2 deletion was achieved in adult male mice once reprogramming is finished and DNA methylation marks are fully acquired. Here we have used an inducible form of ubiquitously expressed ERT2-Cre. Once Cre-recombinase is activated, Miwi2 deletion is induced in all somatic and germ cells in the mice. Miwi2 is strictly expressed in the testes, therefore, there are no effects manifested in other tissues or organs. A similar study was done in order to elucidate Miwi2 function in the adult mice. However, the authors have used Stra8-Cre to induce $Miwi2^{FL}$ allele conversion into $Miwi2^{Null}$ allele (Bao *et al.*, 2014). Stra8 expression starts only in differentiating spermatogonia and usually coincides with c-Kit expression (Sadate-Ngatchou *et al.*, 2008). Therefore, if Miwi2 has a function in spermatogonial stem cell maintenance, it could not be possibly tested in this system. As expected, Bao and colleagues reported that Miwi2 deficient

mice, where Miwi2 deletion was achieved by using Stra8-Cre, had normal testicular morphology and were fertile. On the other hand, our global, inducible Miwi2 deletion strategy showed that the loss of Miwi2 did not impair testicular homeostasis or regeneration. Thus, we made a conclusion that Miwi2 contributes to the spermatogonial stem cell maintenance *via* its role in reprogramming gonadocytes. Nonetheless, it is also possible that spermatogonia employ several redundant maintenance mechanisms and the loss of Miwi2 is easily managed or we were not able to detect to detect function of Miwi2 in the system studied.

Dnmt3L expression in postnatal testes

The experimental evidence presented about Dnmt3L expression in postnatal testes is not unanimous. There are reports of Dnmt3L transcript present not only spermatogonia, but also in meiotic cells (La Salle *et al.*, 2007). Sakai and colleagues could not detect expression of Dnmt3L protein in postnatal mouse testes (Sakai *et al.*, 2004), whereas another group reported that Dnmt3L is expressed in a subpopulation of undifferentiated spermatogonia and it was detected by Western blot (Liao *et al.*, 2014). In contrast our results indicate that Dnmt3L is not expressed in the adult testes. We used *Dnmt3L*^{mKO2} allele to visualize Dnmt3L expressing cells in fetal and adult testes. mKO2-Dnmt3L expression was detected in fetal testes, but not in the adult testes. mKO2 is a bright orange fluorescent protein with characteristics equal or even better than eGFP (Kremers *et al.*, 2011), therefore, it is not likely that detection was limited by a fluorescent tag properties. Additionally, flow cytometry is a sensitive method for detecting even weak fluorescence signals. Moreover, these results were confirmed using yet another allele available in the lab, where Dnmt3L expressing cells are marked by eGFP (data not shown). We could not detect Dnmt3L expression in seminiferous tubules of adult mice by immunofluorescence using anti-V5 antibody. Overall, three different anti-V5 antibodies, one anti-Myc and two anti-mKO2 antibodies were tested by immunofluorescence on whole mount seminiferous tubules of adult and juvenile mice (data not shown). All attempts to detect Dnmt3L in postnatal mouse testes were unavailing. In addition, anti-V5 immunoprecipitation followed by anti-V5 Western blot also did not give positive results. Therefore, overall we conclude that in the conditions tested were could not detect Dnmt3L expression in mouse testes.

The effect of loss of Miwi2 and Dnmt3L on spermatogonial stem cell population

It is known that Dnmt3L is involved in a global DNA methylation in fetal gonadocytes (Bourc'his and Bestor, 2004; Kato *et al.*, 2007; La Salle *et al.*, 2007; Webster *et al.*, 2005), while Miwi2 is responsible for guiding *de novo* DNA methylation of transposable

elements (Aravin *et al.*, 2008; Kuramochi-Miyagawa *et al.*, 2008). We have established that Miwi2 and Dnmt3L do not have a role in adult testes, thus we wished to examine how embryonic functions of Miwi2 and Dnnmt3L contribute to spermatogonial stem cell population establishment. To do so, we sought to assess to what degree the loss of Miwi2 and Dnmt3L has effect on the methylome of spermatogonial precursor cells and what outcome it brings. As expected we have found that Dnmt3L mutant SPCs have lost methylation globally across the genome, while the loss of Miwi2 affected methylation of transposable elements. The loss of DNA methylation has resulted in apparent de-repression of transposable elements. Interestingly, both Miwi2 and Dnmt3L showed nearly the same transposable element de-regulation pattern (Figure 25 B). The same groups of transposable elements were found to be upregulated in the two reprogramming mutants. This outcome is in accordance with the model where Miwi2 leads methylation of transposable elements and acts upstream of DNA methylation machinery. IAPs were the predominant type of transposons upregulated in both mutants. These results were confirmed by immunofluorescence analysis in PLZF expressing undifferentiated spermatogonia (Figure 25 D). It had been reported that IAPs were the most affected transposable element group by the loss of Dnmt3L (Aravin *et al.*, 2008), while LINEs are believed to be mostly affected in Miwi2 mutant cells (Manakov *et al.*, 2015; Nagamori *et al.*, 2015). However, as discussed earlier, it is possible that Miwi2's role in LTR type of transposon methylation is underestimated. Nonetheless, a couple families of LINEs were found to be upregulated by gene expression analysis, while LINE1 ORF1p was not detected in $PLZF^{pos}$ SPCs. It is possible that even if LINE1 mRNA is expressed it is not translated. If LINE1 mRNA is transcribed, most likely it is cleaved and utilized in a piRNA pathway, since Mili should be functional in both Miwi2 and Dnmt3L mutants (Aravin *et al.*, 2008; Kuramochi-Miyagawa *et al.*, 2008). This theory is supported by the fact that in the absence of Dnmt3L a great increase of sense oriented (transposon mRNA-derived) piRNAs is observed (Aravin *et al.*, 2008), indicating that actively transcribed transposon mRNAs successfully enter piRNA pathway, however, only post-transcriptional gene silencing is not enough to silence transposons. Indeed it was established that SPCs also employ repressive chromatin marks to re-enforce silencing of transposable elements. H3K9me2 was found to be enriched at the LINE1 and IAP sequences. This repressive mark is enough to suppress transcription of LINE1, but not IAP elements even in the absence of piRNA mediated methylation (Di Giacomo *et al.*, 2014). This phenomenon explains why a great upregulation of IAP Gag, but not LINE1 ORF1p was detected in $PLZF^{pos}$ undifferentiated spermatogonia in Miwi2 and Dnmt3L mutants.

It has been established that the upregulation of transposable elements leads to an apoptotic cell death in meiotic germ cells (Carmell *et al.*, 2007; Kuramochi-Miyagawa *et al.*, 2004; Webster *et al.*, 2005). It is believed that TE upregulation causes an extensive DNA damage due to transposition events, which leads to a cells death. However, it has been shown that transposon upregulation in meiotic cells does not result in increased DNA damage, but meiotic cells die due to failure to properly align and recombine chromosomes (Zamudio *et al.*, 2015). In accordance to this data, we also did not observed increased DNA damage in $PLZF^{pos}$ undifferentiated spermatogonia. Nonetheless, we detected that both Miwi2 and Dnmt3L deficient mice exhibited a great loss of GFRa1 expressing spermatogonia (Figure 26 C), which make up the compartment of an actual stem cells in the testes. We have shown that an intrinsic transposon activity *per se* cannot be the cause of the spermatogonial stem cell loss. Thus we hypothesized that gene expression changes resulting from re-activation of transposable elements could be a potential cause of stem cell loss.

Several groups have shown that the loss of DNA methylation is accompanied by the changes in the chromatin marks and therefore remodeling creating a permissive environment for transposon gene transcription (Webster *et al.*, 2005; Zamudio *et al.*, 2015). We believe that a transcription of transposable element causes upregulation of transcription of a gene in vicinity. This effect could be executed either by the change in chromatin marks that spread further into nearby sequences and affect transcription of the genes present there or a read-through from transposon locus into a coding gene creates a hybrid transcript which is either not functional or functions aberrantly. This theory is supported by the finding that such a hybrid transcript between LINE1 element and a coding gene was identified in Miwi2 mutant germ cells (Pezic *et al.*, 2014). Additionally, a change in expression of a few genes located near LINE1 was also identified (Pezic *et al.*, 2014). Overall, an active transcription of transposable element genes can deregulate expression of coding genes, which in their turn can cause secondary effects and lead to more extensive gene expression changes. Interestingly, we have found that that a few most upregulated genes in Miwi2 and Dnmt3L deficient SPCs are the same. It is likely that they are affected by transposon upregulation, which is common in both mutants. However, a more detailed research is needed to test whether these genes lie in a close proximity to a transposon gene or are upregulated because form a chimeric transcript with a TE.

All in all, we have showed that Miwi2 and Dnmt3L mutant mice lose the germline because of a failure to maintain a healthy spermatogonial stem cell population. A great reduction of GFRa1 one cells was identified in both Miwi2 and Dnmt3L mutant mice. We believe that the loss of the germline stem cells is caused by de-activation of transposable

elements which affect expression of genes present in vicinity. A misregulation of a few genes by transposons may result in a cascade of gene expression changes that influence spermatogonial stem cell ability to self-renew and differentiate. Overall, embryonic functions of Miwi2 and Dnmt3L affect the maintenance and establishment of a fully functional spermatogonial stem cell population in adult mouse testes.

REFERENCES

Aapola U., Lyle R., Krohn K., Antonarakis S.E., and Peterson P. (2001). Isolation and initial characterization of the mouse Dnmt3l gene. Cytogenetics and cell genetics *92*, 122-126.

Aloisio G.M., Nakada Y., Saatcioglu H.D., Pena C.G., Baker M.D., Tarnawa E.D., Mukherjee J., Manjunath H., Bugde A., Sengupta A.L., *et al.* (2014). PAX7 expression defines germline stem cells in the adult testis. The Journal of clinical investigation *124*, 3929-3944.

Aoki A., Suetake I., Miyagawa J., Fujio T., Chijiwa T., Sasaki H., and Tajima S. (2001). Enzymatic properties of de novo-type mouse DNA (cytosine-5) methyltransferases. Nucleic acids research *29*, 3506-3512.

Aravin A., Gaidatzis D., Pfeffer S., Lagos-Quintana M., Landgraf P., Iovino N., Morris P., Brownstein M.J., Kuramochi-Miyagawa S., Nakano T., *et al.* (2006). A novel class of small RNAs bind to MILI protein in mouse testes. Nature *442*, 203-207.

Aravin A.A., Lagos-Quintana M., Yalcin A., Zavolan M., Marks D., Snyder B., Gaasterland T., Meyer J., and Tuschl T. (2003). The small RNA profile during Drosophila melanogaster development. Developmental cell *5*, 337-350.

Aravin A.A., Naumova N.M., Tulin A.V., Vagin V.V., Rozovsky Y.M., and Gvozdev V.A. (2001). Double-stranded RNA-mediated silencing of genomic tandem repeats and transposable elements in the D. melanogaster germline. Current biology : CB *11*, 1017-1027.

Aravin A.A., Sachidanandam R., Bourc'his D., Schaefer C., Pezic D., Toth K.F., Bestor T., and Hannon G.J. (2008). A piRNA pathway primed by individual transposons is linked to de novo DNA methylation in mice. Molecular cell *31*, 785-799.

Aravin A.A., Sachidanandam R., Girard A., Fejes-Toth K., and Hannon G.J. (2007). Developmentally regulated piRNA clusters implicate MILI in transposon control. Science *316*, 744-747.

Aravin A.A., van der Heijden G.W., Castaneda J., Vagin V.V., Hannon G.J., and Bortvin A. (2009). Cytoplasmic compartmentalization of the fetal piRNA pathway in mice. PLoS genetics *5*, e1000764.

Arnaud P., Hata K., Kaneda M., Li E., Sasaki H., Feil R., and Kelsey G. (2006). Stochastic imprinting in the progeny of Dnmt3L-/- females. Human molecular genetics *15*, 589-598.

Bachman K.E., Rountree M.R., and Baylin S.B. (2001). Dnmt3a and Dnmt3b are transcriptional repressors that exhibit unique localization properties to heterochromatin. The Journal of biological chemistry *276*, 32282-32287.

Bao J., Zhang Y., Schuster A.S., Ortogero N., Nilsson E.E., Skinner M.K., and Yan W. (2014). Conditional inactivation of Miwi2 reveals that MIWI2 is only essential for prospermatogonial development in mice. Cell death and differentiation *21*, 783-796.

Beyret E., Liu N., and Lin H. (2012). piRNA biogenesis during adult spermatogenesis in mice is independent of the ping-pong mechanism. Cell research *22*, 1429-1439.

Bellve A.R., Cavicchia J.C., Millette C.F., O'Brien D.A., Bhatnagar Y.M., and Dym M. (1977). Spermatogenic cells of the prepuberal mouse. Isolation and morphological characterization. The Journal of cell biology *74*, 68-85.

Boitani C., Di Persio S., Esposito V., and Vicini E. (2016). Spermatogonial cells: mouse, monkey and man comparison. Seminars in cell & developmental biology.

Bourc'his D., and Bestor T.H. (2004). Meiotic catastrophe and retrotransposon reactivation in male germ cells lacking Dnmt3L. Nature *431*, 96-99.

Bourc'his D., Xu G.L., Lin C.S., Bollman B., and Bestor T.H. (2001). Dnmt3L and the establishment of maternal genomic imprints. Science *294*, 2536-2539.

Braydich-Stolle L., Kostereva N., Dym M., and Hofmann M.C. (2007). Role of Src family kinases and N-Myc in spermatogonial stem cell proliferation. Developmental biology *304*, 34-45.

Brennecke J., Aravin A.A., Stark A., Dus M., Kellis M., Sachidanandam R., and Hannon G.J. (2007). Discrete small RNA-generating loci as master regulators of transposon activity in Drosophila. Cell *128*, 1089-1103.

Brinster R.L., and Zimmermann J.W. (1994). Spermatogenesis following male germ-cell transplantation. Proceedings of the National Academy of Sciences of the United States of America *91*, 11298-11302.

Buaas F.W., Kirsh A.L., Sharma M., McLean D.J., Morris J.L., Griswold M.D., de Rooij D.G., and Braun R.E. (2004). Plzf is required in adult male germ cells for stem cell self-renewal. Nature genetics *36*, 647-652.

Buageaw A., Sukhwani M., Ben-Yehudah A., Ehmcke J., Rawe V.Y., Pholpramool C., Orwig K.E., and Schlatt S. (2005). GDNF family receptor alpha1 phenotype of spermatogonial stem cells in immature mouse testes. Biology of reproduction *73*, 1011-1016.

Bucci L.R., and Meistrich M.L. (1987). Effects of busulfan on murine spermatogenesis: cytotoxicity, sterility, sperm abnormalities, and dominant lethal mutations. Mutation research *176*, 259-268.

Buehr M., McLaren A., Bartley A., and Darling S. (1993). Proliferation and migration of primordial germ cells in We/We mouse embryos. Developmental dynamics : an official publication of the American Association of Anatomists *198*, 182-189.

Busada J.T., Chappell V.A., Niedenberger B.A., Kaye E.P., Keiper B.D., Hogarth C.A., and Geyer C.B. (2015). Retinoic acid regulates Kit translation during spermatogonial differentiation in the mouse. Developmental biology *397*, 140-149.

Carmell M.A., Girard A., van de Kant H.J., Bourc'his D., Bestor T.H., de Rooij D.G., and Hannon G.J. (2007). MIWI2 is essential for spermatogenesis and repression of transposons in the mouse male germline. Developmental cell *12*, 503-514.

Castaneda J., Genzor P., van der Heijden G.W., Sarkeshik A., Yates J.R., 3rd, Ingolia N.T., and Bortvin A. (2014). Reduced pachytene piRNAs and translation underlie spermiogenic arrest in Maelstrom mutant mice. The EMBO journal *33*, 1999-2019.

Chan F., Oatley M.J., Kaucher A.V., Yang Q.E., Bieberich C.J., Shashikant C.S., and Oatley J.M. (2014). Functional and molecular features of the Id4+ germline stem cell population in mouse testes. Genes & development *28*, 1351-1362.

Chedin F., Lieber M.R., and Hsieh C.L. (2002). The DNA methyltransferase-like protein DNMT3L stimulates de novo methylation by Dnmt3a. Proceedings of the National Academy of Sciences of the United States of America *99*, 16916-16921.

Chen P.Y., Manninga H., Slanchev K., Chien M., Russo J.J., Ju J., Sheridan R., John B., Marks D.S., Gaidatzis D., *et al.* (2005a). The developmental miRNA profiles of zebrafish as determined by small RNA cloning. Genes & development *19*, 1288-1293.

Chen T., Ueda Y., Dodge J.E., Wang Z., and Li E. (2003). Establishment and maintenance of genomic methylation patterns in mouse embryonic stem cells by Dnmt3a and Dnmt3b. Molecular and cellular biology *23*, 5594-5605.

Chen T., Ueda Y., Xie S., and Li E. (2002). A novel Dnmt3a isoform produced from an alternative promoter localizes to euchromatin and its expression correlates with active de novo methylation. The Journal of biological chemistry *277*, 38746-38754.

Chen Z.X., Mann J.R., Hsieh C.L., Riggs A.D., and Chedin F. (2005b). Physical and functional interactions between the human DNMT3L protein and members of the de novo methyltransferase family. Journal of cellular biochemistry *95*, 902-917.

Chiarini-Garcia H., Hornick J.R., Griswold M.D., and Russell L.D. (2001). Distribution of type A spermatogonia in the mouse is not random. Biology of reproduction *65*, 1179-1185.

Chotalia M., Smallwood S.A., Ruf N., Dawson C., Lucifero D., Frontera M., James K., Dean W., and Kelsey G. (2009). Transcription is required for establishment of germline methylation marks at imprinted genes. Genes & development *23*, 105-117.

Chuma S., Hosokawa M., Kitamura K., Kasai S., Fujioka M., Hiyoshi M., Takamune K., Noce T., and Nakatsuji N. (2006). Tdrd1/Mtr-1, a tudor-related gene, is essential for male germ-cell differentiation and nuage/germinal granule formation in mice. Proceedings of the National Academy of Sciences of the United States of America *103*, 15894-15899.

Cook M.S., and Blelloch R. (2013). Small RNAs in germline development. Current topics in developmental biology *102*, 159-205.

Costoya J.A., Hobbs R.M., Barna M., Cattoretti G., Manova K., Sukhwani M., Orwig K.E., Wolgemuth D.J., and Pandolfi P.P. (2004). Essential role of Plzf in maintenance of spermatogonial stem cells. Nature genetics *36*, 653-659.

Cox D.N., Chao A., Baker J., Chang L., Qiao D., and Lin H. (1998). A novel class of evolutionarily conserved genes defined by piwi are essential for stem cell self-renewal. Genes & development *12*, 3715-3727.

Cox D.N., Chao A., and Lin H. (2000). piwi encodes a nucleoplasmic factor whose activity modulates the number and division rate of germline stem cells. Development *127*, 503-514.

Crackower M.A., Kolas N.K., Noguchi J., Sarao R., Kikuchi K., Kaneko H., Kobayashi E., Kawai Y., Kozieradzki I., Landers R., *et al.* (2003). Essential role of Fkbp6 in male fertility and homologous chromosome pairing in meiosis. Science *300*, 1291-1295.

Davis T.L., Yang G.J., McCarrey J.R., and Bartolomei M.S. (2000). The H19 methylation imprint is erased and re-established differentially on the parental alleles during male germ cell development. Human molecular genetics *9*, 2885-2894.

De Fazio S., Bartonicek N., Di Giacomo M., Abreu-Goodger C., Sankar A., Funaya C., Antony C., Moreira P.N., Enright A.J., and O'Carroll D. (2011). The endonuclease activity of Mili fuels piRNA amplification that silences LINE1 elements. Nature *480*, 259-263.

De Rooij D.G. (1988). Regulation of the proliferation of spermatogonial stem cells. Journal of cell science Supplement *10*, 181-194.

de Rooij D.G. (2009). The spermatogonial stem cell niche. Microscopy research and technique *72*, 580-585.

de Rooij D.G., and Grootegoed J.A. (1998). Spermatogonial stem cells. Current opinion in cell biology *10*, 694-701.

Deng W., and Lin H. (2002). miwi, a murine homolog of piwi, encodes a cytoplasmic protein essential for spermatogenesis. Developmental cell *2*, 819-830.

Devor E.J., Huang L., and Samollow P.B. (2008). PiRNA-like RNAs in the marsupial Monodelphis domestica identify transcription clusters and likely marsupial transposon targets. Mammalian genome : official journal of the International Mammalian Genome Society *19*, 581-586.

Dhayalan A., Rajavelu A., Rathert P., Tamas R., Jurkowska R.Z., Ragozin S., and Jeltsch A. (2010). The Dnmt3a PWWP domain reads histone 3 lysine 36 trimethylation and guides DNA methylation. The Journal of biological chemistry *285*, 26114-26120.

Di Giacomo M., Comazzetto S., Saini H., De Fazio S., Carrieri C., Morgan M., Vasiliauskaite L., Benes V., Enright A.J., and O'Carroll D. (2013). Multiple epigenetic mechanisms and the

piRNA pathway enforce LINE1 silencing during adult spermatogenesis. Molecular cell *50*, 601-608.

Di Giacomo M., Comazzetto S., Sampath S.C., Sampath S.C., and O'Carroll D. (2014). G9a co-suppresses LINE1 elements in spermatogonia. Epigenetics & chromatin *7*, 24.

Djikeng A., Shi H., Tschudi C., and Ullu E. (2001). RNA interference in Trypanosoma brucei: cloning of small interfering RNAs provides evidence for retroposon-derived 24-26-nucleotide RNAs. Rna *7*, 1522-1530.

Ebata K.T., Yeh J.R., Zhang X., and Nagano M.C. (2011). Soluble growth factors stimulate spermatogonial stem cell divisions that maintain a stem cell pool and produce progenitors in vitro. Experimental cell research *317*, 1319-1329.

Ebata K.T., Zhang X., and Nagano M.C. (2007). Male germ line stem cells have an altered potential to proliferate and differentiate during postnatal development in mice. Biology of reproduction *76*, 841-847.

Eddy E.M. (1974). Fine structural observations on the form and distribution of nuage in germ cells of the rat. The Anatomical record *178*, 731-757.

Feil R., Wagner J., Metzger D., and Chambon P. (1997). Regulation of Cre recombinase activity by mutated estrogen receptor ligand-binding domains. Biochemical and biophysical research communications *237*, 752-757.

Frost R.J., Hamra F.K., Richardson J.A., Qi X., Bassel-Duby R., and Olson E.N. (2010). MOV10L1 is necessary for protection of spermatocytes against retrotransposons by Piwi-interacting RNAs. Proceedings of the National Academy of Sciences of the United States of America *107*, 11847-11852.

Ghildiyal M., Seitz H., Horwich M.D., Li C., Du T., Lee S., Xu J., Kittler E.L., Zapp M.L., Weng Z., *et al.* (2008). Endogenous siRNAs derived from transposons and mRNAs in Drosophila somatic cells. Science *320*, 1077-1081.

Girard A., Sachidanandam R., Hannon G.J., and Carmell M.A. (2006). A germline-specific class of small RNAs binds mammalian Piwi proteins. Nature *442*, 199-202.

Glass J.L., Fazzari M.J., Ferguson-Smith A.C., and Greally J.M. (2009). CG dinucleotide periodicities recognized by the Dnmt3a-Dnmt3L complex are distinctive at retroelements and imprinted domains. Mammalian genome : official journal of the International Mammalian Genome Society *20*, 633-643.

Goertz M.J., Wu Z., Gallardo T.D., Hamra F.K., and Castrillon D.H. (2011). Foxo1 is required in mouse spermatogonial stem cells for their maintenance and the initiation of spermatogenesis. The Journal of clinical investigation *121*, 3456-3466.

Goh W.S., Falciatori I., Tam O.H., Burgess R., Meikar O., Kotaja N., Hammell M., and Hannon G.J. (2015). piRNA-directed cleavage of meiotic transcripts regulates spermatogenesis. Genes & development *29*, 1032-1044.

Goll M.G., Kirpekar F., Maggert K.A., Yoder J.A., Hsieh C.L., Zhang X., Golic K.G., Jacobsen S.E., and Bestor T.H. (2006). Methylation of tRNAAsp by the DNA methyltransferase homolog Dnmt2. Science *311*, 395-398.

Gonzalez J., Qi H., Liu N., and Lin H. (2015). Piwi Is a Key Regulator of Both Somatic and Germline Stem Cells in the Drosophila Testis. Cell reports *12*, 150-161.

Gou L.T., Dai P., Yang J.H., Xue Y., Hu Y.P., Zhou Y., Kang J.Y., Wang X., Li H., Hua M.M., *et al.* (2014). Pachytene piRNAs instruct massive mRNA elimination during late spermiogenesis. Cell research *24*, 680-700.

Gowher H., Liebert K., Hermann A., Xu G., and Jeltsch A. (2005). Mechanism of stimulation of catalytic activity of Dnmt3A and Dnmt3B DNA-(cytosine-C5)-methyltransferases by Dnmt3L. The Journal of biological chemistry *280*, 13341-13348.

Grasso M., Fuso A., Dovere L., de Rooij D.G., Stefanini M., Boitani C., and Vicini E. (2012). Distribution of GFRA1-expressing spermatogonia in adult mouse testis. Reproduction *143*, 325-332.

Grimson A., Srivastava M., Fahey B., Woodcroft B.J., Chiang H.R., King N., Degnan B.M., Rokhsar D.S., and Bartel D.P. (2008). Early origins and evolution of microRNAs and Piwi-interacting RNAs in animals. Nature *455*, 1193-1197.

Grisanti L., Falciatori I., Grasso M., Dovere L., Fera S., Muciaccia B., Fuso A., Berno V., Boitani C., Stefanini M., *et al.* (2009). Identification of spermatogonial stem cell subsets by morphological analysis and prospective isolation. Stem cells *27*, 3043-3052.

Grivna S.T., Beyret E., Wang Z., and Lin H. (2006a). A novel class of small RNAs in mouse spermatogenic cells. Genes & development *20*, 1709-1714.

Grivna S.T., Pyhtila B., and Lin H. (2006b). MIWI associates with translational machinery and PIWI-interacting RNAs (piRNAs) in regulating spermatogenesis. Proceedings of the National Academy of Sciences of the United States of America *103*, 13415-13420.

Gruenbaum Y., Cedar H., and Razin A. (1982). Substrate and sequence specificity of a eukaryotic DNA methylase. Nature *295*, 620-622.

Gunawardane L.S., Saito K., Nishida K.M., Miyoshi K., Kawamura Y., Nagami T., Siomi H., and Siomi M.C. (2007). A slicer-mediated mechanism for repeat-associated siRNA 5' end formation in Drosophila. Science *315*, 1587-1590.

Hackett J.A., Sengupta R., Zylicz J.J., Murakami K., Lee C., Down T.A., and Surani M.A. (2013). Germline DNA demethylation dynamics and imprint erasure through 5-hydroxymethylcytosine. Science *339*, 448-452.

Hayashi K., Chuva de Sousa Lopes S.M., Kaneda M., Tang F., Hajkova P., Lao K., O'Carroll D., Das P.P., Tarakhovsky A., Miska E.A., *et al.* (2008). MicroRNA biogenesis is required for mouse primordial germ cell development and spermatogenesis. PloS one *3*, e1738.

Hajkova P., Erhardt S., Lane N., Haaf T., El-Maarri O., Reik W., Walter J., and Surani M.A. (2002). Epigenetic reprogramming in mouse primordial germ cells. Mechanisms of development *117*, 15-23.

Han B.W., Wang W., Li C., Weng Z., and Zamore P.D. (2015). Noncoding RNA. piRNA-guided transposon cleavage initiates Zucchini-dependent, phased piRNA production. Science *348*, 817-821.

Hara K., Nakagawa T., Enomoto H., Suzuki M., Yamamoto M., Simons B.D., and Yoshida S. (2014). Mouse spermatogenic stem cells continually interconvert between equipotent singly isolated and syncytial states. Cell stem cell *14*, 658-672.

Hasegawa K., Namekawa S.H., and Saga Y. (2013). MEK/ERK signaling directly and indirectly contributes to the cyclical self-renewal of spermatogonial stem cells. Stem cells *31*, 2517-2527.

Hata K., Kusumi M., Yokomine T., Li E., and Sasaki H. (2006). Meiotic and epigenetic aberrations in Dnmt3L-deficient male germ cells. Molecular reproduction and development *73*, 116-122.

Hata K., Okano M., Lei H., and Li E. (2002). Dnmt3L cooperates with the Dnmt3 family of de novo DNA methyltransferases to establish maternal imprints in mice. Development *129*, 1983-1993.

He Z., Jiang J., Kokkinaki M., Golestaneh N., Hofmann M.C., and Dym M. (2008). Gdnf upregulates c-Fos transcription via the Ras/Erk1/2 pathway to promote mouse spermatogonial stem cell proliferation. Stem cells *26*, 266-278.

Hervouet E., Vallette F.M., and Cartron P.F. (2009). Dnmt3/transcription factor interactions as crucial players in targeted DNA methylation. Epigenetics *4*, 487-499.

Hobbs R.M., Fagoonee S., Papa A., Webster K., Altruda F., Nishinakamura R., Chai L., and Pandolfi P.P. (2012). Functional antagonism between Sall4 and Plzf defines germline progenitors. Cell stem cell *10*, 284-298.

Hobbs R.M., Seandel M., Falciatori I., Rafii S., and Pandolfi P.P. (2010). Plzf regulates germline progenitor self-renewal by opposing mTORC1. Cell *142*, 468-479.

Hofmann M.C., Braydich-Stolle L., and Dym M. (2005). Isolation of male germ-line stem cells; influence of GDNF. Developmental biology *279*, 114-124.

Holz-Schietinger C., and Reich N.O. (2010). The inherent processivity of the human de novo methyltransferase 3A (DNMT3A) is enhanced by DNMT3L. The Journal of biological chemistry *285*, 29091-29100.

Homolka D., Pandey R.R., Goriaux C., Brasset E., Vaury C., Sachidanandam R., Fauvarque M.O., and Pillai R.S. (2015). PIWI Slicing and RNA Elements in Precursors Instruct Directional Primary piRNA Biogenesis. Cell reports *12*, 418-428.

Hosokawa M., Shoji M., Kitamura K., Tanaka T., Noce T., Chuma S., and Nakatsuji N. (2007). Tudor-related proteins TDRD1/MTR-1, TDRD6 and TDRD7/TRAP: domain composition, intracellular localization, and function in male germ cells in mice. Developmental biology *301*, 38-52.

Hsieh C.L. (1999). In vivo activity of murine de novo methyltransferases, Dnmt3a and Dnmt3b. Molecular and cellular biology *19*, 8211-8218.

Hu Y.C., de Rooij D.G., and Page D.C. (2013). Tumor suppressor gene Rb is required for self-renewal of spermatogonial stem cells in mice. Proceedings of the National Academy of Sciences of the United States of America *110*, 12685-12690.

Hu J.L., Zhou B.O., Zhang R.R., Zhang K.L., Zhou J.Q., and Xu G.L. (2009). The N-terminus of histone H3 is required for de novo DNA methylation in chromatin. Proceedings of the National Academy of Sciences of the United States of America *106*, 22187-22192.

Huang H., Gao Q., Peng X., Choi S.Y., Sarma K., Ren H., Morris A.J., and Frohman M.A. (2011). piRNA-associated germline nuage formation and spermatogenesis require MitoPLD profusogenic mitochondrial-surface lipid signaling. Developmental cell *20*, 376-387.

Yabuta Y., Ohta H., Abe T., Kurimoto K., Chuma S., and Saitou M. (2011). TDRD5 is required for retrotransposon silencing, chromatoid body assembly, and spermiogenesis in mice. The Journal of cell biology *192*, 781-795.

Yang Z., Chen K.M., Pandey R.R., Homolka D., Reuter M., Janeiro B.K., Sachidanandam R., Fauvarque M.O., McCarthy A.A., and Pillai R.S. (2016). PIWI Slicing and EXD1 Drive Biogenesis of Nuclear piRNAs from Cytosolic Targets of the Mouse piRNA Pathway. Molecular cell *61*, 138-152.

Ichiyanagi T., Ichiyanagi K., Ogawa A., Kuramochi-Miyagawa S., Nakano T., Chuma S., Sasaki H., and Udono H. (2014). HSP90alpha plays an important role in piRNA biogenesis and retrotransposon repression in mouse. Nucleic acids research *42*, 11903-11911.

Ikami K., Tokue M., Sugimoto R., Noda C., Kobayashi S., Hara K., and Yoshida S. (2015). Hierarchical differentiation competence in response to retinoic acid ensures stem cell maintenance during mouse spermatogenesis. Development *142*, 1582-1592.

Yoder J.A., and Bestor T.H. (1998). A candidate mammalian DNA methyltransferase related to pmt1p of fission yeast. Human molecular genetics *7*, 279-284.

Yoshida S. (2012). Elucidating the identity and behavior of spermatogenic stem cells in the mouse testis. Reproduction *144*, 293-302.

Yoshida S., Sukeno M., and Nabeshima Y. (2007). A vasculature-associated niche for undifferentiated spermatogonia in the mouse testis. Science *317*, 1722-1726.

Yoshida S., Takakura A., Ohbo K., Abe K., Wakabayashi J., Yamamoto M., Suda T., and Nabeshima Y. (2004). Neurogenin3 delineates the earliest stages of spermatogenesis in the mouse testis. Developmental biology *269*, 447-458.

Yoshinaga K., Nishikawa S., Ogawa M., Hayashi S., Kunisada T., Fujimoto T., and Nishikawa S. (1991). Role of c-kit in mouse spermatogenesis: identification of spermatogonia as a specific site of c-kit expression and function. Development *113*, 689-699.

Ishii K., Kanatsu-Shinohara M., Toyokuni S., and Shinohara T. (2012). FGF2 mediates mouse spermatogonial stem cell self-renewal via upregulation of Etv5 and Bcl6b through MAP2K1 activation. Development *139*, 1734-1743.

Jia D., Jurkowska R.Z., Zhang X., Jeltsch A., and Cheng X. (2007). Structure of Dnmt3a bound to Dnmt3L suggests a model for de novo DNA methylation. Nature *449*, 248-251.

Jurka J., Kapitonov V.V., Pavlicek A., Klonowski P., Kohany O., and Walichiewicz J. (2005). Repbase Update, a database of eukaryotic repetitive elements. Cytogenetic and genome research *110*, 462-467.

Kafri T., Ariel M., Brandeis M., Shemer R., Urven L., McCarrey J., Cedar H., and Razin A. (1992). Developmental pattern of gene-specific DNA methylation in the mouse embryo and germ line. Genes & development *6*, 705-714.

Kalmykova A.I., Klenov M.S., and Gvozdev V.A. (2005). Argonaute protein PIWI controls mobilization of retrotransposons in the Drosophila male germline. Nucleic acids research *33*, 2052-2059.

Kanatsu-Shinohara M., Ogonuki N., Inoue K., Miki H., Ogura A., Toyokuni S., and Shinohara T. (2003). Long-term proliferation in culture and germline transmission of mouse male germline stem cells. Biology of reproduction *69*, 612-616.

Kanatsu-Shinohara M., Takashima S., Ishii K., and Shinohara T. (2011). Dynamic changes in EPCAM expression during spermatogonial stem cell differentiation in the mouse testis. PloS one *6*, e23663.

Kanatsu-Shinohara M., Toyokuni S., and Shinohara T. (2004). CD9 is a surface marker on mouse and rat male germline stem cells. Biology of reproduction *70*, 70-75.

Kanatsu-Shinohara M., Toyokuni S., and Shinohara T. (2005). Genetic selection of mouse male germline stem cells in vitro: offspring from single stem cells. Biology of reproduction *72*, 236-240.

Kaneda M., Okano M., Hata K., Sado T., Tsujimoto N., Li E., and Sasaki H. (2004). Essential role for de novo DNA methyltransferase Dnmt3a in paternal and maternal imprinting. Nature *429*, 900-903.

Kareta M.S., Botello Z.M., Ennis J.J., Chou C., and Chedin F. (2006). Reconstitution and mechanism of the stimulation of de novo methylation by human DNMT3L. The Journal of biological chemistry *281*, 25893-25902.

Kato Y., Kaneda M., Hata K., Kumaki K., Hisano M., Kohara Y., Okano M., Li E., Nozaki M., and Sasaki H. (2007). Role of the Dnmt3 family in de novo methylation of imprinted and repetitive sequences during male germ cell development in the mouse. Human molecular genetics *16*, 2272-2280.

Kawaoka S., Izumi N., Katsuma S., and Tomari Y. (2011). 3' end formation of PIWI-interacting RNAs in vitro. Molecular cell *43*, 1015-1022.

Kim V.N., Han J., and Siomi M.C. (2009). Biogenesis of small RNAs in animals. Nature reviews Molecular cell biology *10*, 126-139.

Klein A.M., Nakagawa T., Ichikawa R., Yoshida S., and Simons B.D. (2010). Mouse germ line stem cells undergo rapid and stochastic turnover. Cell stem cell *7*, 214-224.

Klenov M.S., Sokolova O.A., Yakushev E.Y., Stolyarenko A.D., Mikhaleva E.A., Lavrov S.A., and Gvozdev V.A. (2011). Separation of stem cell maintenance and transposon silencing functions of Piwi protein. Proceedings of the National Academy of Sciences of the United States of America *108*, 18760-18765.

Kotaja N., Lin H., Parvinen M., and Sassone-Corsi P. (2006). Interplay of PIWI/Argonaute protein MIWI and kinesin KIF17b in chromatoid bodies of male germ cells. Journal of cell science *119*, 2819-2825.

Kotaja N., and Sassone-Corsi P. (2007). The chromatoid body: a germ-cell-specific RNA-processing centre. Nature reviews Molecular cell biology *8*, 85-90.

Kremers G.J., Gilbert S.G., Cranfill P.J., Davidson M.W., and Piston D.W. (2011). Fluorescent proteins at a glance. Journal of cell science *124*, 157-160.

Kuramochi-Miyagawa S., Kimura T., Ijiri T.W., Isobe T., Asada N., Fujita Y., Ikawa M., Iwai N., Okabe M., Deng W., *et al.* (2004). Mili, a mammalian member of piwi family gene, is essential for spermatogenesis. Development *131*, 839-849.

Kuramochi-Miyagawa S., Kimura T., Yomogida K., Kuroiwa A., Tadokoro Y., Fujita Y., Sato M., Matsuda Y., and Nakano T. (2001). Two mouse piwi-related genes: miwi and mili. Mechanisms of development *108*, 121-133.

Kuramochi-Miyagawa S., Watanabe T., Gotoh K., Takamatsu K., Chuma S., Kojima-Kita K., Shiromoto Y., Asada N., Toyoda A., Fujiyama A., *et al.* (2010). MVH in piRNA processing and gene silencing of retrotransposons. Genes & development *24*, 887-892.

Kuramochi-Miyagawa S., Watanabe T., Gotoh K., Totoki Y., Toyoda A., Ikawa M., Asada N., Kojima K., Yamaguchi Y., Ijiri T.W., *et al.* (2008). DNA methylation of retrotransposon genes is regulated by Piwi family members MILI and MIWI2 in murine fetal testes. Genes & development *22*, 908-917.

La Salle S., Mertineit C., Taketo T., Moens P.B., Bestor T.H., and Trasler J.M. (2004). Windows for sex-specific methylation marked by DNA methyltransferase expression profiles in mouse germ cells. Developmental biology *268*, 403-415.

La Salle S., Oakes C.C., Neaga O.R., Bourc'his D., Bestor T.H., and Trasler J.M. (2007). Loss of spermatogonia and wide-spread DNA methylation defects in newborn male mice deficient in DNMT3L. BMC developmental biology *7*, 104.

La Salle S., and Trasler J.M. (2006). Dynamic expression of DNMT3a and DNMT3b isoforms during male germ cell development in the mouse. Developmental biology *296*, 71-82.

Lane N., Dean W., Erhardt S., Hajkova P., Surani A., Walter J., and Reik W. (2003). Resistance of IAPs to methylation reprogramming may provide a mechanism for epigenetic inheritance in the mouse. Genesis *35*, 88-93.

Lau N.C., Seto A.G., Kim J., Kuramochi-Miyagawa S., Nakano T., Bartel D.P., and Kingston R.E. (2006). Characterization of the piRNA complex from rat testes. Science *313*, 363-367.

Lee J., Kanatsu-Shinohara M., Inoue K., Ogonuki N., Miki H., Toyokuni S., Kimura T., Nakano T., Ogura A., and Shinohara T. (2007). Akt mediates self-renewal division of mouse spermatogonial stem cells. Development *134*, 1853-1859.

Lees-Murdock D.J., De Felici M., and Walsh C.P. (2003). Methylation dynamics of repetitive DNA elements in the mouse germ cell lineage. Genomics *82*, 230-237.

Lees-Murdock D.J., Shovlin T.C., Gardiner T., De Felici M., and Walsh C.P. (2005). DNA methyltransferase expression in the mouse germ line during periods of de novo methylation. Developmental dynamics : an official publication of the American Association of Anatomists *232*, 992-1002.

Lees-Murdock D.J., and Walsh C.P. (2008). DNA methylation reprogramming in the germ line. Epigenetics *3*, 5-13.

Lei H., Oh S.P., Okano M., Juttermann R., Goss K.A., Jaenisch R., and Li E. (1996). De novo DNA cytosine methyltransferase activities in mouse embryonic stem cells. Development *122*, 3195-3205.

Leonhardt H., Page A.W., Weier H.U., and Bestor T.H. (1992). A targeting sequence directs DNA methyltransferase to sites of DNA replication in mammalian nuclei. Cell *71*, 865-873.

Li C., Vagin V.V., Lee S., Xu J., Ma S., Xi H., Seitz H., Horwich M.D., Syrzycka M., Honda B.M., *et al.* (2009). Collapse of germline piRNAs in the absence of Argonaute3 reveals somatic piRNAs in flies. Cell *137*, 509-521.

Li E., Bestor T.H., and Jaenisch R. (1992). Targeted mutation of the DNA methyltransferase gene results in embryonic lethality. Cell *69*, 915-926.

Li J.Y., Lees-Murdock D.J., Xu G.L., and Walsh C.P. (2004). Timing of establishment of paternal methylation imprints in the mouse. Genomics *84*, 952-960.

Li R., Vannitamby A., Zhang J.G., Fehmel E.L., Southwell B.R., and Hutson J.M. (2015). Oct4-GFP expression during transformation of gonocytes into spermatogonial stem cells in the perinatal mouse testis. Journal of pediatric surgery *50*, 2084-2089.

Li X.Z., Roy C.K., Dong X., Bolcun-Filas E., Wang J., Han B.W., Xu J., Moore M.J., Schimenti J.C., Weng Z., *et al.* (2013). An ancient transcription factor initiates the burst of piRNA production during early meiosis in mouse testes. Molecular cell *50*, 67-81.

Liao H.F., Chen W.S., Chen Y.H., Kao T.H., Tseng Y.T., Lee C.Y., Chiu Y.C., Lee P.L., Lin Q.J., Ching Y.H., *et al.* (2014). DNMT3L promotes quiescence in postnatal spermatogonial progenitor cells. Development *141*, 2402-2413.

Lim S.L., Qu Z.P., Kortschak R.D., Lawrence D.M., Geoghegan J., Hempfling A.L., Bergmann M., Goodnow C.C., Ormandy C.J., Wong L., *et al.* (2015). HENMT1 and piRNA Stability Are Required for Adult Male Germ Cell Transposon Repression and to Define the Spermatogenic Program in the Mouse. PLoS genetics *11*, e1005620.

Lin H., and Spradling A.C. (1997). A novel group of pumilio mutations affects the asymmetric division of germline stem cells in the Drosophila ovary. Development *124*, 2463-2476.

Liu J., Carmell M.A., Rivas F.V., Marsden C.G., Thomson J.M., Song J.J., Hammond S.M., Joshua-Tor L., and Hannon G.J. (2004). Argonaute2 is the catalytic engine of mammalian RNAi. Science *305*, 1437-1441.

Ma L., Buchold G.M., Greenbaum M.P., Roy A., Burns K.H., Zhu H., Han D.Y., Harris R.A., Coarfa C., Gunaratne P.H., *et al.* (2009). GASZ is essential for male meiosis and suppression of retrotransposon expression in the male germline. PLoS genetics *5*, e1000635.

Malone C.D., Brennecke J., Dus M., Stark A., McCombie W.R., Sachidanandam R., and Hannon G.J. (2009). Specialized piRNA pathways act in germline and somatic tissues of the Drosophila ovary. Cell *137*, 522-535.

Manakov S.A., Pezic D., Marinov G.K., Pastor W.A., Sachidanandam R., and Aravin A.A. (2015). MIWI2 and MILI Have Differential Effects on piRNA Biogenesis and DNA Methylation. Cell reports *12*, 1234-1243.

McLaren A., and Southee D. (1997). Entry of mouse embryonic germ cells into meiosis. Developmental biology *187*, 107-113.

Meng X., Lindahl M., Hyvonen M.E., Parvinen M., de Rooij D.G., Hess M.W., Raatikainen-Ahokas A., Sainio K., Rauvala H., Lakso M., *et al.* (2000). Regulation of cell fate decision of undifferentiated spermatogonia by GDNF. Science *287*, 1489-1493.

Merchant-Larios H., Moreno-Mendoza N., and Buehr M. (1993). The role of the mesonephros in cell differentiation and morphogenesis of the mouse fetal testis. The International journal of developmental biology *37*, 407-415.

Miura F., and Ito T. (2015). Highly sensitive targeted methylome sequencing by post-bisulfite adaptor tagging. DNA research : an international journal for rapid publication of reports on genes and genomes *22*, 13-18.

Mochizuki K., Fine N.A., Fujisawa T., and Gorovsky M.A. (2002). Analysis of a piwi-related gene implicates small RNAs in genome rearrangement in tetrahymena. Cell *110*, 689-699.

Mohn F., Handler D., and Brennecke J. (2015). Noncoding RNA. piRNA-guided slicing specifies transcripts for Zucchini-dependent, phased piRNA biogenesis. Science *348*, 812-817.

Molaro A., Falciatori I., Hodges E., Aravin A.A., Marran K., Rafii S., McCombie W.R., Smith A.D., and Hannon G.J. (2014). Two waves of de novo methylation during mouse germ cell development. Genes & development *28*, 1544-1549.

Morimoto H., Iwata K., Ogonuki N., Inoue K., Atsuo O., Kanatsu-Shinohara M., Morimoto T., Yabe-Nishimura C., and Shinohara T. (2013). ROS are required for mouse spermatogonial stem cell self-renewal. Cell stem cell *12*, 774-786.

Mouse Genome Sequencing C., Waterston R.H., Lindblad-Toh K., Birney E., Rogers J., Abril J.F., Agarwal P., Agarwala R., Ainscough R., Alexandersson M., *et al.* (2002). Initial sequencing and comparative analysis of the mouse genome. Nature *420*, 520-562.

Murchison E.P., Kheradpour P., Sachidanandam R., Smith C., Hodges E., Xuan Z., Kellis M., Grutzner F., Stark A., and Hannon G.J. (2008). Conservation of small RNA pathways in platypus. Genome research *18*, 995-1004.

Nagamori I., Kobayashi H., Shiromoto Y., Nishimura T., Kuramochi-Miyagawa S., Kono T., and Nakano T. (2015). Comprehensive DNA Methylation Analysis of Retrotransposons in Male Germ Cells. Cell reports *12*, 1541-1547.

Nakagawa T., Nabeshima Y., and Yoshida S. (2007). Functional identification of the actual and potential stem cell compartments in mouse spermatogenesis. Developmental cell *12*, 195-206.

Nakagawa T., Sharma M., Nabeshima Y., Braun R.E., and Yoshida S. (2010). Functional hierarchy and reversibility within the murine spermatogenic stem cell compartment. Science *328*, 62-67.

Nakanishi K., Weinberg D.E., Bartel D.P., and Patel D.J. (2012). Structure of yeast Argonaute with guide RNA. Nature *486*, 368-374.

Naughton C.K., Jain S., Strickland A.M., Gupta A., and Milbrandt J. (2006). Glial cell-line derived neurotrophic factor-mediated RET signaling regulates spermatogonial stem cell fate. Biology of reproduction *74*, 314-321.

Nebel B.R., Amarose A.P., and Hacket E.M. (1961). Calendar of gametogenic development in the prepuberal male mouse. Science *134*, 832-833.

Niles K.M., Chan D., La Salle S., Oakes C.C., and Trasler J.M. (2011). Critical period of nonpromoter DNA methylation acquisition during prenatal male germ cell development. PloS one *6*, e24156.

Nimura K., Ishida C., Koriyama H., Hata K., Yamanaka S., Li E., Ura K., and Kaneda Y. (2006). Dnmt3a2 targets endogenous Dnmt3L to ES cell chromatin and induces regional DNA methylation. Genes to cells : devoted to molecular & cellular mechanisms *11*, 1225-1237.

Nishibu T., Hayashida Y., Tani S., Kurono S., Kojima-Kita K., Ukekawa R., Kurokawa T., Kuramochi-Miyagawa S., Nakano T., Inoue K., *et al.* (2012). Identification of MIWI-associated Poly(A) RNAs by immunoprecipitation with an anti-MIWI monoclonal antibody. Bioscience trends *6*, 248-261.

O'Doherty A.M., Rutledge C.E., Sato S., Thakur A., Lees-Murdock D.J., Hata K., and Walsh C.P. (2011). DNA methylation plays an important role in promoter choice and protein production at the mouse Dnmt3L locus. Developmental biology *356*, 411-420.

Oakberg E.F. (1956). Duration of spermatogenesis in the mouse and timing of stages of the cycle of the seminiferous epithelium. The American journal of anatomy *99*, 507-516.

Oakberg E.F. (1971). Spermatogonial stem-cell renewal in the mouse. The Anatomical record *169*, 515-531.

Oatley J.M., Avarbock M.R., and Brinster R.L. (2007). Glial cell line-derived neurotrophic factor regulation of genes essential for self-renewal of mouse spermatogonial stem cells is dependent on Src family kinase signaling. The Journal of biological chemistry *282*, 25842-25851.

Oatley J.M., Oatley M.J., Avarbock M.R., Tobias J.W., and Brinster R.L. (2009). Colony stimulating factor 1 is an extrinsic stimulator of mouse spermatogonial stem cell self-renewal. Development *136*, 1191-1199.

Oatley M.J., Kaucher A.V., Racicot K.E., and Oatley J.M. (2011a). Inhibitor of DNA binding 4 is expressed selectively by single spermatogonia in the male germline and regulates the self-renewal of spermatogonial stem cells in mice. Biology of reproduction *85*, 347-356.

Oatley M.J., Racicot K.E., and Oatley J.M. (2011b). Sertoli cells dictate spermatogonial stem cell niches in the mouse testis. Biology of reproduction *84*, 639-645.

Ogawa T., Ohmura M., Yumura Y., Sawada H., and Kubota Y. (2003). Expansion of murine spermatogonial stem cells through serial transplantation. Biology of reproduction *68*, 316-322.

Ohbo K., Yoshida S., Ohmura M., Ohneda O., Ogawa T., Tsuchiya H., Kuwana T., Kehler J., Abe K., Scholer H.R., *et al.* (2003). Identification and characterization of stem cells in prepubertal spermatogenesis in mice. Developmental biology *258*, 209-225.

Ohinata Y., Payer B., O'Carroll D., Ancelin K., Ono Y., Sano M., Barton S.C., Obukhanych T., Nussenzweig M., Tarakhovsky A., *et al.* (2005). Blimp1 is a critical determinant of the germ cell lineage in mice. Nature *436*, 207-213.

Okano M., Bell D.W., Haber D.A., and Li E. (1999). DNA methyltransferases Dnmt3a and Dnmt3b are essential for de novo methylation and mammalian development. Cell *99*, 247-257.

Okano M., Xie S., and Li E. (1998a). Cloning and characterization of a family of novel mammalian DNA (cytosine-5) methyltransferases. Nature genetics *19*, 219-220.

Okano M., Xie S., and Li E. (1998b). Dnmt2 is not required for de novo and maintenance methylation of viral DNA in embryonic stem cells. Nucleic acids research *26*, 2536-2540.

Ooi S.K., Qiu C., Bernstein E., Li K., Jia D., Yang Z., Erdjument-Bromage H., Tempst P., Lin S.P., Allis C.D., *et al.* (2007). DNMT3L connects unmethylated lysine 4 of histone H3 to de novo methylation of DNA. Nature *448*, 714-717.

Pacaud R., Sery Q., Oliver L., Vallette F.M., Tost J., and Cartron P.F. (2014). DNMT3L interacts with transcription factors to target DNMT3L/DNMT3B to specific DNA sequences: role of the DNMT3L/DNMT3B/p65-NFkappaB complex in the (de-)methylation of TRAF1. Biochimie *104*, 36-49.

Palakodeti D., Smielewska M., Lu Y.C., Yeo G.W., and Graveley B.R. (2008). The PIWI proteins SMEDWI-2 and SMEDWI-3 are required for stem cell function and piRNA expression in planarians. Rna *14*, 1174-1186.

Pan J., Goodheart M., Chuma S., Nakatsuji N., Page D.C., and Wang P.J. (2005). RNF17, a component of the mammalian germ cell nuage, is essential for spermiogenesis. Development *132*, 4029-4039.

Papaioannou M.D., Pitetti J.L., Ro S., Park C., Aubry F., Schaad O., Vejnar C.E., Kuhne F., Descombes P., Zdobnov E.M., *et al.* (2009). Sertoli cell Dicer is essential for spermatogenesis in mice. Developmental biology *326*, 250-259.

Parker N., Falk H., Singh D., Fidaleo A., Smith B., Lopez M.S., Shokat K.M., and Wright W.W. (2014). Responses to glial cell line-derived neurotrophic factor change in mice as

spermatogonial stem cells form progenitor spermatogonia which replicate and give rise to more differentiated progeny. Biology of reproduction *91*, 92.

Pastor W.A., Stroud H., Nee K., Liu W., Pezic D., Manakov S., Lee S.A., Moissiard G., Zamudio N., Bourc'his D., *et al.* (2014). MORC1 represses transposable elements in the mouse male germline. Nature communications *5*, 5795.

Pech M.F., Garbuzov A., Hasegawa K., Sukhwani M., Zhang R.J., Benayoun B.A., Brockman S.A., Lin S., Brunet A., Orwig K.E., *et al.* (2015). High telomerase is a hallmark of undifferentiated spermatogonia and is required for maintenance of male germline stem cells. Genes & development *29*, 2420-2434.

Pezic D., Manakov S.A., Sachidanandam R., and Aravin A.A. (2014). piRNA pathway targets active LINE1 elements to establish the repressive H3K9me3 mark in germ cells. Genes & development *28*, 1410-1428.

Phillips B.T., Gassei K., and Orwig K.E. (2010). Spermatogonial stem cell regulation and spermatogenesis. Philosophical transactions of the Royal Society of London Series B, Biological sciences *365*, 1663-1678.

Raju P., Nyamsuren G., Elkenani M., Kata A., Tsagaan E., Engel W., and Adham I.M. (2015). Pelota mediates gonocyte maturation and maintenance of spermatogonial stem cells in mouse testes. Reproduction *149*, 213-221.

Reddien P.W., Oviedo N.J., Jennings J.R., Jenkin J.C., and Sanchez Alvarado A. (2005). SMEDWI-2 is a PIWI-like protein that regulates planarian stem cells. Science *310*, 1327-1330.

Reuter M., Berninger P., Chuma S., Shah H., Hosokawa M., Funaya C., Antony C., Sachidanandam R., and Pillai R.S. (2011). Miwi catalysis is required for piRNA amplification-independent LINE1 transposon silencing. Nature *480*, 264-267.

Reuter M., Chuma S., Tanaka T., Franz T., Stark A., and Pillai R.S. (2009). Loss of the Mili-interacting Tudor domain-containing protein-1 activates transposons and alters the Mili-associated small RNA profile. Nature structural & molecular biology *16*, 639-646.

Ritchie M.E., Phipson B., Wu D., Hu Y., Law C.W., Shi W., and Smyth G.K. (2015). limma powers differential expression analyses for RNA-sequencing and microarray studies. Nucleic acids research *43*, e47.

Ryu B.Y., Orwig K.E., Oatley J.M., Avarbock M.R., and Brinster R.L. (2006). Effects of aging and niche microenvironment on spermatogonial stem cell self-renewal. Stem cells *24*, 1505-1511.

Ro S., Park C., Song R., Nguyen D., Jin J., Sanders K.M., McCarrey J.R., and Yan W. (2007). Cloning and expression profiling of testis-expressed piRNA-like RNAs. Rna *13*, 1693-1702.

Ruby J.G., Jan C., Player C., Axtell M.J., Lee W., Nusbaum C., Ge H., and Bartel D.P. (2006). Large-scale sequencing reveals 21U-RNAs and additional microRNAs and endogenous siRNAs in C. elegans. Cell *127*, 1193-1207.

Sada A., Hasegawa K., Pin P.H., and Saga Y. (2012). NANOS2 acts downstream of glial cell line-derived neurotrophic factor signaling to suppress differentiation of spermatogonial stem cells. Stem cells *30*, 280-291.

Sada A., Suzuki A., Suzuki H., and Saga Y. (2009). The RNA-binding protein NANOS2 is required to maintain murine spermatogonial stem cells. Science *325*, 1394-1398.

Sadate-Ngatchou P.I., Payne C.J., Dearth A.T., and Braun R.E. (2008). Cre recombinase activity specific to postnatal, premeiotic male germ cells in transgenic mice. Genesis *46*, 738-742.

Sai Lakshmi S., and Agrawal S. (2008). piRNABank: a web resource on classified and clustered Piwi-interacting RNAs. Nucleic acids research *36*, D173-177.

Saito K., Nishida K.M., Mori T., Kawamura Y., Miyoshi K., Nagami T., Siomi H., and Siomi M.C. (2006). Specific association of Piwi with rasiRNAs derived from retrotransposon and heterochromatic regions in the Drosophila genome. Genes & development *20*, 2214-2222.

Sakai Y., Suetake I., Itoh K., Mizugaki M., Tajima S., and Yamashina S. (2001). Expression of DNA methyltransferase (Dnmt1) in testicular germ cells during development of mouse embryo. Cell structure and function *26*, 685-691.

Sakai Y., Suetake I., Shinozaki F., Yamashina S., and Tajima S. (2004). Co-expression of de novo DNA methyltransferases Dnmt3a2 and Dnmt3L in gonocytes of mouse embryos. Gene expression patterns : GEP *5*, 231-237.

Sasaki H., and Matsui Y. (2008). Epigenetic events in mammalian germ-cell development: reprogramming and beyond. Nature reviews Genetics *9*, 129-140.

Saxe J.P., Chen M., Zhao H., and Lin H. (2013). Tdrkh is essential for spermatogenesis and participates in primary piRNA biogenesis in the germline. The EMBO journal *32*, 1869-1885.

Schlesser H.N., Simon L., Hofmann M.C., Murphy K.M., Murphy T., Hess R.A., and Cooke P.S. (2008). Effects of ETV5 (ets variant gene 5) on testis and body growth, time course of spermatogonial stem cell loss, and fertility in mice. Biology of reproduction *78*, 483-489.

Schrans-Stassen B.H., van de Kant H.J., de Rooij D.G., and van Pelt A.M. (1999). Differential expression of c-kit in mouse undifferentiated and differentiating type A spermatogonia. Endocrinology *140*, 5894-5900.

Seki Y., Hayashi K., Itoh K., Mizugaki M., Saitou M., and Matsui Y. (2005). Extensive and orderly reprogramming of genome-wide chromatin modifications associated with specification and early development of germ cells in mice. Developmental biology *278*, 440-458.

Shinohara T., Avarbock M.R., and Brinster R.L. (1999). beta1- and alpha6-integrin are surface markers on mouse spermatogonial stem cells. Proceedings of the National Academy of Sciences of the United States of America *96*, 5504-5509.

Shinohara T., Orwig K.E., Avarbock M.R., and Brinster R.L. (2000). Spermatogonial stem cell enrichment by multiparameter selection of mouse testis cells. Proceedings of the National Academy of Sciences of the United States of America *97*, 8346-8351.

Shoji M., Tanaka T., Hosokawa M., Reuter M., Stark A., Kato Y., Kondoh G., Okawa K., Chujo T., Suzuki T., *et al.* (2009). The TDRD9-MIWI2 complex is essential for piRNA-mediated retrotransposon silencing in the mouse male germline. Developmental cell *17*, 775-787.

Shovlin T.C., Bourc'his D., La Salle S., O'Doherty A., Trasler J.M., Bestor T.H., and Walsh C.P. (2007). Sex-specific promoters regulate Dnmt3L expression in mouse germ cells. Human reproduction *22*, 457-467.

Sijen T., and Plasterk R.H. (2003). Transposon silencing in the Caenorhabditis elegans germ line by natural RNAi. Nature *426*, 310-314.

Soper S.F., van der Heijden G.W., Hardiman T.C., Goodheart M., Martin S.L., de Boer P., and Bortvin A. (2008). Mouse maelstrom, a component of nuage, is essential for spermatogenesis and transposon repression in meiosis. Developmental cell *15*, 285-297.

Suetake I., Shinozaki F., Miyagawa J., Takeshima H., and Tajima S. (2004). DNMT3L stimulates the DNA methylation activity of Dnmt3a and Dnmt3b through a direct interaction. The Journal of biological chemistry *279*, 27816-27823.

Sun F., Xu Q., Zhao D., and Degui Chen C. (2015). Id4 Marks Spermatogonial Stem Cells in the Mouse Testis. Scientific reports *5*, 17594.

Suzuki H., Sada A., Yoshida S., and Saga Y. (2009). The heterogeneity of spermatogonia is revealed by their topology and expression of marker proteins including the germ cell-specific proteins Nanos2 and Nanos3. Developmental biology *336*, 222-231.

Takase H.M., and Nusse R. (2016). Paracrine Wnt/beta-catenin signaling mediates proliferation of undifferentiated spermatogonia in the adult mouse testis. Proceedings of the National Academy of Sciences of the United States of America *113*, E1489-1497.

Takashima S., Kanatsu-Shinohara M., Tanaka T., Morimoto H., Inoue K., Ogonuki N., Jijiwa M., Takahashi M., Ogura A., and Shinohara T. (2015). Functional differences between GDNF-dependent and FGF2-dependent mouse spermatogonial stem cell self-renewal. Stem cell reports *4*, 489-502.

Takashima S., Takehashi M., Lee J., Chuma S., Okano M., Hata K., Suetake I., Nakatsuji N., Miyoshi H., Tajima S., *et al.* (2009). Abnormal DNA methyltransferase expression in mouse germline stem cells results in spermatogenic defects. Biology of reproduction *81*, 155-164.

Tanaka S.S., Toyooka Y., Akasu R., Katoh-Fukui Y., Nakahara Y., Suzuki R., Yokoyama M., and Noce T. (2000). The mouse homolog of Drosophila Vasa is required for the development of male germ cells. Genes & development *14*, 841-853.

Tanaka T., Hosokawa M., Vagin V.V., Reuter M., Hayashi E., Mochizuki A.L., Kitamura K., Yamanaka H., Kondoh G., Okawa K., *et al.* (2011). Tudor domain containing 7 (Tdrd7) is essential for dynamic ribonucleoprotein (RNP) remodeling of chromatoid bodies during spermatogenesis. Proceedings of the National Academy of Sciences of the United States of America *108*, 10579-10584.

Tokuda M., Kadokawa Y., Kurahashi H., and Marunouchi T. (2007). CDH1 is a specific marker for undifferentiated spermatogonia in mouse testes. Biology of reproduction *76*, 130-141.

Tsuda M., Sasaoka Y., Kiso M., Abe K., Haraguchi S., Kobayashi S., and Saga Y. (2003). Conserved role of nanos proteins in germ cell development. Science *301*, 1239-1241.

Uysal F., Akkoyunlu G., and Ozturk S. (2015). Dynamic expression of DNA methyltransferases (DNMTs) in oocytes and early embryos. Biochimie *116*, 103-113.

Unhavaithaya Y., Hao Y., Beyret E., Yin H., Kuramochi-Miyagawa S., Nakano T., and Lin H. (2009). MILI, a PIWI-interacting RNA-binding protein, is required for germ line stem cell self-renewal and appears to positively regulate translation. The Journal of biological chemistry *284*, 6507-6519.

Vagin V.V., Sigova A., Li C., Seitz H., Gvozdev V., and Zamore P.D. (2006). A distinct small RNA pathway silences selfish genetic elements in the germline. Science *313*, 320-324.

Vagin V.V., Wohlschlegel J., Qu J., Jonsson Z., Huang X., Chuma S., Girard A., Sachidanandam R., Hannon G.J., and Aravin A.A. (2009). Proteomic analysis of murine Piwi proteins reveals a role for arginine methylation in specifying interaction with Tudor family members. Genes & development *23*, 1749-1762.

van Wolfswinkel J.C. (2014). Piwi and potency: PIWI proteins in animal stem cells and regeneration. Integrative and comparative biology *54*, 700-713.

Vasileva A., Tiedau D., Firooznia A., Muller-Reichert T., and Jessberger R. (2009). Tdrd6 is required for spermiogenesis, chromatoid body architecture, and regulation of miRNA expression. Current biology : CB *19*, 630-639.

Vourekas A., Zheng Q., Alexiou P., Maragkakis M., Kirino Y., Gregory B.D., and Mourelatos Z. (2012). Mili and Miwi target RNA repertoire reveals piRNA biogenesis and function of Miwi in spermiogenesis. Nature structural & molecular biology *19*, 773-781.

Wasik K.A., Tam O.H., Knott S.R., Falciatori I., Hammell M., Vagin V.V., and Hannon G.J. (2015). RNF17 blocks promiscuous activity of PIWI proteins in mouse testes. Genes & development *29*, 1403-1415.

Watanabe D., Suetake I., Tada T., and Tajima S. (2002). Stage- and cell-specific expression of Dnmt3a and Dnmt3b during embryogenesis. Mechanisms of development *118*, 187-190.

Watanabe D., Suetake I., Tajima S., and Hanaoka K. (2004). Expression of Dnmt3b in mouse hematopoietic progenitor cells and spermatogonia at specific stages. Gene expression patterns : GEP *5*, 43-49.

Watanabe T., Cheng E.C., Zhong M., and Lin H. (2015). Retrotransposons and pseudogenes regulate mRNAs and lncRNAs via the piRNA pathway in the germline. Genome research *25*, 368-380.

Watanabe T., Chuma S., Yamamoto Y., Kuramochi-Miyagawa S., Totoki Y., Toyoda A., Hoki Y., Fujiyama A., Shibata T., Sado T., *et al.* (2011a). MITOPLD is a mitochondrial protein essential for nuage formation and piRNA biogenesis in the mouse germline. Developmental cell *20*, 364-375.

Watanabe T., Takeda A., Tsukiyama T., Mise K., Okuno T., Sasaki H., Minami N., and Imai H. (2006). Identification and characterization of two novel classes of small RNAs in the mouse germline: retrotransposon-derived siRNAs in oocytes and germline small RNAs in testes. Genes & development *20*, 1732-1743.

Watanabe T., Tomizawa S., Mitsuya K., Totoki Y., Yamamoto Y., Kuramochi-Miyagawa S., Iida N., Hoki Y., Murphy P.J., Toyoda A., *et al.* (2011b). Role for piRNAs and noncoding RNA in de novo DNA methylation of the imprinted mouse Rasgrf1 locus. Science *332*, 848-852.

Watson M.L., Zinn A.R., Inoue N., Hess K.D., Cobb J., Handel M.A., Halaban R., Duchene C.C., Albright G.M., and Moreadith R.W. (1998). Identification of morc (microrchidia), a mutation that results in arrest of spermatogenesis at an early meiotic stage in the mouse.

Proceedings of the National Academy of Sciences of the United States of America *95*, 14361-14366.

Webster K.E., O'Bryan M.K., Fletcher S., Crewther P.E., Aapola U., Craig J., Harrison D.K., Aung H., Phutikanit N., Lyle R., *et al.* (2005). Meiotic and epigenetic defects in Dnmt3L-knockout mouse spermatogenesis. Proceedings of the National Academy of Sciences of the United States of America *102*, 4068-4073.

Wu Q., Song R., Ortogero N., Zheng H., Evanoff R., Small C.L., Griswold M.D., Namekawa S.H., Royo H., Turner J.M., *et al.* (2012). The RNase III enzyme DROSHA is essential for microRNA production and spermatogenesis. The Journal of biological chemistry *287*, 25173-25190.

Xiol J., Cora E., Koglgruber R., Chuma S., Subramanian S., Hosokawa M., Reuter M., Yang Z., Berninger P., Palencia A., *et al.* (2012). A role for Fkbp6 and the chaperone machinery in piRNA amplification and transposon silencing. Molecular cell *47*, 970-979.

Zamudio N., Barau J., Teissandier A., Walter M., Borsos M., Servant N., and Bourc'his D. (2015). DNA methylation restrains transposons from adopting a chromatin signature permissive for meiotic recombination. Genes & development *29*, 1256-1270.

Zhang P., Kang J.Y., Gou L.T., Wang J., Xue Y., Skogerboe G., Dai P., Huang D.W., Chen R., Fu X.D., *et al.* (2015). MIWI and piRNA-mediated cleavage of messenger RNAs in mouse testes. Cell research *25*, 193-207.

Zhang X., Ebata K.T., Robaire B., and Nagano M.C. (2006). Aging of male germ line stem cells in mice. Biology of reproduction *74*, 119-124.

Zhao Q., Rank G., Tan Y.T., Li H., Moritz R.L., Simpson R.J., Cerruti L., Curtis D.J., Patel D.J., Allis C.D., *et al.* (2009). PRMT5-mediated methylation of histone H4R3 recruits DNMT3A, coupling histone and DNA methylation in gene silencing. Nature structural & molecular biology *16*, 304-311.

Zheng K., and Wang P.J. (2012). Blockade of pachytene piRNA biogenesis reveals a novel requirement for maintaining post-meiotic germline genome integrity. PLoS genetics *8*, e1003038.

Zheng K., Wu X., Kaestner K.H., and Wang P.J. (2009). The pluripotency factor LIN28 marks undifferentiated spermatogonia in mouse. BMC developmental biology *9*, 38.

Zheng K., Xiol J., Reuter M., Eckardt S., Leu N.A., McLaughlin K.J., Stark A., Sachidanandam R., Pillai R.S., and Wang P.J. (2010). Mouse MOV10L1 associates with Piwi proteins and is an essential component of the Piwi-interacting RNA (piRNA) pathway. Proceedings of the National Academy of Sciences of the United States of America *107*, 11841-11846.